



INTERNATIONAL
HELLENIC
UNIVERSITY

Numerical modeling of a hybrid parabolic trough Concentrating Solar Power Plant

Constantinos Sioumis

SID: 3302100035

SCHOOL OF SCIENCE & TECHNOLOGY

A thesis submitted for the degree of

Master of Science (MSc) in Information and Communication Systems

FEBRUARY 2013

THESSALONIKI – GREECE



INTERNATIONAL
HELLENIC
UNIVERSITY

Numerical modeling of a hybrid parabolic trough Concentrating Solar Power Plant

Constantinos Sioumis

SID: 3302100035

Supervisor: Dr. George Giannakidis
Supervising Committee Assoc. Prof. Name Surname
Members: Assist. Prof. Name Surname

SCHOOL OF SCIENCE & TECHNOLOGY

A thesis submitted for the degree of

Master of Science (MSc) in Information and Communication Systems

FEBRUARY 2013

THESSALONIKI – GREECE

Abstract

This dissertation was written as a part of the MSc in Energy Systems at the International Hellenic University. Its scope is to review researching efforts in the field of Concentrating Solar Power Plants (CSPP) modeling and to apply appropriately well-established related modeling principles into a 20 MW hybrid parabolic trough CSPP.

For this reason the introductory section documents the importance of appropriate modeling of CSPP by examining the ground of RES promotion, distinguishing the prospects of CSPPs and illustrating the parties that would be interested in such a research. This document goes on with the review of 3 major dilemmas faced by someone who aims at estimating the production of a CSPP: a) acknowledgment of uncertainty inherent in these systems, b) building a custom-made model to evaluate the appropriateness of available modeling tools and c) using commercial integrated CSPP modeling software. Information provided in that section is being matched with illustrated needs, restrictions and specificities related to input data required in the modeling process of a hybrid parabolic trough CSPP with thermal storage. This correlation made the use of System Advisor Model seem as the most appropriate tool in order that a 20 MW plant to be modeled. Parametric, statistical and financial analysis is also performed supporting the exportation of useful conclusions.

Although simulating the operation of a CSPP is a highly demanding process requiring extensive knowledge of several scientific fields (physics, mathematics, electrical and mechanical engineering, informatics), sincere support and scientific guidance provided by Dr. George Giannakides have been proven to be enough for the successful completion of this study. Acknowledging his contribution and deeply thanking him for this is the least that I could do.

Constantinos Sioumis

February 15th, 2013

Contents

ABSTRACT.....	III
CONTENTS.....	IV
LIST OF FIGURES.....	VII
1 INTRODUCTION.....	1
1.1 THE NEED FOR LOW CO ₂ EMISSIONS.....	1
1.2 THE ROLE OF CSP IN LESS CO ₂	4
1.3 CSP AS A MEANS OF SAVING COSTS	6
1.4 CSP PLANTS: UNDER RESEARCH AND DEVELOPMENT.....	11
1.5 ESTIMATING ELECTRICITY GENERATION: A KEY FACTOR.....	13
1.6 THE THESIS IN A NUTSHELL	15
2 MODELING CSP PLANTS.....	17
2.1 INTRODUCTION.....	17
2.2 CERTAINTY VS PROBABILITY	17
2.2.1 <i>Deterministic Models</i>	18
2.2.2 <i>Probabilistic Models</i>	18
2.3 MODELING TOOLS	20
2.3.1 <i>Fortran</i>	20
2.3.2 <i>Mathematica</i>	21
2.3.3 <i>MATLAB</i>	21
2.3.4 <i>Spreadsheets</i>	22
2.3.5 <i>Other Modeling Tools</i>	23
2.4 INTEGRATED CSP PLANT MODELS	24
2.4.1 <i>RETScreen</i>	25
2.4.2 <i>TRNSYS</i>	29
2.4.3 <i>System Advisor Model</i>	32
2.4.4 <i>Other Integrated CSPP Models</i>	36
3 CHALLENGES ON MODELING A PARABOLIC TROUGH CSP PLANT .	39
3.1 INTRODUCTION.....	39

3.2	INSTALLATION SITE	41
3.2.1	<i>Sun Relative Position</i>	41
3.2.2	<i>Atmospheric Attenuation</i>	41
3.2.3	<i>External Shading</i>	42
3.3	CLIMATE.....	42
3.3.1	<i>Solar Data</i>	43
3.3.2	<i>Non-solar Data</i>	43
3.4	SOLAR FIELD	43
3.4.1	<i>Lay-out</i>	44
3.4.2	<i>Solar Collector Assemblies</i>	44
3.4.3	<i>Heat Collection Element</i>	46
3.4.4	<i>Heat Transfer Fluid</i>	47
3.5	POWER CYCLE.....	48
3.5.1	<i>Fossil Fuel-fired Boiler</i>	49
3.5.2	<i>Steam Generator – Feedwater Heaters</i>	50
3.5.3	<i>Steam Turbines - Electricity Generator</i>	50
3.5.4	<i>Condenser</i>	50
3.6	THERMAL ENERGY STORAGE SYSTEM.....	51
3.7	PIPING SYSTEM.....	51
3.7.1	<i>Tubular Components</i>	52
3.7.2	<i>Non-tubular Components</i>	52
3.8	COMMENTS.....	52
4	A 20 MW CSPP MODEL	53
4.1	INTRODUCTION.....	53
4.2	THE OBJECTIVES	54
4.3	INITIAL SETUP	54
4.3.1	<i>Climate</i>	55
4.3.2	<i>Annual Performance</i>	57
4.3.3	<i>Solar Field</i>	58
4.3.4	<i>Collectors</i>	64
4.3.5	<i>Receivers</i>	65
4.3.6	<i>Power Cycle</i>	66
4.3.7	<i>Thermal Storage</i>	70

4.3.8	<i>Parasitics</i>	73
4.4	DETERMINISTIC MODELING	74
4.4.1	<i>Alternative Locations</i>	74
4.4.2	<i>Output of the Initial Setup</i>	75
4.4.3	<i>Parametric Analysis</i>	77
4.5	PROBABILISTIC MODELING	82
4.6	FINANCIAL MODELING	85
4.6.1	<i>Trough System Costs</i>	85
4.6.2	<i>Financing</i>	86
4.6.3	<i>Tax Credit and Payment Incentives</i>	88
4.6.4	<i>Sizing the Solar Field</i>	88
4.6.5	<i>Technical Optimization</i>	90
4.6.6	<i>Feasibility Analysis</i>	91
5	CONCLUSIONS	99
	BIBLIOGRAPHY	101

List of Figures

Figure 1.1: Global surface air temperature anomalies relative to 1951-1980 base period for annual and 5-year running means. Green vertical bars are 2σ error estimates. 1

Figure 1.2: 420.000 years of ice core data from Vostok, Antarctica research station. ... 2

Figure 1.3: Kyoto Protocol participation map as of February, 2012..... 3

Figure 1.4: World CO₂ emissions by sector in 2009..... 4

Figure 1.5: Comparison of as-published lifecycle GHG emission estimates for electricity generation technologies. The impacts of the land use change are excluded from this analysis. 5

Figure 1.6: Comparison of as-published and harmonized lifecycle GHG emission estimates for electricity generation technologies. 5

Figure 1.7: Composition of U.S. energy use. Electricity refers to power from primary sources only: nuclear, hydropower, solar, wind and geothermal..... 6

Figure 1.8: 1973 and 2009 world fuel shares of electricity generation. ** Other includes geothermal, solar, wind, biofuels and waste and heat. 6

Figure 1.9: Oil reserves-to-production (R/P) ratios..... 7

Figure 1.10: Crude oil prices 1861-2011. US dollars per barrel. World events..... 7

Figure 1.11: Gold to Oil Ratio (barrels/ounce). Smoothed prices using 1-year moving average. 8

Figure 1.12: Progress of energy efficiency for heat engines and luminous devices 8

Figure 1.13: Fossil Fuel Prices (constant USD prices of 2008 per BOE). 9

Figure 1.14: Electricity Share in the EU Energy Mix (values shown as final consumption)..... 9

Figure 1.15: Regional ranges of LCOE for nuclear, coal, gas and onshore wind power plants. 9

Figure 1.16: LCOE ranges for 14 technologies.....10

Figure 1.17: LCOE for a plant in US Southwest by technology.....10

Figure 1.18: LCOE Forecast by technology, 2010-2020.11

Figure 1.19: CSP global cumulative installed capacity and annual electricity production.11

Figure 1.20: CSP project pipeline atlas.....	12
Figure 1.21: Expected installed capacity of solar-thermal power plants in GW.	12
Figure 1.22: EU-MENA project of the DESERTEC Foundation.....	13
Figure 1.23: EU Renewable Shares of Final Energy, 2005 and 2009, with Targets for 2020.	13
Figure 1.24: Renewable Energy Support Policies.....	14
Figure 2.1: Histograms (left) and cumulative distribution functions (right) of parameters with normal (top) and uniform distribution (bottom).....	19
Figure 2.2: The total-system modeling pyramid.	24
Figure 2.3: A new total-system modeling scheme.....	25
Figure 2.4: The RETScreen start-up sheet.	26
Figure 2.5: The RETScreen standard input climate data.	26
Figure 2.6: The RETScreen manual input climate data.....	27
Figure 2.7: The RETScreen energy model sheet.....	28
Figure 2.8: The RETScreen Power System Load Definition – Base, Intermediate & Peak.....	28
Figure 2.9: The TRNSYS Simulation Studio start-up sheet.....	29
Figure 2.10: a) Left – Adjustable parameters, b) Right – Component output data categories.....	30
Figure 2.11: The TRNSYS screen for the linkage of two components.	31
Figure 2.12: The TRNSYS online result plotter.....	31
Figure 2.13: SAM Solar Field Sheet.	33
Figure 2.14: SAM Power Cycle sheet.	34
Figure 2.15: SAM Thermal Storage sheet.....	35
Figure 2.16: The insertion module of a variable containing uncertainty.....	35
Figure 2.17: The SIMPLESYS energy model.....	36
Figure 2.18: The “Climate” data input tabs.....	37
Figure 2.19: The “Solar field” data input tab and the “Time Graphics” results tab	37
Figure 2.20: DinaCET’s solar field simulation sheet.....	38
Figure 2.21: DinaCET’s simulation of a cloudy day operation	38
Figure 3.1: Diagram of a hybrid parabolic trough with thermal storage	39
Figure 3.3: DNI as a function of AOD	41

Figure 3.4: AOD as a function of elevation	41
Figure 3.5: An example in which neither the final nor the average of initial and final temperature provides a reliable representation of the temperature over the time step.	42
Figure 3.6: Three indicative solar field lay-outs.....	44
Figure 3.7: Three indicative solar field lay-outs.....	44
Figure 3.8: Comparison of thermal power production of 2 solar field multiples	45
Figure 3.9: A typical HCE for parabolic troughs	46
Figure 3.10: Efficiency chart of different annulus gases.....	47
Figure 3.11: An indicative Rankine cycle configuration.....	48
Figure 3.12: Two alternatives of Solar-Fossil Fuel Hybrids	49
Figure 4.1: Actual and modeled solar output	53
Figure 4.2: Actual and modeled parasitic loads	53
Figure 4.3: Schematic view of a hybrid parabolic trough CSPP with thermal storage ..	55
Figure 4.4: The 3 locations.	55
Figure 4.5: SAM weather file library.....	56
Figure 4.6: SAM suggested weather file web links.....	56
Figure 4.7: SAM TMY3 creator.	56
Figure 4.8: SAM weather and location data summary.	57
Figure 4.9: Two indicative levels of weather data analysis.....	57
Figure 4.10: The annual system performance tab in average form.....	58
Figure 4.11: The module for the definition of variable system performance factors for each year.	58
Figure 4.12: The solar collector arrangement.	58
Figure 4.13: The probability of a CSPP with SM=1 to operate at its rated capacity.....	59
Figure 4.14: An example of LCOE as a function of SM and full hours of thermal storage	59
Figure 4.15: The maximum DNI-cosine effect product.....	60
Figure 4.16: The monthly profile of the dumped thermal energy.	60
Figure 4.17: The arrangement of SCA's per loop.	61
Figure 4.18: Land requirements.....	62
Figure 4.19: Defining an alternative HTF.	62
Figure 4.20: Summary of the solar field parameters and HTF properties.....	63

Figure 4.21: Water needs and plant heat capacity.....	63
Figure 4.22: The EuroTrough collector	64
Figure 4.23: The SAM collectors tab.....	64
Figure 4.24: The HCE geometrical parameters.....	65
Figure 4.25: The module enabling the definition of emittance for different temperature values.....	65
Figure 4.26: Various HCE parameters and variations.....	66
Figure 4.27: Estimating the plant capacity.	67
Figure 4.28: Conditions at design point for the basis Rankine cycle.	67
Figure 4.29: Power block variables at the design point.....	68
Figure 4.30: Plant control dataset.....	68
Figure 4.31: Parameters and variables conceding the cooling system.....	69
Figure 4.32: Input data to the SAM dry cooling model.	70
Figure 4.33: Input data to the SAM TES system.....	71
Figure 4.34: The thermal storage and fossil energy dispatch schedule.....	72
Figure 4.35: Assumed values for a) Pipe sizing schedules (up left), b) Piping lengths (up right), c) Various configurations regarding the piping equipment (down).....	73
Figure 4.36: The assumed parasitic coefficients.	74
Figure 4.37: The assumed parasitic coefficients.....	74
Figure 4.38: The correlation of annual solar field energy and, the DNI and collectors tilt.	75
Figure 4.39: The monthly distribution of gross and net electric output.	75
Figure 4.40: Net electric power output and freeze protection energy.	76
Figure 4.41: Solar thermal output and thermal energy produced by the auxiliary heaters.	76
Figure 4.42: The monthly profile of the dumped thermal energy.	77
Figure 4.43: The SAM parametric analysis module.	78
Figure 4.44: The optimal stow and deploy angles.....	79
Figure 4.45: The optimal annular gas type used in the receivers.	79
Figure 4.46: No low resource standby period is proposed.	80
Figure 4.47: Mitigation of benefits leads to the preservation of the current TES capacity.	80

Figure 4.49: Sensitivity analysis of net electric output to selected parasitic loads.	82
Figure 4.50: Defining whether an input variable follows a uniform or a normal distribution.....	83
Figure 4.51: The histogram/cumulative distribution function of the general optical error.	83
Figure 4.52: The histogram/cumulative distribution function of the net annual energy.	84
Figure 4.53: Estimated δR^2 s of the uncertain variables.	84
Figure 4.54: Trough system costs.	86
Figure 4.55: The financing dataset of the investment.	87
Figure 4.56: The optimal solar multiple-storage capacity combination for Athens.....	89
Figure 4.57: The optimal solar multiple-storage capacity combination for Thessaloniki.	89
Figure 4.58: The optimal solar multiple-storage capacity combination for Andravida.	90
Figure 4.59: The optimal tank heater capacity for Athens.	90
Figure 4.60: Sensitivity analysis between the NPV and the trough system costs (Andravida).....	92
Figure 4.61: Parametric analysis concerning the investment capital mix (Andravida).	92
Figure 4.62: Parametric analysis concerning the cost of capital (Andravida).	93
Figure 4.63: Parametric analysis concerning the cost of capital (Andravida).	93
Figure 4.64: Sensitivity analysis between the NPV and the trough system costs (Thessaloniki).....	94
Figure 4.65: Parametric analysis concerning the investment capital mix (Thessaloniki).	94
Figure 4.66: Parametric analysis concerning the cost of capital (Thessaloniki).....	95
Figure 4.67: Sensitivity analysis between the NPV and the trough system costs (Athens).	95
Figure 4.68: Parametric analysis concerning the investment capital mix (Athens).	96
Figure 4.69: Parametric analysis concerning the cost of capital (Athens).	96
Figure 4.70: The values of the 3 locations' major calculations.	97

1 Introduction

The scope of this introductory section is to ratify the importance of accurate forecasting of the electricity produced by hybrid concentrating solar power (CSP) plants and to present briefly the upcoming sections and their between cohesion.

1.1 The need for low CO₂ emissions

The weather in 2011 caused no major surprise to climate researchers. Although the Global Land-Ocean Temperature Index presented a slight decrease compared to 2010, its powerful uptrend (see Figure 1.1), which started in the late 19th century, remained totally in force [1].

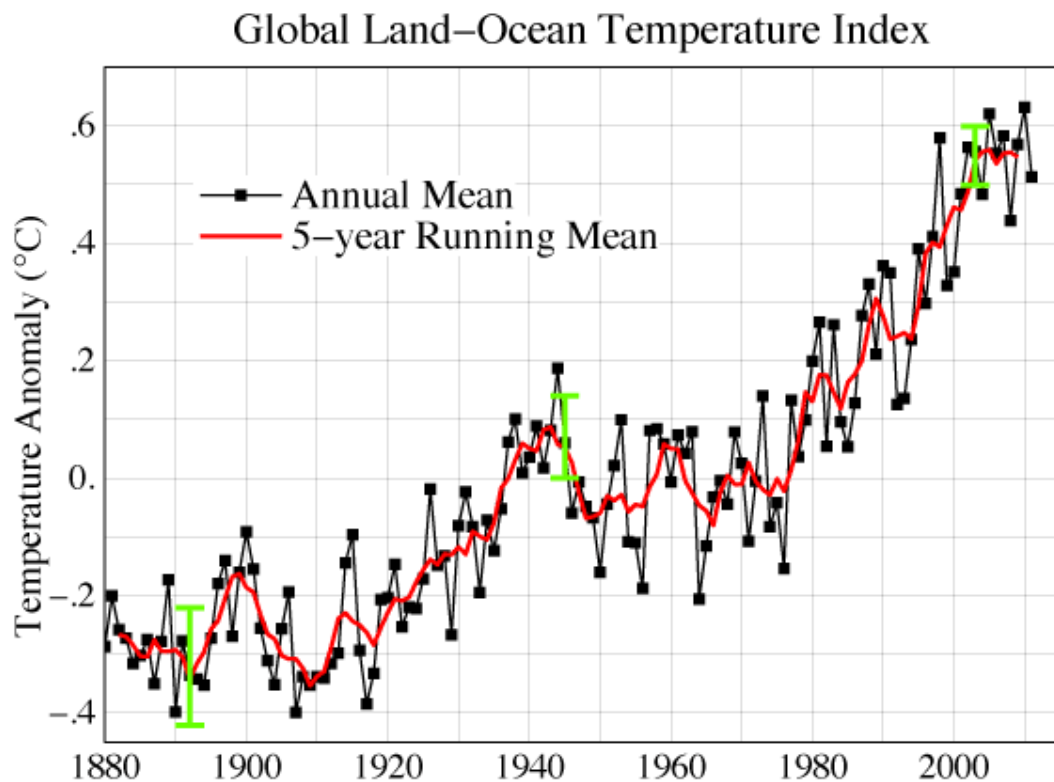


Figure 1.1: Global surface air temperature anomalies relative to 1951-1980 base period for annual and 5-year running means. Green vertical bars are 2σ error estimates.

Global warming is still here. This makes someone believe that observations noted in 2007 in the Fourth Assessment Report of the United Nations' Intergovernmental Panel on Climate Change (IPCC) are still valid; the atmosphere keeps getting full of harmful gases, warmth supplants coldness, snow level decreases, sea level rises, hurricanes strengthened [2]. Can we really do anything in order to deter these continuously growing threats?

In the early 20th century, Milutin Milanković argued that Earth's climate variations, insolation and temperature included, are not just reasonable but predictable too, as it spins around its axis and orbits around the Sun [3]. This theory has repeatedly been tested and confirmed as a) the project CLIMAP (Climate: Long Range Investigation, Mapping and Production) was fully in line with it [4], b) the project COHMAP (Cooperative Holocene Mapping Project) correlated global climate change with several astronomical factors [5] and c) the project SPECMAP (Spectral Mapping Project), proved that the climate responds to changes in solar radiation of different astronomical cycles [6].

On the other hand, over time Milanković's theory has faced massive dispute, mainly caused in the 1970s by the publication of marine sediment records knocking Milanković's estimations on ice-age cycles [7]. Indeed, in 1999 disputers of Milanković managed to correlate Earth's temperature with levels of carbon dioxide (CO₂), levels of methane (CH₄) and insolation (see Figure 1.2) [8].

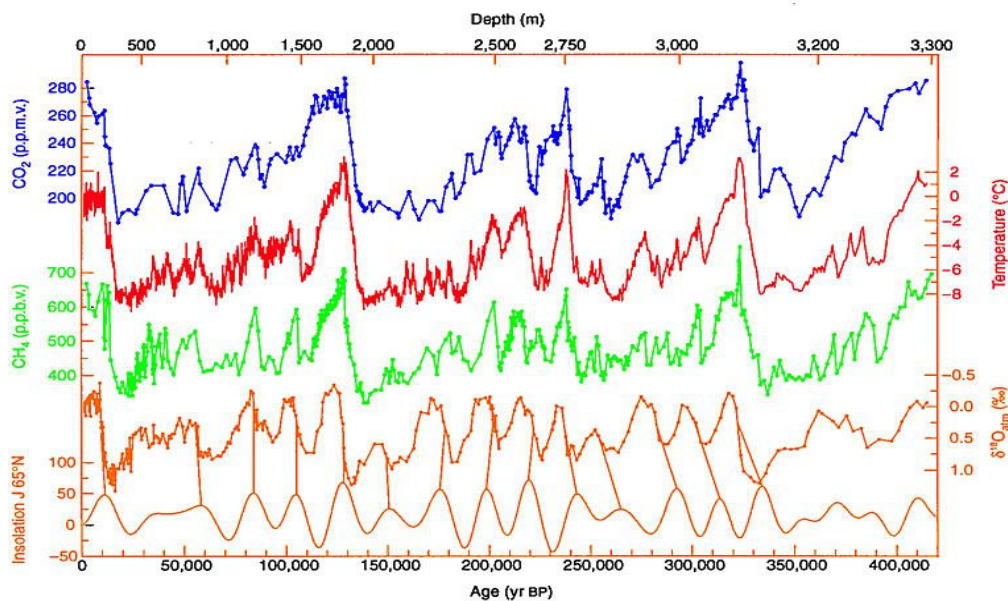


Figure 1.2: 420.000 years of ice core data from Vostok, Antarctica research station.

Although the abovementioned juxtaposition was partially mitigated in 2006, when W.F. Ruddiman introduced his carbon dioxide feedback hypothesis, combining Sun's and CO₂'s effect on Earth's climate [9], we won't argue on this topic any more. Besides it seems that humanity has reached a decision; CO₂ emissions have to be reduced.

Obviously this comes from the environmentally-friendly, low-CO₂-emission energy policies promoted through the United Nations Framework Convention on Climate Change (UNFCCC or FCCC) since its initial establishment in 1992 and especially since 1997 when the Kyoto Protocol was signed [10]. However, trying to preserve a rather dispassionate view of the situation, we should not neglect to underline the serious challenges faced by the Treaty in 2009 in Copenhagen [11] and the limited progress succeeded afterwards in Cancún and Durban summits. Canada's withdrawal in 2011 and USA having never ratified the Treaty [12] reinforce our skepticism on governments' unity and commitment on CO₂ emissions reduction, although in 2009 these two countries produced only 5.715,77 Mt of CO₂ or 19,7% of the global CO₂ emissions [13].

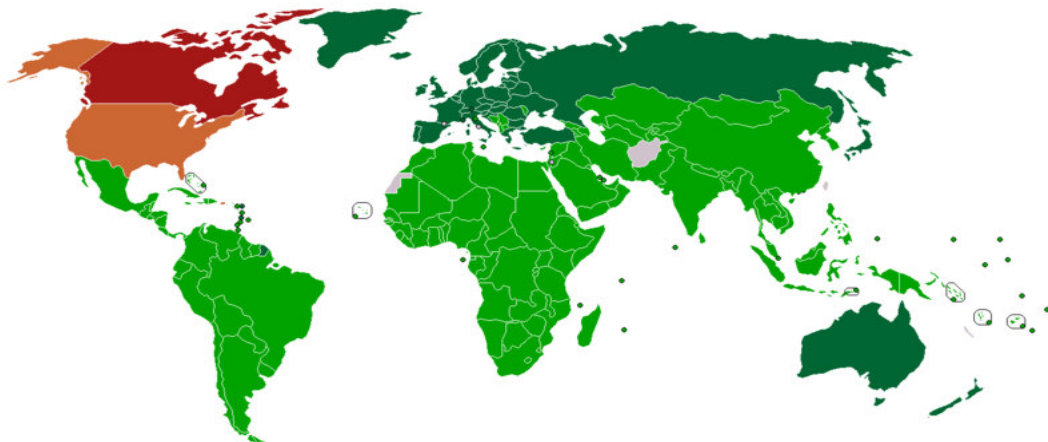


Figure 1.3: Kyoto Protocol participation map as of February, 2012.

Green = Ratified the treaty. Brown = No intention to ratify. Red = Withdrawn from the Protocol. Grey = No position taken or position unknown.

Concluding, although an extended debate is still taking place on whether CO₂ emissions are harmful and should be avoided, the majority of the world (see Figure 1.3) is committed to their reduction. Some pieces of related evidence are the 3 European Commission's Directives on RES promotion (2001/77, 2003/30 and 2009/28) and, Greek Government's Law 3468/2006 and its amendments thereafter.

1.2 The role of CSP in less CO₂

As it is clearly shown in Figure 1.4, electricity and heat cause more than 40% of global CO₂ emissions [14], making this sector an ideal candidate for emission reduction measures that will lead to a cleaner environment.

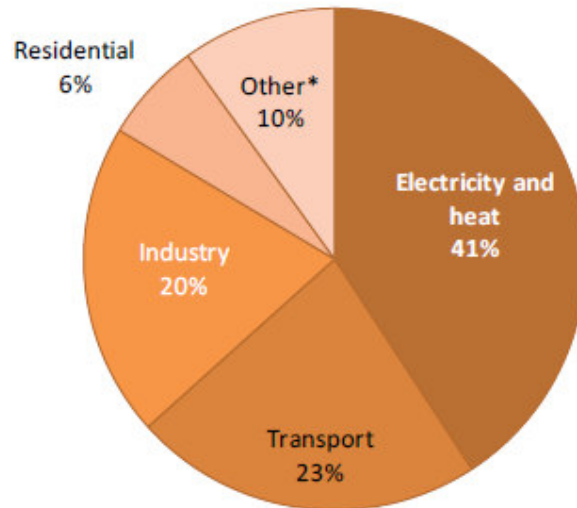


Figure 1.4: World CO₂ emissions by sector in 2009.

* Other includes commercial/public services, agriculture/forestry, fishing, energy industries other than electricity and heat generation, and other emissions not specified elsewhere.

Working on this purpose, the National Renewable Energy Laboratory of the USA edited data referring to lifecycle greenhouse gas (GHG) estimates for various electricity generation technologies. As-published data (Figure 1.5) [15] [16] compared to harmonized data (Figure 1.6) [17] exclude the impact of the land use change as well as oil and natural gas technologies. A quick look at these figures makes it more than clear that electricity generation technologies based on renewable sources produce significantly less CO₂ during their lifecycle, than those using fossil fuels; nuclear technologies are not taken into account due to their controversial categorization and overall attractiveness.

Furthermore the level of as-published CO₂ emissions produced by CSP technologies is noticeably lower than these of biopower and photovoltaics, while corresponding harmonized data prove that exploitation of CSP and wind power produces by far the least CO₂ among all power technologies.

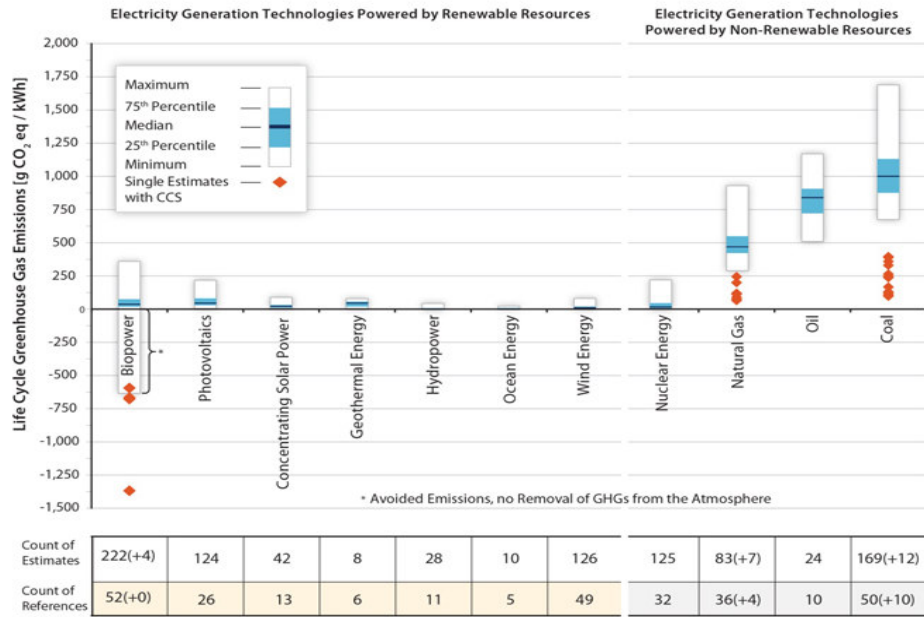


Figure 1.5: Comparison of as-published lifecycle GHG emission estimates for electricity generation technologies. The impacts of the land use change are excluded from this analysis.

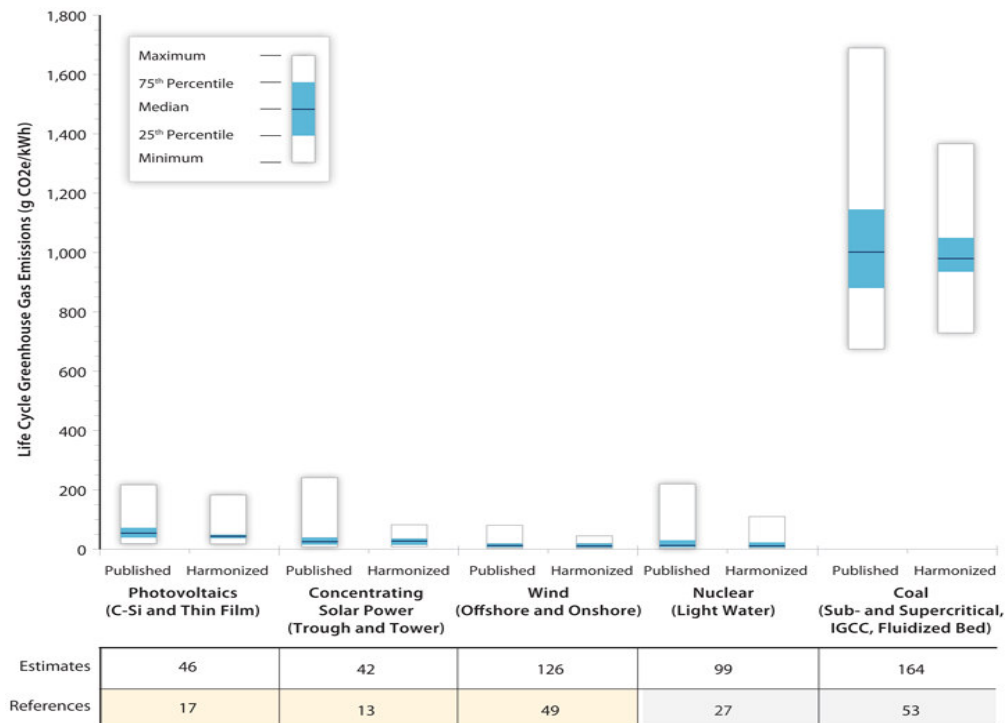


Figure 1.6: Comparison of as-published and harmonized lifecycle GHG emission estimates for electricity generation technologies.

1.3 CSP as a means of saving costs

Figures 1.5 and 1.6 presented in the previous section show that fossil fuels are the largest CO₂ emitters among all available electricity generation technologies. But, is it this fact that keeps forcing United States of America in replacing these primary energy sources with renewable ones [18]?

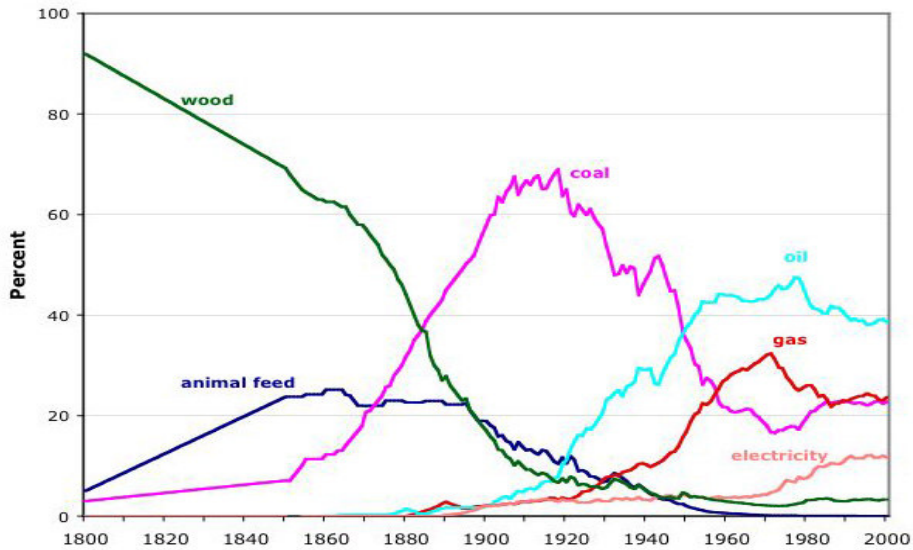


Fig-

ure 1.7: Composition of U.S. energy use. Electricity refers to power from primary sources only: nuclear, hydropower, solar, wind and geothermal.

Since USA even today is not committed in reducing CO₂ emissions, obviously past environmental concerns are not enough to explain Figure 1.7. Globally and focused on the electricity sector this trend is even more clear as coal, natural gas and oil covered 75,1% of the world electricity needs in 1973 but only 67,1% in 2009 [13].

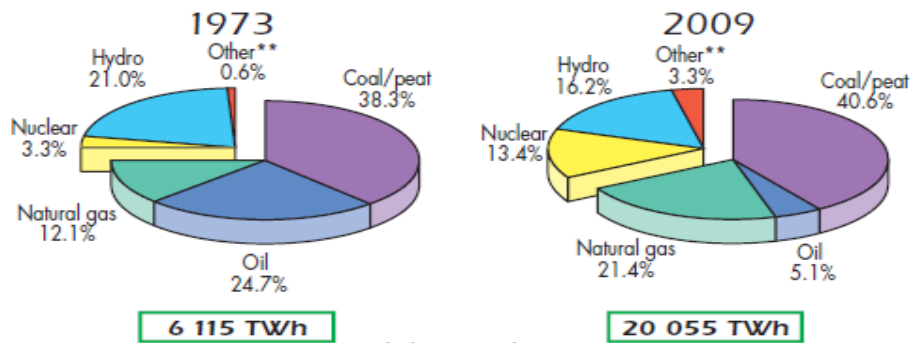


Figure 1.8: 1973 and 2009 world fuel shares of electricity generation. ** Other includes geothermal, solar, wind, biofuels and waste and heat.

Maybe it's the threat that fuels, i.e. oil reserves, are heading to depletion. However Figure 1.9 shows that a lucky guess and a proper drilling can save the day [19].

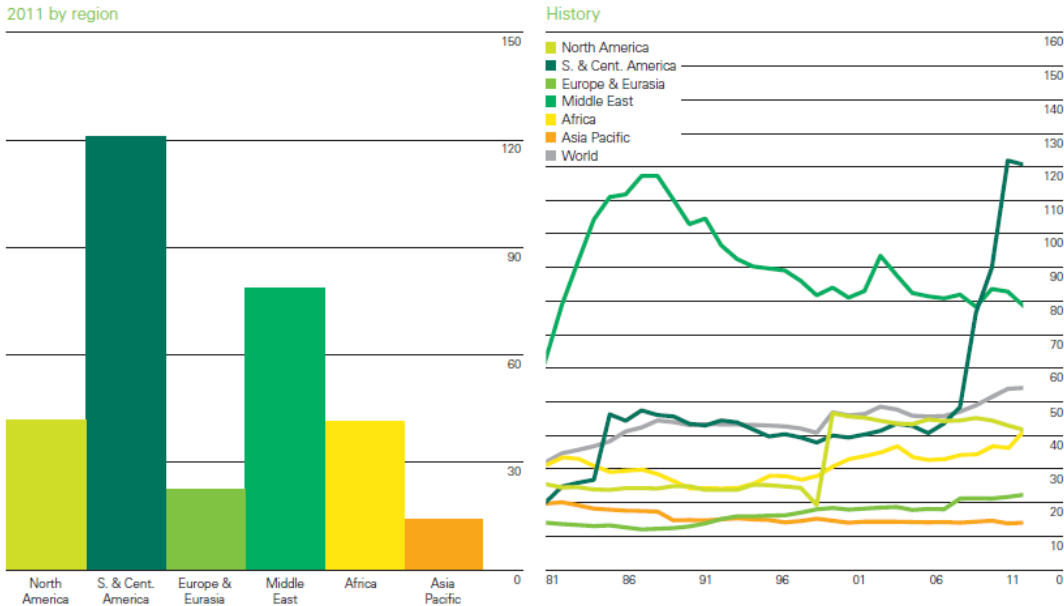


Figure 1.9: Oil reserves-to-production (R/P) ratios.

Last but not least is the possibility that the major decline in oil and natural gas share in total primary energy sources, observed since the early 1980's, is caused by Adam Smith's invisible hand of the market [20].

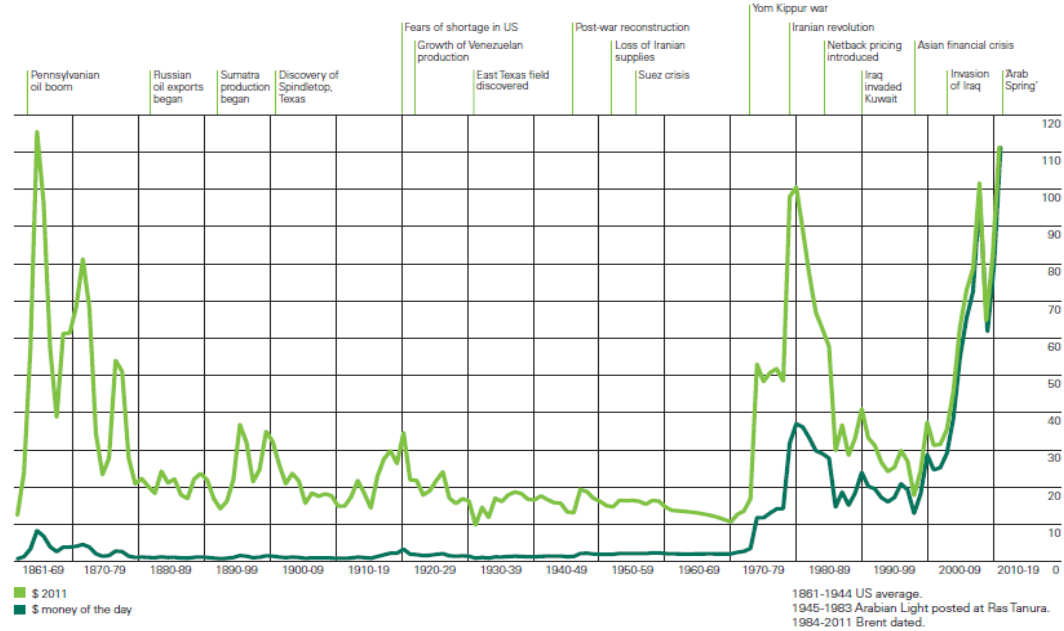


Figure 1.10: Crude oil prices 1861-2011. US dollars per barrel. World events.

Indeed, the chart above (Figure 1.10) [19] could support such a hypothesis as it shows that deflated price of crude oil started surging in the early 1970's until the peak of 1980, plunged forming a local bottom in 1998 and recently has exceeded previous high reaching the historical peak observed in the mid of 1860's. On the other hand, considering gold as the unique constant value in the global economy, one could counter this assumption simply by presenting the chart shown in Figure 1.11 [21] which proves that currently oil compared to gold is neither cheap nor expensive, historically speaking.

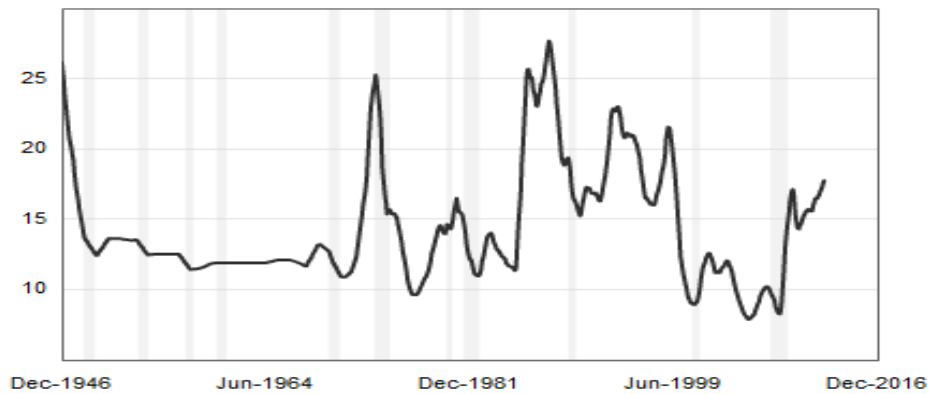


Figure 1.11: Gold to Oil Ratio (barrels/ounce). Smoothed prices using 1-year moving average.

Nevertheless, as the efficiency of fossil fuel technologies, used to generate electricity, tends to reach its upper limit soon (see Figure 1.12) [22], increased fuel prices definitely result in increased electricity cost.

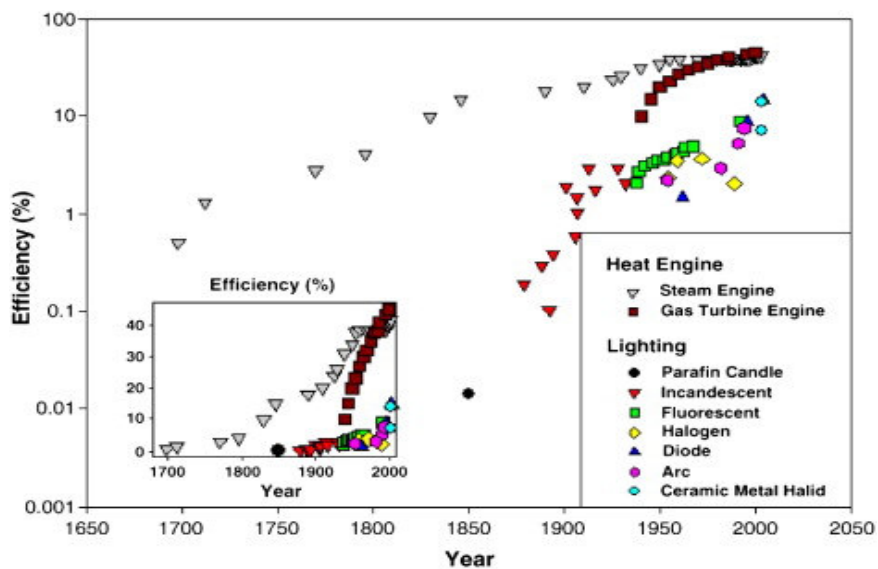


Figure 1.12: Progress of energy efficiency for heat engines and luminous devices

This would motivate somebody to search for an alternative. Europe is not excluded as the corresponding data (Figures 1.13 and 1.14) does not really differ [23] [24].

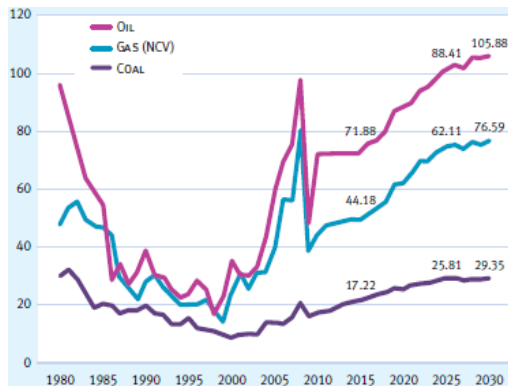


Figure 1.13: Fossil Fuel Prices (constant USD prices of 2008 per BOE).

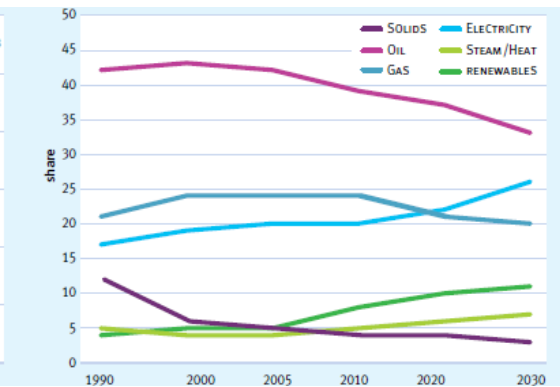


Figure 1.14: Electricity Share in the EU Energy Mix (values shown as final consumption).

However, choosing an electricity generation technology, even if the only factor that had to be optimized was “cost per kWh produced”, is not an easy task. Variations in a) daily prices of raw materials and fuels, b) companies engaged in the production of related equipment, c) climate and non-climate data (i.e. grid availability and tax incentives) among different locations and d) assumptions concerning other kinds of needed data (i.e. discount rate), cause extreme variations among estimations of the Levelized Cost of Electricity (LCOE) [25]. Figure 1.15 definitely supports this claim [26].

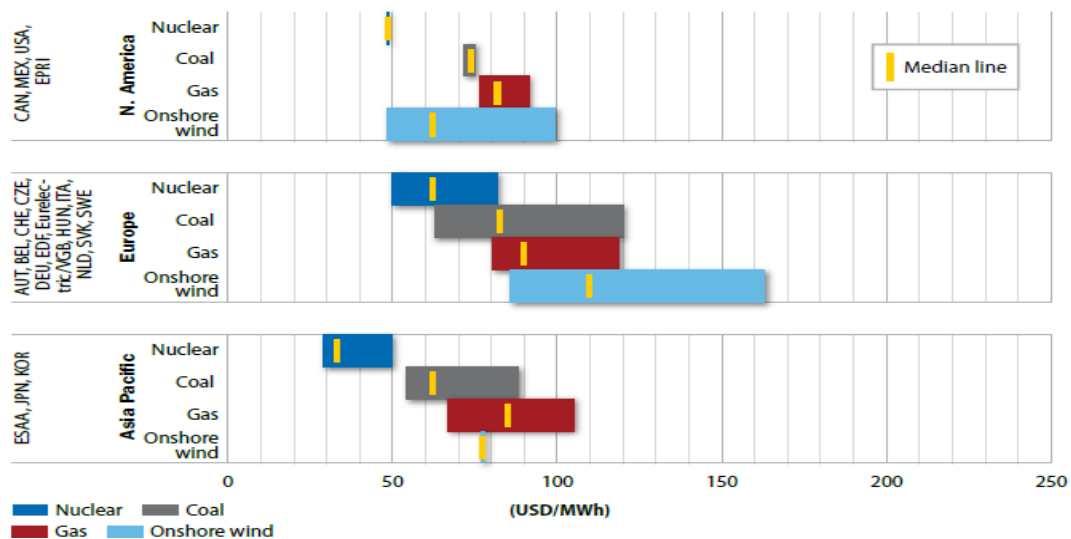


Figure 1.15: Regional ranges of LCOE for nuclear, coal, gas and onshore wind power plants.

In addition, if someone takes into account other external costs related to each technology, widely known as externalities, things become even more complex [27].

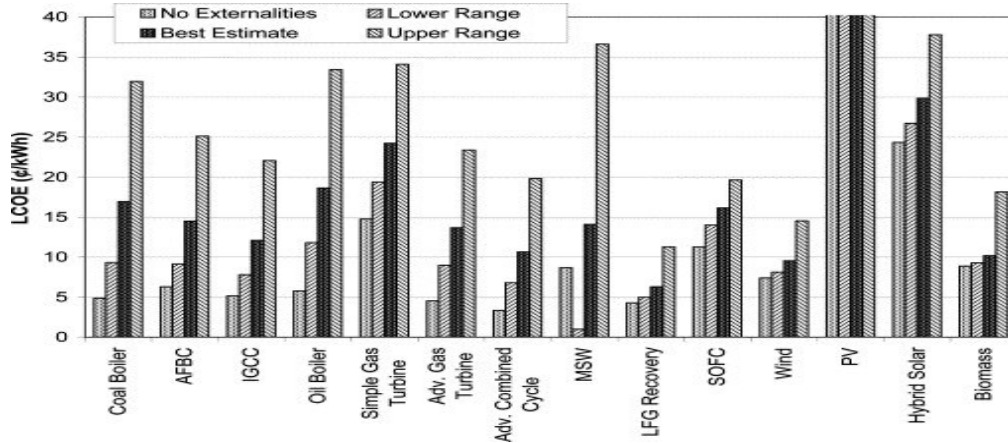


Figure 1.16: LCOE ranges for 14 technologies.

According to Figure 1.16, discarding externalities, electricity generation technologies using fossil fuels can be hardly compared, economically speaking, to these using RES other than wind. This fact changes dramatically when costs related to i.e. social health and environmental downgrade are counted in, since under certain conditions hybrid CSP plants seem to become attractive. This view is further strengthened by the findings of a GTM Research’s recent study shown in Figures 1.17 and 1.18 [28], according to which the LCOE of CSP plants in the USA vary from 0,168 to 0,117 \$/kWh and, estimations concerning the near future make CSP plants look cost-effective.

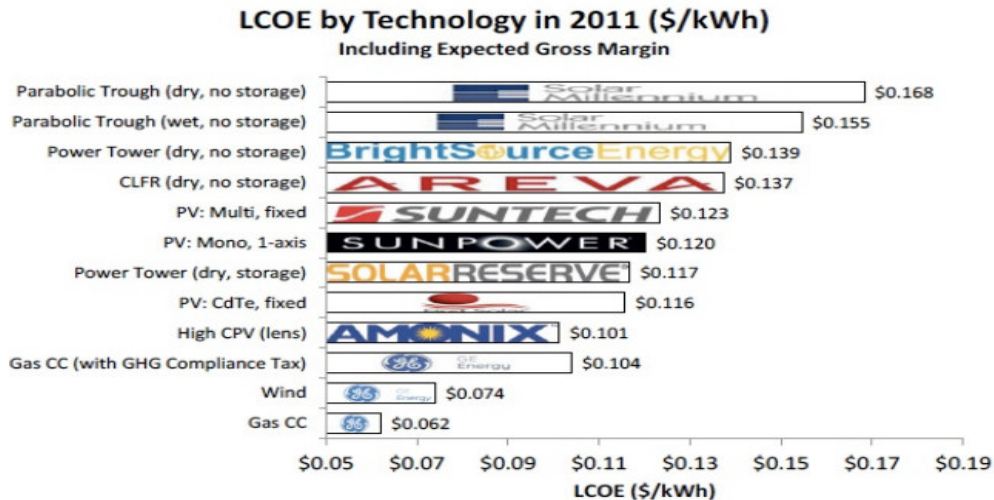


Figure 1.17: LCOE for a plant in US Southwest by technology.

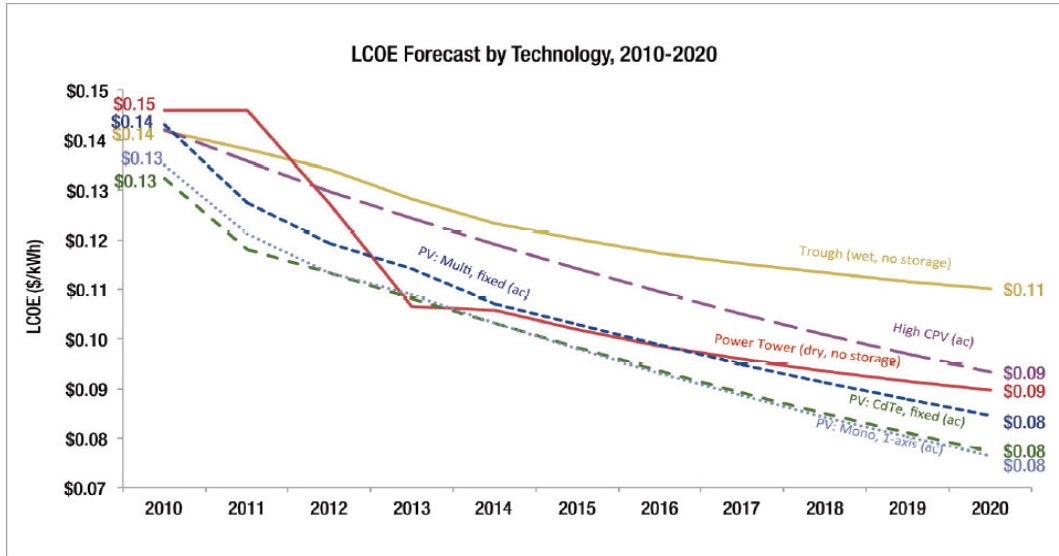


Figure 1.18: LCOE Forecast by technology, 2010-2020.

1.4 CSP plants: Under research and development

"Within 6 hours deserts receive more energy from the sun than humankind consumes within a year". This calculation made by Dr. G. Knies [33], combined with evidence that a) CSP technologies cause relatively few CO₂ emissions during their life-cycle and b) the corresponding LCOE is currently, under certain conditions, acceptable and will soon become attractive, probably are the main drivers that motivated plenty of industrially developed countries to pay attention to this technology. As a consequence USA and EU have diachronically invested important amounts of time and money in CSP research [29] [30], while installed capacity surges (see Figure 1.19) [31].

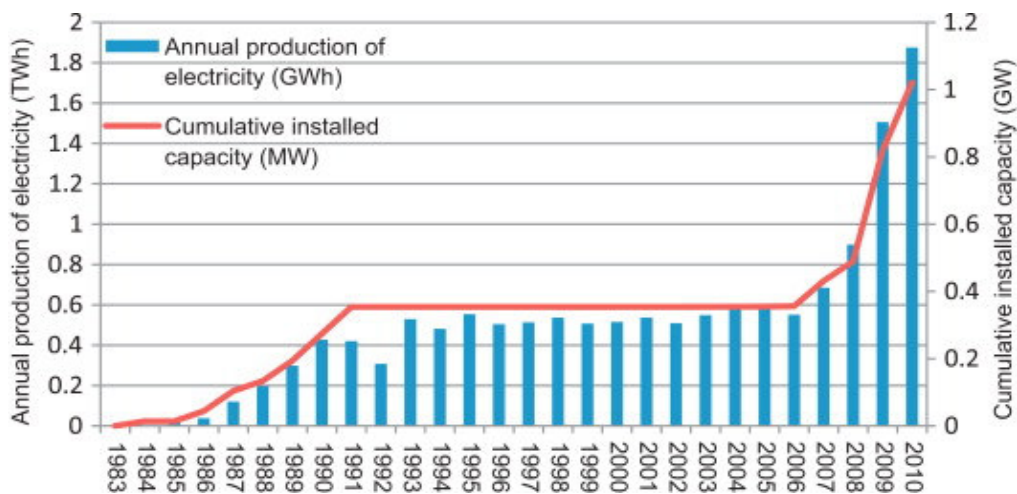


Figure 1.19: CSP global cumulative installed capacity and annual electricity production.

This trend seems really powerful as a large number of projects are still under development (Figure 1.20) [28] while 7 related studies shown in Figure 1.21 outline a rather brilliant future for CSP [32].

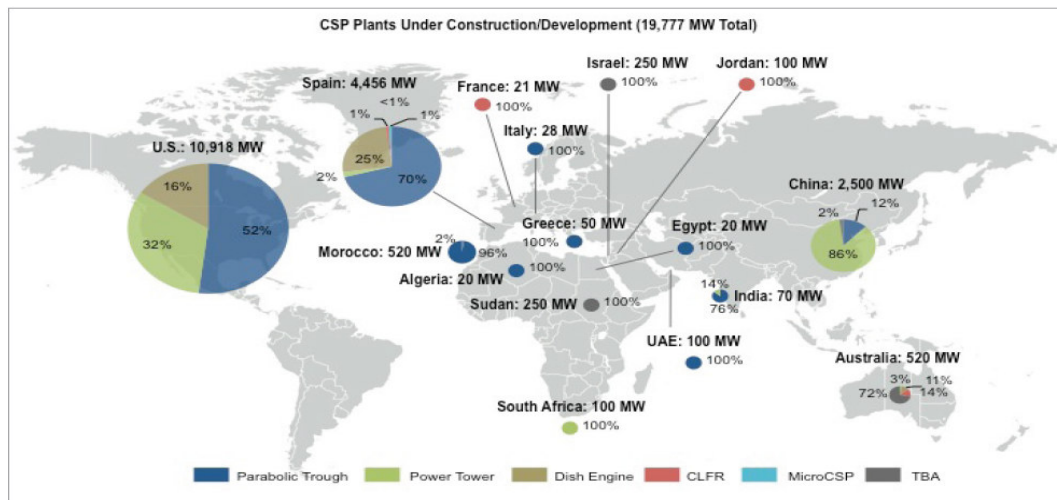


Figure 1.20: CSP project pipeline atlas.

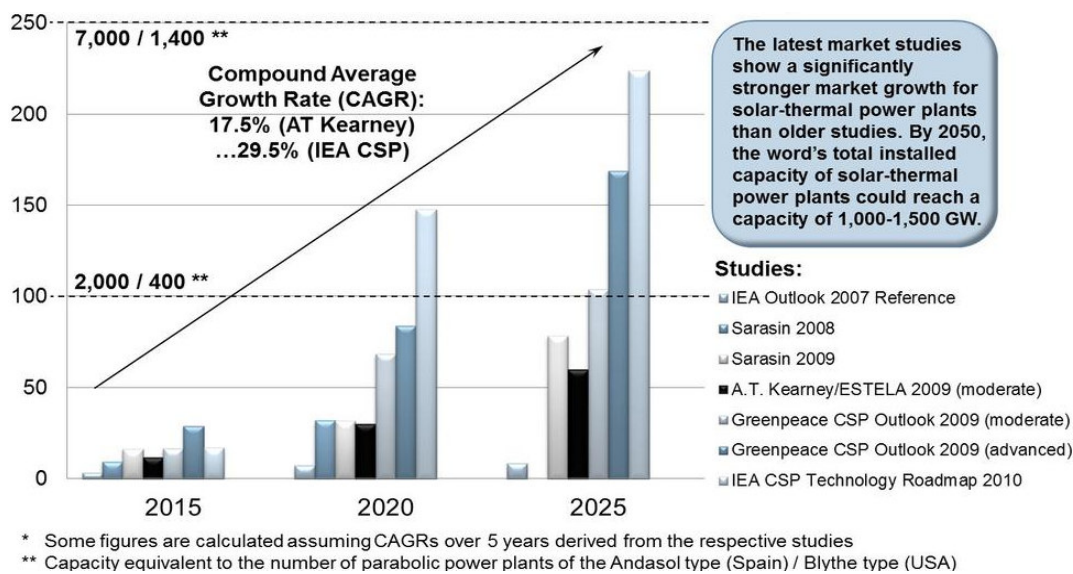


Figure 1.21: Expected installed capacity of solar-thermal power plants in GW.

Furthermore, somebody should not neglect the dominant position in this emerging sector held by the projects of DESERTEC Foundation (see Figure 1.22) [33]. The fact that these projects include Greece too strengthens the choice made by investors who applied for the licensing of 1.084,42 MW of CSP in the country [34].



Figure 1.22: EU-MENA project of the DESERTEC Foundation.

1.5 Estimating electricity generation: A key factor

In the very beginning of this Chapter the commitment of the majority of the world in promoting RES was clearly presented. However, reaching ambitious targets, like those of the Figure 1.23 [35], prerequisites the establishment of numerous measures.

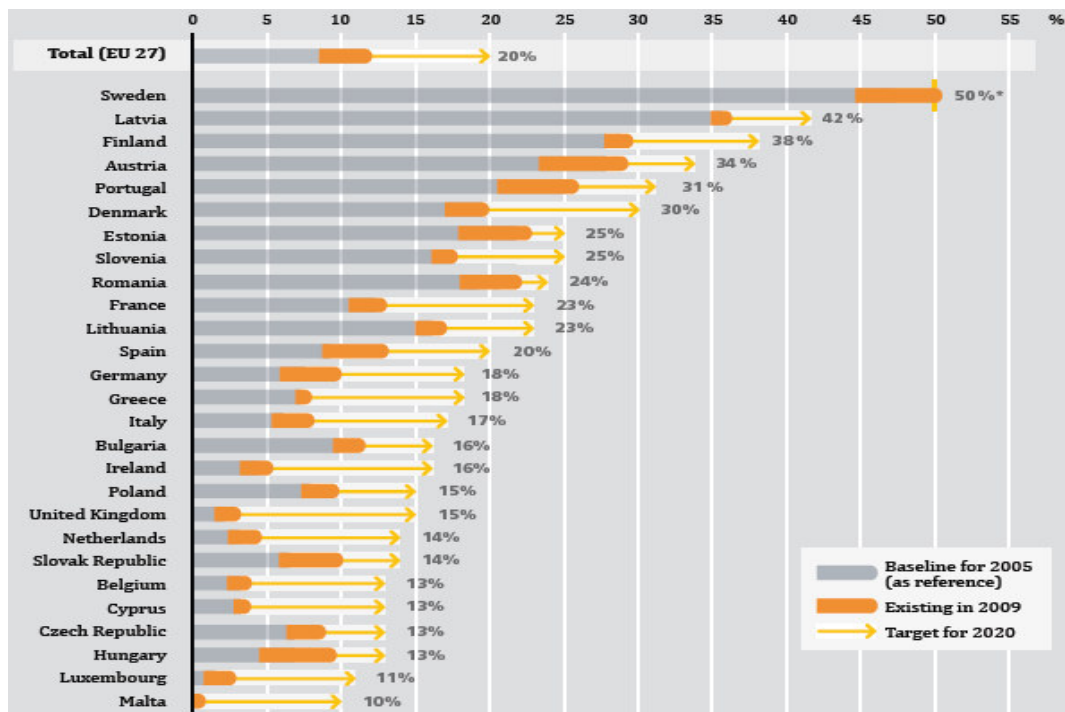


Figure 1.23: EU Renewable Shares of Final Energy, 2005 and 2009, with Targets for 2020.

As Figure 1.24 shows [35], these measures aim at overcoming both technical and financial constraints faced in the promotion of RES. Focusing on the fiscal part the most common incentives are feed-in-tariff (f-i-t), capital subsidy and tax credits/reductions.

On what level should these fiscal incentives be granted though? A quick view, i.e. in the f-i-t measure and the way it is applied i.e. in Greece, makes clear that each technology is subsidized on a different level [36]. Apparently this has to do with the ensuring of the investment feasibility, since according to data given in section 1.3 the LCOE of fossil fuels is much lower than this of RES. Expected income is one of the most important factors that determine the feasibility of an investment and in the case of RES plants their sole income is highly correlated to their production amount (the other major factor is the selling price). As such, a reliable annual estimation of their electricity generation becomes highly important for governments willing to promote RES.

	REGULATORY POLICIES						FISCAL INCENTIVES				PUBLIC FINANCING	
	Feed-in tariff (incl. premium payments)	Electricity quota/obligation/ RPS	Net metering	Renewable obligation/ mandate	Renewable obligation/ mandate	Tradeable RPS	Capital subsidy grant, or rebate	Investment or production tax credits	Reductions in sales, energy, CO ₂ , VAT or other taxes	Energy production payments	Public investment, loans, or grants	Public competitive bidding
HIGH-INCOME COUNTRIES												
Australia	▲			▲		●	●				●	
Austria	●			●		●	●			●		
Belgium		▲	●	●		●	●			●		
Canada	▲	▲	●	●		●	●	●		●	●	
Croatia	●						●			●		
Cyprus	●						●			●		
Czech Republic	●			●		●	●	●				
Denmark	●		●	●		●	●	●		●	●	
Estonia	●			●		●	●		●			
Finland	●			●		●	●		●			
France	●			●		●	●	●		●		●
Germany	●			●	●	●	●	●		●		●
Greece	●		●				●			●		
Hungary	●			●			●			●		
Ireland	●					●						●
Israel	●				▲	●				●		●
Italy	●	●	●	●		●	●			●		●
Japan	●	●	●	●		●	●			●		●
Latvia	●			●			●			●		●
Luxembourg	●						●			●		
Malta			●				●					
Netherlands				●		●	●	●	●			
New Zealand							●					
Norway				●		●	●			●		
Poland		●		●		●	●			●		●
Portugal	●	●	●	●	●	●	●	●		●		●
Singapore												
Slovakia	●						●					
Slovenia	●					●	●	●		●		●
South Korea ¹		●		●		●	●	●		●		●
Spain ²	●			●	●		▲	●	●	●		●
Sweden		●		●		●	●	●	●	●		
Switzerland	●						●	●	●			
Trinidad & Tobago							●	●				
United Kingdom	●	●		●		●	●	●	●	●		●
United States	▲	▲	▲	●	▲	●	●	●	●	●		●

Figure 1.24: Renewable Energy Support Policies.

Similar needs exist in the case of parties interested in investing in electricity generation, and RES in particular, as they would definitely desire high quality estimations on the revenues that such an investment would generate.

On the other hand, annual production forecasts are by no means enough in the case of national grid operators in order to secure electricity supply. For example the Greek Operator of Electricity Market (OEM) is running the domestic electricity market according to the pool model, implementing the Day-Ahead-System (DAS) and dividing the day into 24 hourly periods [37]. This practically means that OEM needs, except from an availability statement of the plant's administrator [37], accurate estimations on the expected production on an hourly basis.

1.6 The Thesis in a Nutshell

Having previously set the ground of RES development importance, CSPPs potential role and the need for their precise modeling, this study goes on with the review of related models building process. For this purpose significant effort is made in determining pros and cons of adopting either a deterministic or a probabilistic approach, while the ability of probabilistic modeling, which is concluded to be the most appropriate for CSPPs, constitutes a typical comparison measure of all modeling tools (programming languages and software) and integrated CSPP models presented afterwards.

Our next concern has been the nature of the input data needed so that a respective model is built, the review of which strengthens our notion of probabilistic modeling appropriateness. The installation site, the equipment and materials used and the plant's set-up and operation objectives are the four main categories in which these data sets could be distinguished.

On the other hand, increased reliability sought in the output of such a model constitutes the development of a new one a rather complex and time-consuming process and certainly far beyond the scope of this study. For these reasons this study utilizes the System Advisor Model, possibly the most highly performing, widely available, CSPP model, by the use of which a hybrid parabolic tough CSPP with thermal storage located in Greece is simulated. Further analysis is executed with respect to the way that installation site, equipment, system's uncertainty and cost affect that plant's performance.

This study ends with the summary of major conclusions and the provision of recommendations to researchers interested in this field.

2 Modeling CSP Plants

In this section we present the three major and consecutive dilemmas faced by someone who aims at estimating the production of a CSP plant, as well as a short review of each one of these options.

2.1 Introduction

Estimating the production of a hybrid CSP plant can be achieved by either spending some extra time and developing a new model from scratch or quitting from tailor-made claims and using an existing one. With regard to the latter option someone can choose between using already available total system models and establishing an improvised model using common programming codes, either exploiting existing component/process sub-models or not; pros and cons do not really change compared to the first dilemma.

Notwithstanding the first and probably the most crucial decision, that has to be reached, concerns the level of uncertainty that someone would like that model to incorporate. Faith to robust variable states leads to adoption of deterministic models while an “everything flows” approach is better supported by probabilistic ones.

2.2 Certainty vs Probability

A mathematical model describes a system by the use of mathematical concepts and language, supporting efforts made for a) system’s logical explanation, b) analysis of its components’ effect and c) estimations on system’s behaviour under different conditions [38]. With regard to the latter, mathematical models are classified, in terms of their variable states, in either deterministic or probabilistic.

The following two subparagraphs provide comprehensive data regarding CSP plant models, classified on the basis on whether they acknowledge or not the inherent uncertainty of the related systems.

2.2.1 Deterministic Models

Deterministic models are distinguished for their consistency as the same deterministic model produces always the same output unless initial conditions (input) change. This derives from the major principle underlying deterministic models according to which each one of the variable states they include are described by unique (central) values based on model's parameters and previous states of these variables.

According to Gelman et al. (2009) [39], models of this class require less effort to be built and are easier to fit and understand. Probably benefits mentioned above have been the main reasons for which until today deterministic models constitute the majority of available modeling tools for CSP plants.

On the other hand, although sensitivity analyses are not excluded in the case of deterministic models, this process is proved to be laborious in the case of large number of parameters, while sensitivities examined may mislead due to interactions among mutually depended parameters [40].

2.2.2 Probabilistic Models

On the opposite side stand probabilistic models, that is to say models which identify and quantify, by the use of probability distributions, uncertainties inherent in a system, and determine their impact in system's performance. This kind of models estimates the confidence and reliability of their results while they perform solid sensitivity analyses identifying the most crucial parameters and processes [40].

This modeling approach requires the completion of three major phases: a) the building of a probability distribution for each uncertain (stochastic) parameter and sampling the corresponding distribution(s), b) running the system model and c) evaluation of the distribution(s) results [41].

a) Stochastic Parameters: Distributions and Sampling

Uncertain parameters are considered to be these for which specific data is not available or variability is expected while the choice of the distribution type that is to be used for each of these parameters is based on actual data, bibliography or personal judgment. Figure 2.1 indicatively presents probabilistic charts and functions of two distributions stratified into 5 equally probable parts.

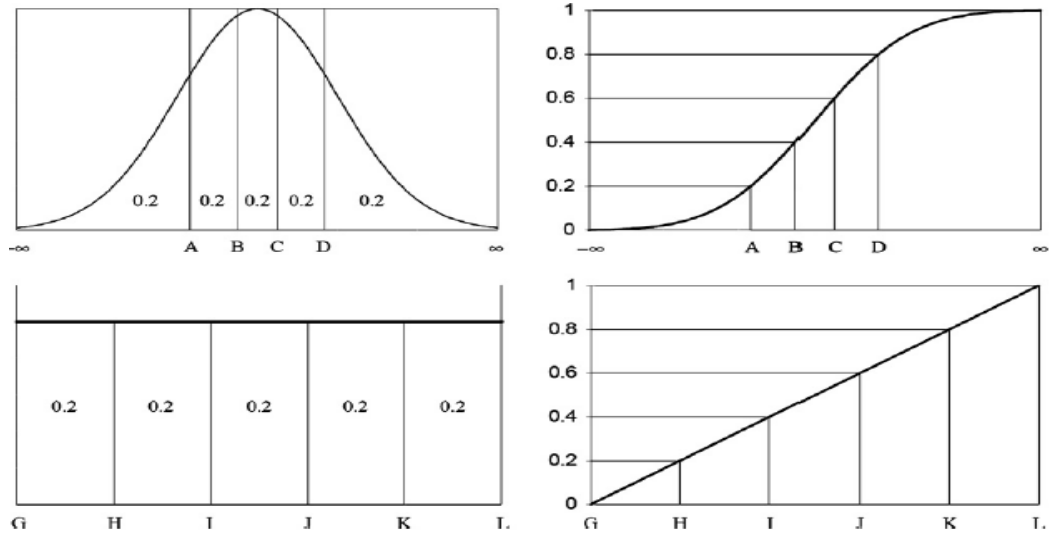


Figure 2.1: Histograms (left) and cumulative distribution functions (right) of parameters with normal (top) and uniform distribution (bottom) [41].

The most common sampling methods for the selected distributions are Monte Carlo and Latin Hypercube Sampling (LHS). Nowadays both these two methods are widely used in sampling, although LHS’s superiority has been pointed out quite many years ago [42]. Please note that the sampling process could also include the pairing of stochastic parameters so that potential correlations among them to be taken into account [43].

As far as the needed number of the samplings per variable is concerned, except from the rule of thumb according to which “the more the better”, there are plenty of related techniques available, depending on each case’s special features [44].

b) Probabilistic System Modeling

Sampled distributions built in the previous phase constitute the input, or a part of it, of a probabilistic model which is run so many times as the distributions are sampled.

Although the abovementioned imply more effort during the model building and running processes, this has to be compared to the added value of model’s results. Notwithstanding, only one out of the five below presented CSP plant models was primarily developed adopting the probabilistic approach.

c) Evaluation of Results

As implied above, probabilistic models return highly valuable results as a) through a cumulative distribution function they indicate the probability that a system achieves a

specific metric and b) by the use of regression, linear or not, the researcher becomes able to rank the impact caused by stochastic parameters to the model outcome.

2.3 Modeling tools

After a decision is reached, on whether counting in uncertainty and evaluating its possible impact on a CSPP performance is important or not, interested researchers may choose among a variety of programming languages and computing environment in order to build a custom-made CSPP model. Below, their major alternatives are reviewed in brief.

2.3.1 Fortran

Fortran is one of the most popular programming languages being mainly applied to numeric computations and scientific computing. Since the 1950's, when IBM developed it, it has repeatedly been evolved – from the structured programming of Fortran 77 to concurrent programming of Fortran 2008, dominating this area [45]. Furthermore Fortran, along with C and C++, seems to constitute maybe the most preferable alternative for scientific codes building thanks to its extended calculating abilities, while it is widely used by engineers seeking for efficiency and high execution speed [46].

Undoubtedly, Fortran is not an ideal programming language suitable for all models as it lacks a user-friendly interactive interface and carries strict and time-consuming processes – calling libraries, declaring dimensions and intrinsic type of variables etc [47]. Still its wide applicability, and specifically in CSPP modeling, can be assessed by the number of codes written in Fortran, such as a) DELSOL – mostly an optical design and performance of heliostat fields code suitable only for tower power systems [48], b) CIRCE – an optics modeling code suitable for both troughs and dishes [49], c) SOLERGY – a total performance CSPP model suitable of tower power systems [50], and d) TRNSYS – an integrated computing package mainly used in the renewable energy and buildings engineering (see 2.4.2).

Fortran can also successfully support probabilistic modeling, a conclusion deriving from the numerous of related models found [51] [52]. Particularly in CSPP modeling, in 2010 Ho et al. [41] presented the SOLERGY Batch Mode. The latter is a program allowing SOLERGY, an initially deterministic model, to run in a probabilistic mode by

introducing an input file containing stochastic parameters and delivering multiply simulated output values – i.e. energy output, LCOE etc.

2.3.2 Mathematica

Moving from single programming languages to integrated computational software programs, Mathematica holds an exceptional position among the latter. Initially developed in 1988 by Wolfram Research, Mathematica is widely used in several areas of technical computing, such as engineering and mathematics. The program is written in Mathematica and C languages and since its first version (ver. 1.0) it has repeatedly been modified being evolved into a powerful computing and analyzing tool with a rich mathematical function library, high compatibility with other programs and languages, advanced visualization abilities and a smart two-part interface (ver. 8.0.4) [53].

Probably these features have been some of the major reasons for which Mathematica is widely used in modeling [54] [55] and particularly in CSPPs. Some of the models developed in Mathematica in the latter field are: a) a thermal energy storage-system model aiming at the facilitation of heat transfer [56], b) a mathematical model arguing that the decarbonation of the energy infrastructure is technically plausible [57], c) a statistical model of hybrid solar power cycles evaluating the capacity and analyzing the performance of thermal storage [58], d) a simulation model estimating the performance of CSPPs with thermal storage [59] and e) a numerical model simulating the base load electricity demand in order a suitable thermal storage system to be sized [60] Last but not least stands the SimulCET, an integrated CSPP performance model (see 2.4.4).

Although none of the models above, except from the SimulCET, counts in uncertainty of the treated variables, Mathematica is capable of supporting a great range of probabilistic modeling [61] [62].

2.3.3 MATLAB

MATLAB is also distinguished for its dual nature as it constitutes both a high-level programming language and an interactive environment, written in C and Java languages, suitable for visualization and complex computations [63]. It was released in 1984 (MATLAB 1.0) by MathWorks and since then it has been updated several times reaching its current form (MATLAB 8). MATLAB has an extended range of applications among of which stand function and data plotting, matrix manipulations and model-

ing, while it can easily interface with other programming languages such as C, Fortran and Java. Furthermore, by the use of MuPAD symbolic engine and Simulink, MATLAB users are allowed to perform symbolic computations, and graphical simulations and model-based designing respectively [64]. It is also notable that a MATLAB code is often significantly shorter than this that a compiled language would generate [65], while it is interpreted when the program is executed, decreasing the execution speed but, freeing the researcher from memory management and allowing dynamic typing and interactive sessions [46].

MATLAB's advantageous features, among which stands its user friendliness with regard to displaying results both graphically and in tabular mode [66], made it highly attractive for both academic and industrial researchers while it is widely applied in solar energy field too [67] [68] [69]. As far as CSPP modeling is concerned, MATLAB is one of researchers' top choices. Pieces of related evidence are: a) a model evaluating the coupling of desalination units to parabolic-trough solar power plants [70], b) a total performance model of a parabolic-trough solar power plant [71], c) a model determining the solar field size of CSPP coupled to a desalination unit [72], d) a model analyzing the levelized energy cost of various CSPPs and locations [73], e) calculation of the solar flux concentration through a solar tower system [74], and f) a model calculating the output of hybrid systems of solar towers with gas turbine [75].

For once more, models and codes referred above do not take into account systems' inherent uncertainties. Nevertheless, MATLAB is definitely suitable for probabilistic modeling [76] [77] [78].

2.3.4 Spreadsheets

Spreadsheets are computer software used in data management and analysis. Their computational attributes combined with their user-friendliness have made them highly popular among computational/modeling tools. Currently plenty of related applications are commercially available although Microsoft Excel, using Visual Basic for Applications as its programming language, has clearly dominated the corresponding market [79]. Probably this has been the reason for which numerous of add-in packages have been developed for this particular application, extending basic version's computational abilities.

Diachronically engineering has been one of the most important boosters of spreadsheets development and blooming due to its advanced computational needs. Indicatively we mention that even the very first spreadsheet application, VisiCalc, was developed for engineering purposes [80]. Some of the CSPP models developed in spreadsheets are: a) EXCELERGY – an integrated model built, by the National Renewable Energy Laboratory (NREL) to simulate solar thermal trough power plants, which is not maintained any more but it has been partially transferred to probably the most popular CSPP integrated model, System Advisor Model (see 2.4.3) [81], b) RETScreen – a performance model used in various renewable technologies (see 2.4.1), c) Dish Field Systems Model – a model estimating the dish/engine systems’ energy performance [82], d) an economics model comparing different reflecting materials in a CSP plant [83], and e) a cost model used to compare concentrated solar-based combined heat and power to alternate technologies [84] .

Finally we underline discretion, provided to researchers building spreadsheet-based models, in selecting between a deterministic or probabilistic mode. Although System Advisor Model is the only spreadsheet-based CSPP model providing such an option, other codes developed in this modeling tool prove its ability to support probabilistic modeling [85] [86] [87] [88]. Particularly in the case of Microsoft Excel, due to limited abilities of its basic version, enhanced management of systems’ uncertainty is achieved by the use of various risk analysis add-in packages [89].

2.3.5 Other Modeling Tools

A. JavaScript: JavaScript is a scripting-language, using syntax similar to this of C language. It was developed by Brendan Eich and its major use is limited in Web browsers, creating advanced interfaces and dynamic websites, although it also used in non-Web applications such as PDF documents [90]. Since JavaScript has only first-class functions, and consequently limited computational abilities, it is not used widely in engineering and the only CSPP model written in this language is SIMPLESYS (see 2.4.1). Despite JavaScript’s ability to incorporate uncertainty into generated models, only one model found to have taken advantage of this attribute [91]. This supports our notion that this programming language is rather not preferable in building demanding computational models.

B. C++: It is a compiled, intermediate-level programming language developed by B. Stroustrup in 1979 at Bell Labs [92]. Being one of the most popular programming languages [93], it is applied on a large number of fields [94], engineering included [95].

Nevertheless, despite its ability to support probabilistic modeling too [96], it seems that it is not really attractive for CSPP modeling as the only model found being written in C++ is the integrated CSPP model “DinaCET” (see 2.4.4).

C. Eclipse: Eclipse IDE (Integrated Development Environment) is open source software supporting multiple programming languages. Initially developed by IBM VisualAge, it is written in Java as it is addressed mainly to Java developers [97]. Eclipse IDE is found to be applied in engineering [98] and limitedly in CSPP modeling too as it was used for the building of “Tonatiuh” – a software package using Monte Carlo ray tracer for the optical simulation of CSPPs [99]. Probabilistic modeling is also included in this software’s features [100].

2.4 Integrated CSP Plant Models

Integrated CSPP models stand at the top of the total-system modeling pyramid, proposed by C. K. Ho and G. J. Kolb [40], as they execute calculations with regard to the overall system performance, while usually they are capable of economics modeling too (Figure 2.2).

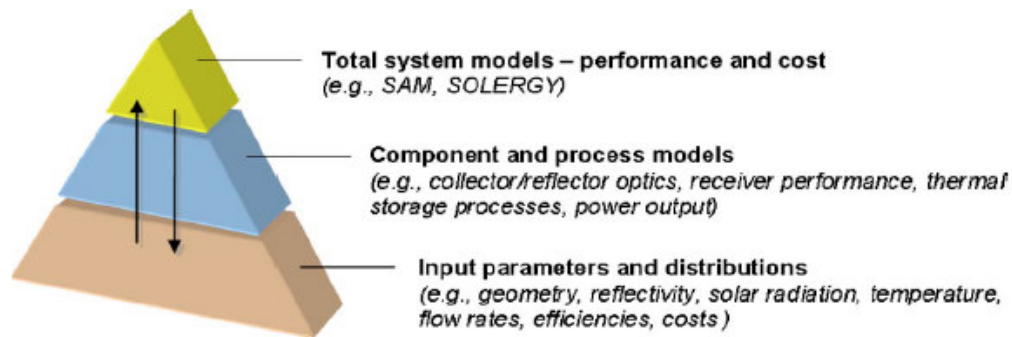


Figure 2.2: The total-system modeling pyramid.

Taking this opportunity it would be meaningful to mention that this approach, partially modified, is also adopted in this study (Figure 2.3): a) in 2.2 we examined the differences between models incorporating uncertainty or not, b) in 2.3 we reviewed some of the major modeling tools available for building, component by component, a total-system model, and c) in this paragraph the most popular ready-to-use integrated CSP models are presented, regardless of their deterministic or probabilistic approach.

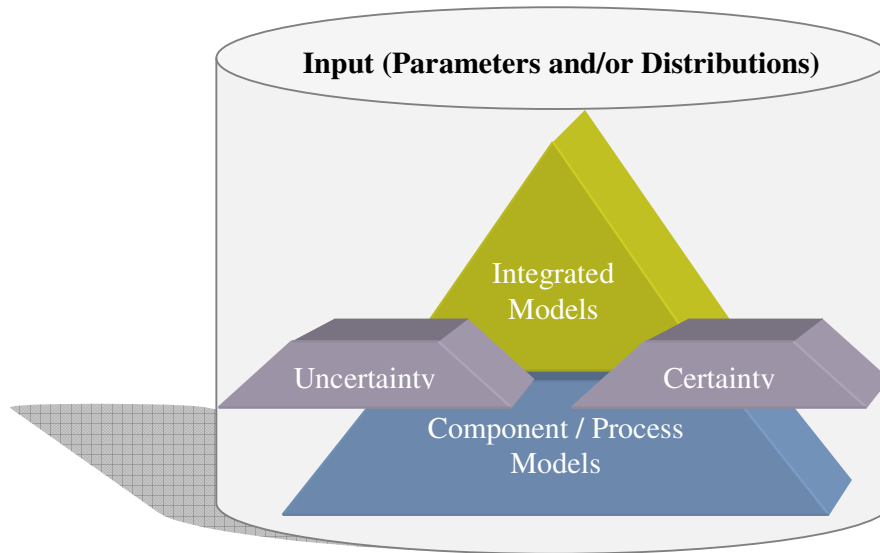


Figure 2.3: A new total-system modeling scheme.

Please note that challenges emerging by the nature of a model’s input are considered to be so highly important, that applicability of information provided in this section becomes meaningful only after thorough examination of variables that are to be counted in by the model (see section 3).

Finally, we justify the number and features of the integrated CSPP models presented below reminding that scope of this study is to model the performance of a hybrid parabolic trough power plant. On this basis, corresponding models applied only to other CSP technologies were neglected.

2.4.1 RETScreen

RETScreen – Clean Energy Project Analysis Software, is a decision support tool calculating energy production and savings, and performing economics and risk analysis with regard to a variety of renewable-energy and energy-efficient technologies, solar thermal power included. This Excel-based software is developed and maintained by the CanmetENERGY research centre and its extended popularity lead to the release of the most recent 4th version [101].

With regard to CSPP modeling, RETScreen provides a single model for all CSP technologies, while there is no provision for a potential coupled storage system. Nevertheless on its start-up sheet (Figure 2.4), the user is able to choose between a single- and a multiple-sources power station, either connected to the grid – with internal load or not, or isolated. The last major user-defined parameter of this sheet is the “heating value ref-

erence” which is related to the cycle of the fuel combustion and particularly to whether the combustion product is condensed or not.

Project information [See project database](#)

Project name	20 MW CSPP
Project location	Crete
Prepared for	IHU
Prepared by	C. Sioumis
Project type	Power - multiple technologies
Grid type	Central-grid & internal load
Analysis type	Method 1
Heating value reference	Higher heating value (HHV)
Show settings	<input checked="" type="checkbox"/>
Language - Langue	English - Anglais
User manual	English - Anglais
Currency	Euro
Units	Metric units

Figure 2.4: The RETScreen start-up sheet.

Climatic data used for the simulation of CSPPs come via the NASA Prediction of Worldwide Energy Resource (POWER) project, developed by NASA's Langley Research Center and CanmetENERGY (Figure 2.5).

The screenshot shows the RETScreen software interface. At the top, there are dropdown menus for Country - region (Greece), Province / State (n/a), and Climate data location (Iraklion (Civ/AFB)). Below these are input fields for Latitude (35,3 °N), Longitude (25,2 °E), and Elevation (39 m). There are also fields for Heating design temperature (6,9 °C), Cooling design temperature (30,2 °C), and Earth temperature amplitude (9,2 °C). A NASA logo is visible in the top right corner.

	Air temperature °C	Relative humidity %	Daily solar radiation - horizontal kWh/m²/d	Atmospheric pressure kPa	Wind speed m/s	Earth temperature °C	Heating degree-days °C-d	Cooling degree-days °C-d
Jan	12,0	68,2%	2,39	101,3	5,2	15,2	186	62
Feb	11,7	66,1%	3,31	101,2	5,6	15,1	176	48
Mar	13,0	65,7%	4,68	101,0	4,9	16,0	155	93
Apr	16,0	62,2%	6,29	100,9	4,4	18,1	60	180
May	19,5	61,4%	7,48	100,8	4,0	21,3	0	295
Jun	23,4	57,6%	8,47	100,7	4,2	24,8	0	402
Jul	25,7	57,9%	8,43	100,5	5,3	26,8	0	487
Aug	25,7	60,5%	7,59	100,5	5,1	27,4	0	487
Sep	23,3	62,8%	6,19	100,9	4,4	25,8	0	399
Oct	20,1	65,8%	4,33	101,2	4,5	22,9	0	313
Nov	16,4	68,0%	2,77	101,2	4,8	19,4	48	192
Dec	13,4	68,9%	2,09	101,2	5,0	16,5	143	105
Annual	18,4	63,8%	5,35	100,9	4,8	20,8	768	3,062
Source	Ground	Ground	NASA	NASA	Ground	NASA	Ground	Ground

Measured at: m, 10, 0

Figure 2.5: The RETScreen standard input climate data.

Nevertheless, users are allowed to enter their own climatic data too (Figure 2.6). Particularly regarding solar radiation, corresponding values refer to solar energy received on average during one day on a horizontal surface for each month.

	Climate data location	Project location
Latitude	35,3	35,3
Longitude	25,2	25,2
Elevation	39	39
Heating design temperature	6,9	
Cooling design temperature	30,2	
Earth temperature amplitude	9,2	

Month	Air temperature	Relative humidity	Daily solar radiation - horizontal	Atmospheric pressure	Wind speed	Earth temperature	Heating degree-days	Cooling degree-days
	°C	%	kWh/m ² /d	kPa	m/s	°C	°C-d	°C-d
January	12,0	68,2%	2,39	101,3	5,2	15,2	186	62
February	11,7	66,1%	3,31	101,2	5,6	15,1	176	48
March	13,0	65,7%	4,68	101,0	4,9	16,0	155	93
April	16,0	62,2%	6,29	100,9	4,4	18,1	60	180
May	19,5	61,4%	7,48	100,8	4,0	21,3	0	295
June	23,4	57,6%	8,47	100,7	4,2	24,8	0	402
July	25,7	57,9%	8,43	100,5	5,3	26,8	0	487
August	25,7	60,5%	7,59	100,5	5,1	27,4	0	487
September	23,3	62,8%	6,19	100,9	4,4	25,8	0	399
October	20,1	65,8%	4,33	101,2	4,5	22,9	0	313
November	16,4	68,0%	2,77	101,2	4,8	19,4	48	192
December	13,4	68,9%	2,09	101,2	5,0	16,5	143	105
Annual	18,4	63,8%	5,35	100,9	4,8	20,8	768	3.062
Measured at	m				10,0	0,0		

Figure 2.6: The RETScreen manual input climate data.

After declaring the above, the user enters values regarding the estimated “internal load” of the CSPP per month, while the last sheet contains the “energy model” (Figure 2.7). The latter requires the completion of a data set regarding a) the base load power system, b) the intermediate load power system, c) the base peak power system and d) the back-up power system. On the same sheet estimated energy delivered to the internal load and to the grid is presented.

Focusing on the modeling of the CSPP we underline that the plant’s estimated output is calculated on the basis of installed power (power capacity) and the capacity factor. Since the latter refers to the ratio of the average power produced by the power plant over a year to its rated power capacity, the software does not handle directly the interaction between the climate data of a specific location and a CSPP’s output while help provided to the user is limited to the provision of a typical capacity factor rate of 20 to 70%. The same applies to other aspects of potential differentiations among CSPPs (see Section 3).

Moreover, although the provision that a power plant uses multiple technologies imply the existence of several interactions among them, surprisingly enough the software adopts a rather simplified approach on this alternative (Figure 2.8) neglecting the auxiliary alternative.

Proposed case power system		Incremental initial costs	
Base load power system			
Technology	Solar thermal power		
Solar thermal power #1			
Power capacity	20,000 kW	20000.0%	
Manufacturer	Abengoa Solar		
Model	PS10		
Capacity factor	50.0%		
Electricity delivered to load	712 MWh	100.0%	
Electricity exported to grid	86.888 MWh		
Intermediate load power system			
Technology	Gas turbine		
Availability	90.0%		7,884 h
Fuel selection method			
Single fuel			
Fuel type	Natural gas - m ³		
Fuel rate	€ / m ³		
Gas turbine #2			
Power capacity	2,000 kW	2000.0%	
Minimum capacity	0.0%		
Electricity delivered to load	0 MWh	0.0%	
Electricity exported to grid	15,788 MWh		
Manufacturer			
Model			
Heat rate	10,000 kJ/kWh		
Fuel required	20.0 GJ/h		
Electricity rate - base case	€ / MWh	0.00	
Fuel rate - proposed case power system	€ / MWh	0.00	
Electricity export rate	€ / MWh		
Electricity rate - proposed case	€ / MWh		
Operating strategy			
Full power capacity output	0 MWh	15,788 MWh	0 MWh
Power load following	0 MWh	0 MWh	0 MWh
Power system fuel	43,800 MWh	0 MWh	0 MWh
Operating profit (loss)	€	0	0
Efficiency	%	36.0%	
Remaining electricity required	MWh	0	0
Select base load power system	Power system #1	Solar thermal power #1	
Select operating strategy	Full power capacity output		

Proposed case system characteristics	Unit	Estimate	%	Incremental initial costs	System design graph
Power					
Base load power system					
Technology	Solar thermal power				
Operating strategy	Full power capacity output				
Capacity	kW	20,000	20000.0%		
Electricity delivered to load	MWh	712	100.0%		
Electricity exported to grid	MWh	86.888			
Electricity delivered to load	MWh	0	0.0%		
Intermediate load power system					
Technology	Gas turbine				
Operating strategy	Full power capacity output				
Capacity	kW	2,000	2000.0%		
Electricity delivered to load	MWh	0	0.0%		
Electricity exported to grid	MWh	15,788			
Peak load power system					
Technology	Grid electricity				
Suggested capacity	kW	0.0			
Capacity	kW	1,000	1000.0%		
Electricity delivered to load	MWh	0	0.0%		
Back-up power system (optional)					
Technology					
Capacity	kW	0			

Proposed case system summary	Fuel type	Fuel consumption - unit	Fuel consumption	Capacity (kW)	Energy delivered (MWh)
Power					
Base load	Solar	m ²	0	20,000	712
Intermediate load	Natural gas	m ³	4,206,066	2,000	0
Peak load	Electricity	MWh	0	1,000	0
Electricity exported to grid					102,656
Total				23,000	103,368

Figure 2.7: The RETScreen energy model sheet.

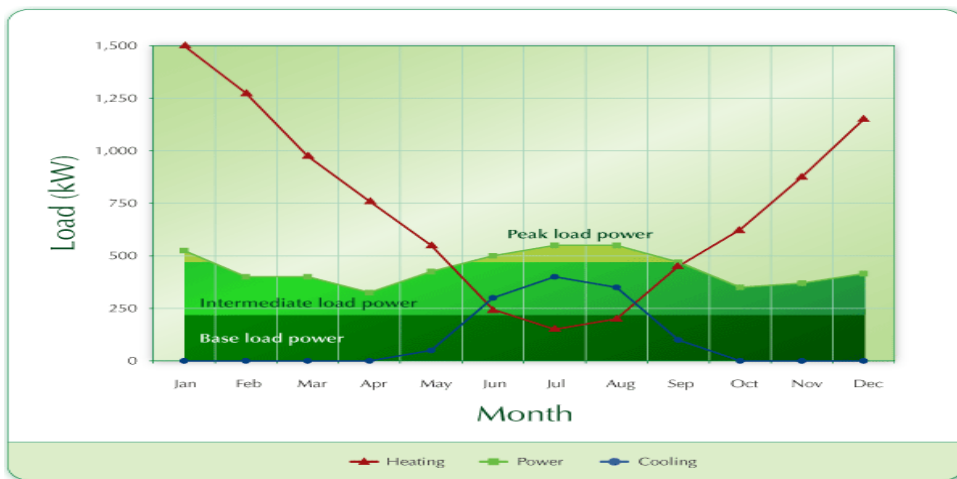


Figure 2.8: The RETScreen Power System Load Definition – Base, Intermediate & Peak.

Finally, it might be helpful to notice that all RETScreen energy models are deterministic despite that feasibility analysis performed includes an important level of risk analysis too. Probably weaknesses mentioned above are the main reasons for which RETScreen does not seem to stand among the top choices for CSPP modeling.

2.4.2 TRNSYS

TRNSYS is a software platform enabling users, through a modular structure, to simulate the performance of transient systems and particularly solar energy systems [102]. Its engine, the typical component library, is written in Fortran while users may add their custom-made components developed also in Fortran, C, C++ or any other language creating a DLL [103]. TRNSYS was developed at the University of Wisconsin [104], became commercially available in 1975 and today is maintained by the collaboration of four entities based in US, France and Germany [105]. In the rest of this paragraph we will provide short information on the process followed in order a CSPP model is built in TRNSYS 17.

So, after the design of the system to be modeled is completed, the user needs to decide the components that will be used in the simulation, to add them in the TRNSYS Simulation Studio and to configure them. Simulation Studio is one of the core modules of TRNSYS including numerous tools such as simulation engine and graphical connection programs as well as plotting and spreadsheet software.

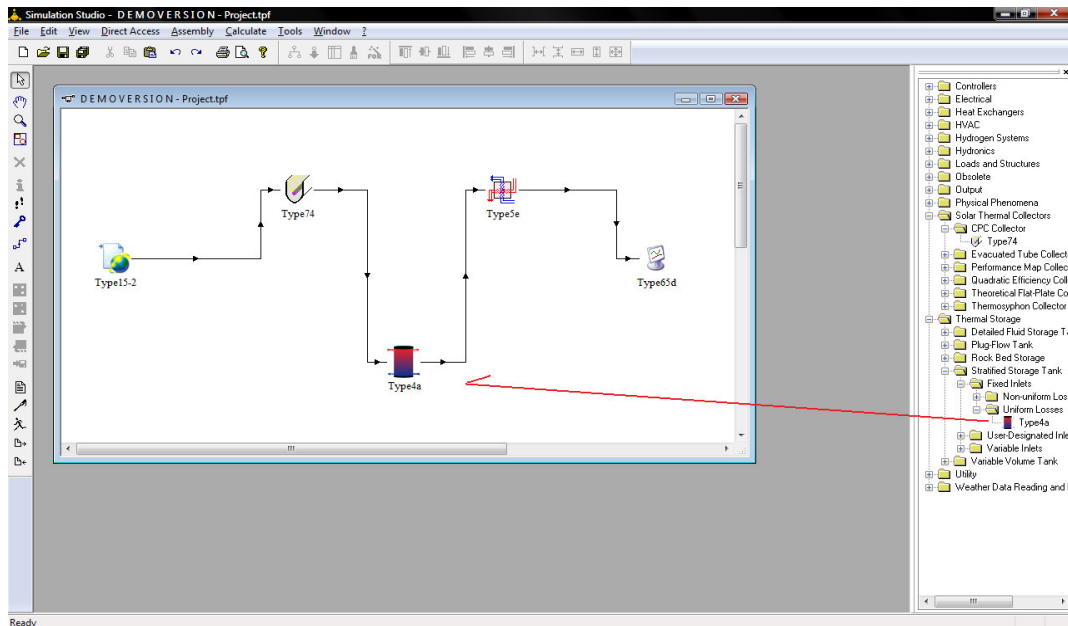


Figure 2.9: The TRNSYS Simulation Studio start-up sheet.

As Figure 2.9 presents, creating a new model on this module starts from a blank sheet on which users are enabled to drag and drop ready to use but also further configurable components, either included in the default TRNSYS library or custom-made by the users.

In the case i.e. of a simplified¹ parabolic trough CSPP with thermal storage, the first component comes from the category “Weather Data Reading and Processing”. TRNSYS library contains more than 1.000 related files concerning more than 150 countries, containing almost 60 kinds of related output data – temperature, wind, solar radiation etc (Figure 2.10), although users can create their own files too. Moreover this kind of components count in adjustable parameters such as the CSPP tracking mode, the ground reflectance etc (Figure 2.10).

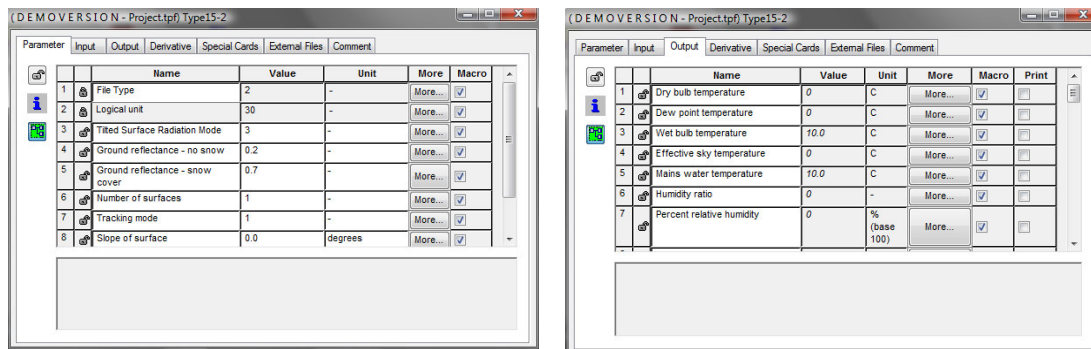


Figure 2.10: a) Left – Adjustable parameters, b) Right – Component output data categories.

Secondly we add the component handling the solar collectors. In this case among the 13 related parameters stand the number of series, the collector area and the fluid specific heat while component’s output is limited to outlet temperature and flow rate and useful energy gain. This time users are enabled to interfere with a set of 12 kinds of input data processed by this component too, as another one stands right before this – the “Weather Data Reading and Processing” component. The same rationale applies to the rest two components – “Thermal Storage” and “Heat Exchanger”, which also enable users to choose among and adjust plenty of parameters and input and output data.

After the insertion of one component into the project sheet, the user takes care of linking it with other already added components. Figure 2.11 indicatively shows a related

¹ Due to the fact that the TRNSYS version used is a demo-version, the presented project could not include more than five components. Due to this fact analysis ends at the exit of the heat exchanger.

screen and particularly some of the connections between the output of the “Weather Data Reading and Processing” component and the input of the “Solar Collector” component. Obviously these linkages are essential for the establishment of data flow and the execution of the respective calculations. After all appropriate links have been set, model’s operation can be simulated and the results are shown online and/or printed in a file (Figure 2.12).

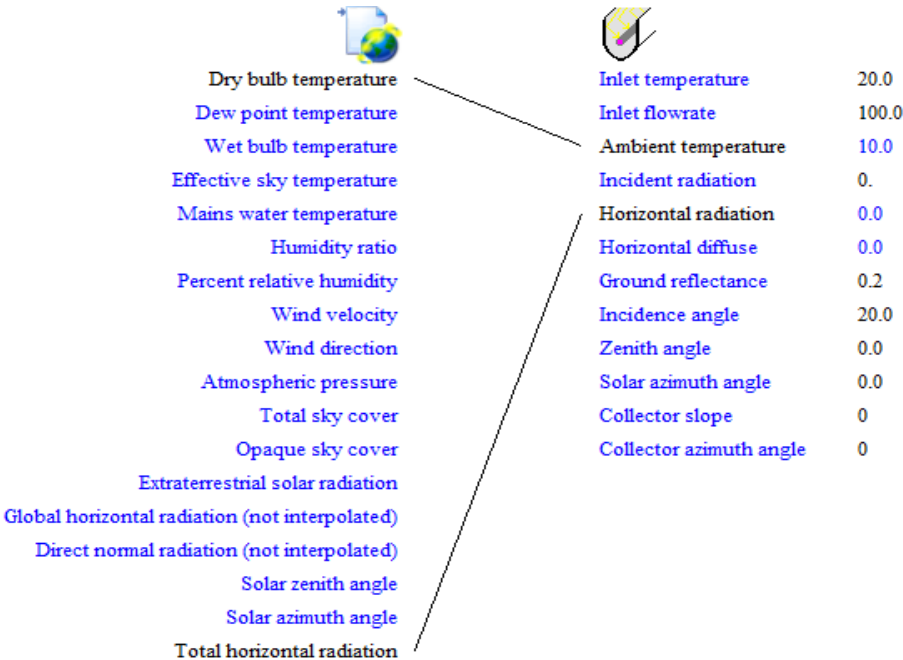


Figure 2.11: The TRNSYS screen for the linkage of two components.

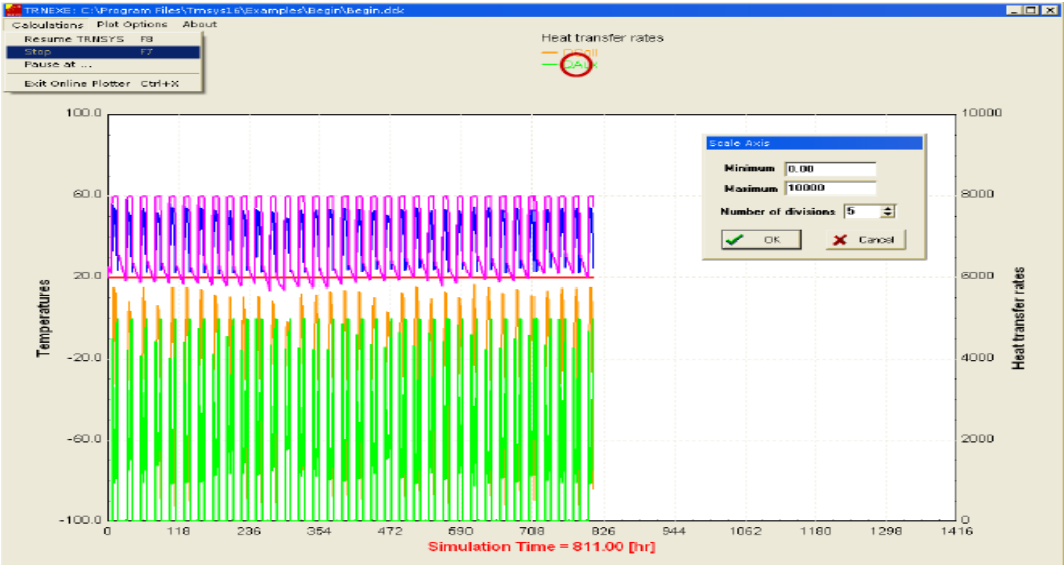


Figure 2.12: The TRNSYS online result plotter.

Summarizing the impression left by this short review of TRNSYS, we underline a) the user-friendliness, b) its extended capabilities – particularly regarding the way it handles step-like time functions despite the fact that example above did not demonstrate them, c) its wide adjustability to a wide range of needs and d) interactivity with plenty of other programs and programming languages. On the other hand we cannot neglect that TRNSYS requires highly detailed input data in order that expected plant performance is reliably calculated and that it does not support probabilistic modeling. In any case, the large number of CSPP models built in TRNSYS is considered to be a well-established proof of its value [74] [81] [106] [107] [108] [109] [110].

2.4.3 System Advisor Model

System Advisor Model (SAM), originally called the “Solar Advisor Model”, is one of the most recognizable integrated CSPP models. Although SAM is an Excel-based software, we should not neglect that it keeps wrapping around TRNSYS for the CSPPs energy performance simulation. Having been developed by the National Renewable Energy Laboratory in cooperation with Sandia National Laboratories in 2005, the model is regularly maintained and updated reaching its current form (Version 2012.5.11) [111].

Starting a new simulation of a parabolic trough CSPP in SAM, users are enabled to choose between two kinds of models - a physical and an empirical one. The former estimates the plant’s performance counting in first principles of engineering and thermodynamics while the latter uses a set of equations formed through the exploitation of data gathered from the SEGS projects in the USA.

After the desired model is initialized, the first sheet that is to be completed concerns climate data. Please note that respective data is not entered as stand-alone values but as a file (TM2, TM3 or EPW), coming from either SAM library or a user-defined location. Direct normal radiation, dry-bulb temperature, atmospheric pressure and wind speed are some of the data elements that such a file includes while all of the respective values refer to hourly time-spaces. Summary of the data contained in input files can be displayed by the use of SAM’s Weather Data Viewer, a module enabling the generation of several types of graphs such as time series, heat map, monthly profile and duration curve.

The next sheet, called “Annual Performance”, requires the completion of two cells: a) the estimated system degradation caused by system aging and b) the availability expected counting in regular and contingent outages.

Having completed the above, let's say preliminary, sheets, users start configuring the vital parts of a parabolic trough CSP starting with the solar field. Values needed in this particular sheet are distinguished in several categories such as the solar field parameters, the heat transfer fluid and the design point (Figure 2.13). What is important to mention is that users are enabled either to enter a solar multiple looking for the total required aperture and number of loops or vice versa.

Solar Field Parameters

Option 1: Solar multiple

Option 2: Field aperture m²

Row spacing m

Stow angle deg

Deploy angle deg

Number of field subsections

Header pipe roughness m

HTF pump efficiency

Freeze protection temp °C

Irradiation at design W/m²

Allow partial defocusing

Heat Transfer Fluid

Field HTF fluid

User-defined HTF fluid

Design loop inlet temp °C

Design loop outlet temp °C

Min single loop flow rate kg/s

Max single loop flow rate kg/s

Min field flow velocity m/s

Max field flow velocity m/s

Header design min flow velocity m/s

Header design max flow velocity m/s

Design Point

Single loop aperture <input type="text" value="3762.4"/> m ²	Actual number of loops <input type="text" value="230"/>
Loop optical efficiency <input type="text" value="0.744601"/>	Actual aperture <input type="text" value="865352"/> m ²
Total loop conversion efficiency <input type="text" value="0.716894"/>	Actual solar multiple <input type="text" value="2"/>
Total required aperture, SM=1 <input type="text" value="431859"/> m ²	Field thermal output <input type="text" value="588.235"/> MWt
Required number of loops, SM=1 <input type="text" value="114.783"/>	

Collector Orientation

Collector tilt deg Tilt: horizontal=0, vertical=90

Collector azimuth deg Azimuth: equator=0, west=90, east=-90

Mirror Washing

Water usage per wash L/m²,aper.

Washes per year

Plant Heat Capacity

Hot piping thermal inertia kWh/K-MWt

Cold piping thermal inertia kWh/K-MWt

Field loop piping thermal inertia Wh/K-m

Land Area

Solar Field Area acres Non-Solar Field Land Area Multiplier Total Land Area acres

Single Loop Configuration

Note: The specification below is only for one loop in the solar field.
Usage tip: To configure the loop, choose whether to edit SCA's, HCE's or defocus order. Select assemblies by clicking one or dragging the mouse over multiple items. Assign types to selected items by pressing keys 1-4.

Number of SCA/HCE assemblies per loop: Edit SCAs Edit HCEs Edit Defocus Order

SCA: 1	SCA: 1	SCA: 1	SCA: 1	SCA: 1	SCA: 1
HCE: 1	HCE: 1	HCE: 1	HCE: 1	HCE: 1	HCE: 1
DF# 8	DF# 7	DF# 6	DF# 5	DF# 4	DF# 3
				SCA: 1	SCA: 1
				HCE: 1	HCE: 1
				DF# 1	DF# 2

Figure 2.13: SAM Solar Field Sheet.

The following two sheets particularize variables related to the solar collectors and receivers enabling users to incorporate sufficient details in their models, while next

comes the configuration of the power cycle which may also be coupled with a fossil backup boiler (Figure 2.14)

Plant Capacity	
Design gross output	111 MWe
Estimated gross to net conversion factor	0.9
Estimated net output at design (nameplate)	100 MWe
Note: Parasitic losses typically reduce net output to approximately 90 % of design gross power	

Power Block Design Point	
Rated cycle conversion efficiency	0.3774
Design inlet temperature	391 °C
Design outlet temperature	293 °C
Boiler operating pressure	100 bar
Fossil backup boiler LHV efficiency	0.9
Steam cycle blowdown fraction	0.02

Plant Control	
Low resource standby period	2 hrs
Fraction of thermal power needed for standby	0.2
Power block startup time	0.5 hr
Fraction of thermal power needed for startup	0.2
Minimum required startup temp	300 °C
Max turbine over design operation	1.05
Min turbine operation	0.25
Turbine Inlet Pressure Control	Fixed pressure

Cooling System	
Condenser type	Evaporative
Ambient temp at design	20 °C
Ref. Condenser Water dT	10 °C
Approach temperature	5 °C
ITD at design point	16 °C
Condenser pressure ratio	1.0028
Min condenser pressure	1.25 inHg
Cooling system part load levels	2
Note: Hybrid dispatch control parameters refer to the dispatch periods defined on the thermal storage page.	

Hybrid Dispatch	
Period 1:	0
Period 2:	0
Period 3:	0
Period 4:	0
Period 5:	0
Period 6:	0
Period 7:	0
Period 8:	0
Period 9:	0

Figure 2.14: SAM Power Cycle sheet.

Close to the end stands the completion of the “Thermal Storage” sheet, in which users also define whether the fossil backup system a) aims at a minimum backup level or b) operates supplementary. In most cases the second option fits better in grid connected CSPPs with a PPA (Figure 2.15).

Storage System	
Full load hours of TES	6 hr
Storage volume	26268.7 m ³
TES Thermal capacity	1764.71 MWt
Parallel tank pairs	1
Tank height	20 m
Tank fluid min height	1 m
Tank diameter	40.894 m
Min fluid volume	1313.43 m ³
Tank loss coeff	0.4 W/m ² -K
Estimated heat loss	0.500115 MWt
Cold tank heater set point	250 °C
Hot tank heater set point	365 °C
Fossil dispatch mode	Supplemental operation
Aux heater outlet set temp	391
Tank heater capacity	25 MWt
Tank heater efficiency	0.98
Hot side HX approach temp	5 °C
Cold side HX approach temp	7 °C
Heat exchanger derate	0.877551
Initial TES fluid temp	300 °C
Storage HTF fluid	Solar Salt
User-defined HTF fluid	Edit...
Fluid Temperature	342 °C
TES fluid density	1872.49 kg/m ³
TES specific heat	1.50182 kJ/kg-K

Figure 2.15: SAM Thermal Storage sheet.

Having completed the last sheet, referring to internal loads, too, users are enabled to choose among a large set of simulation options such as parametric and sensitivity analysis, optimization etc. Probabilistic modeling is also supported as SAM may generate histograms showing the frequency distribution of selected output values counting in as input the distribution followed by one or more variables (Figure 2.16).

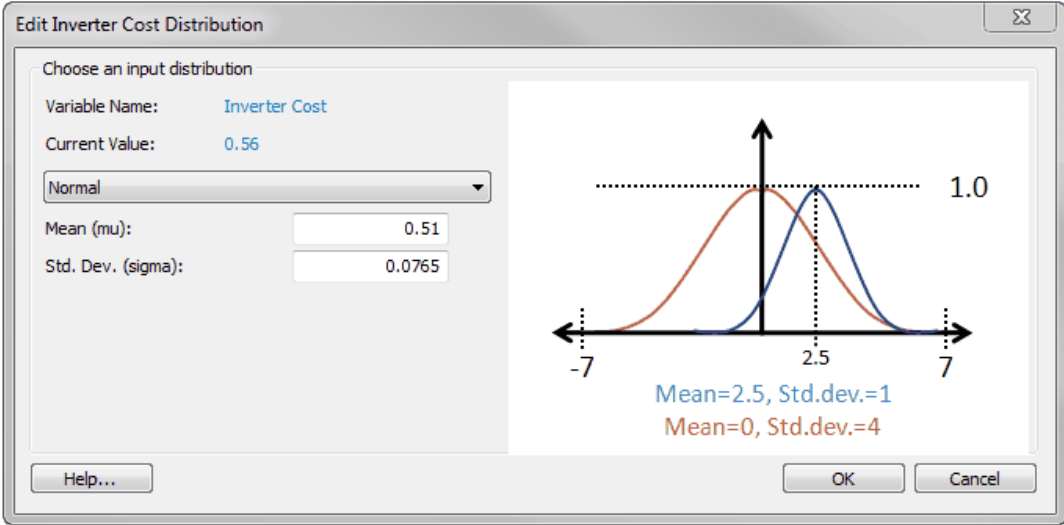


Figure 2.16: The insertion module of a variable containing uncertainty.

Obviously this software’s holistic approach on parabolic trough CSP plant modeling has been the ground on which several researchers were based in order to develop their custom-made SAM models [112] [113] [114] [115] [116] [117].

2.4.4 Other Integrated CSPP Models

A. SIMPLESYS: SIMPLESYS is an oversimplified Web-based model and not surprisingly the programming language used is JavaScript. It utilizes an instantaneous energy balance and a constant-temperature control system providing estimations on the thermal output of a CSP system with storage, regardless of the CPS technology used [118]. In order that a CSP plant operation is simulated, the user fills in estimated values with regard to the features shown in Figure 2.17.

Rate of Energy Demand (QL) - (kW) =	<input type="text" value="150"/>
Maximum (noon) Collector Field Output (CM) - (kW) =	<input type="text" value="500"/>
Energy to Heat-up Field Piping (EP) - (kWh) =	<input type="text" value="200"/>
Rate of Energy Loss from Field Piping (QF) - (kW) =	<input type="text" value="10"/>
Storage Capacity (SM) - (kWh) =	<input type="text" value="500"/>
Energy Initially in Storage (ES) - (kWh) =	<input type="text" value="0"/>
Rate of Energy Loss from Storage (SL) - (kW) =	<input type="text" value="10"/>
System Turn-on Time (h) =	<input type="text" value="0"/>
System Turn-off Time (h) =	<input type="text" value="24"/>
Number of Days to Run This Simulation =	<input type="text" value="3"/>

Figure 2.17: The SIMPLESYS energy model.

Although the model is useful for preliminary calculations and may be further refined in order to take also into account more variables and to estimate the electrical output, it definitely falls short compared to analysis quality provided by other CSPP modeling software.

B. SimulCET: SimulCET is a Mathematica-based software package developed by the National Renewable Energy Centre of Spain (CENER) exclusively for the assessment of parabolic trough CSPPs’ performance. In the above framework this modeling program, based on both empirically and physically derived correlations, analyzes the impact of different operational strategies on the expected outcome as well as the way that gas utilization and thermal storage affect a CSPP’s energy performance [119]. Although SimulCET is not widely commercially available, it seems that except from CENER, privately held companies also take advantage of its limitedly promoted fea-

tures [120], among of which probabilistic modeling stands prominently [121]. As we did not have the chance to be directly engaged with this software package, this review is limited in the provision of a few program’s screenshots found in other sources (Figures 2.18 & 2.19).

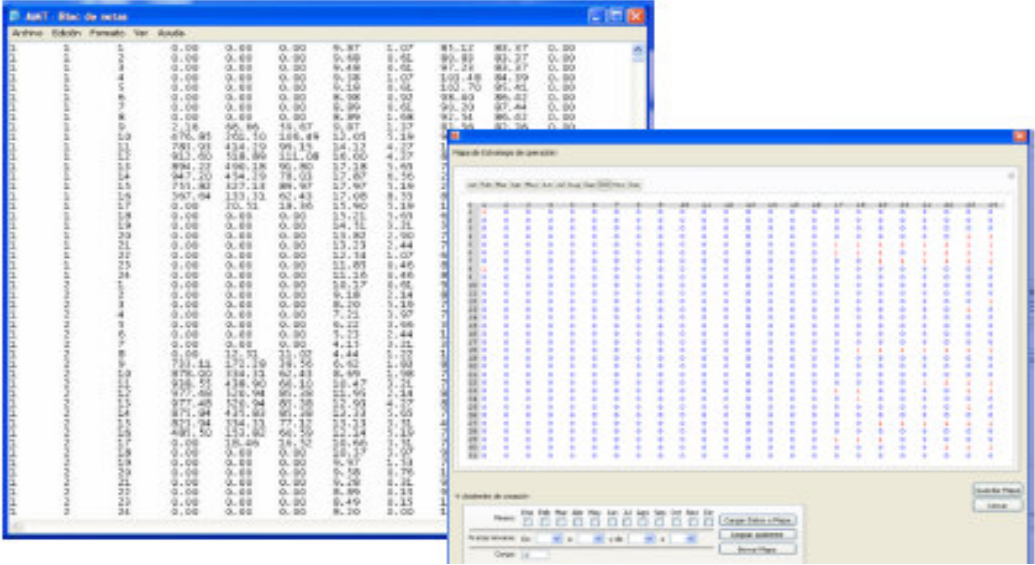


Figure 2.18: The “Climate” data input tabs [122].

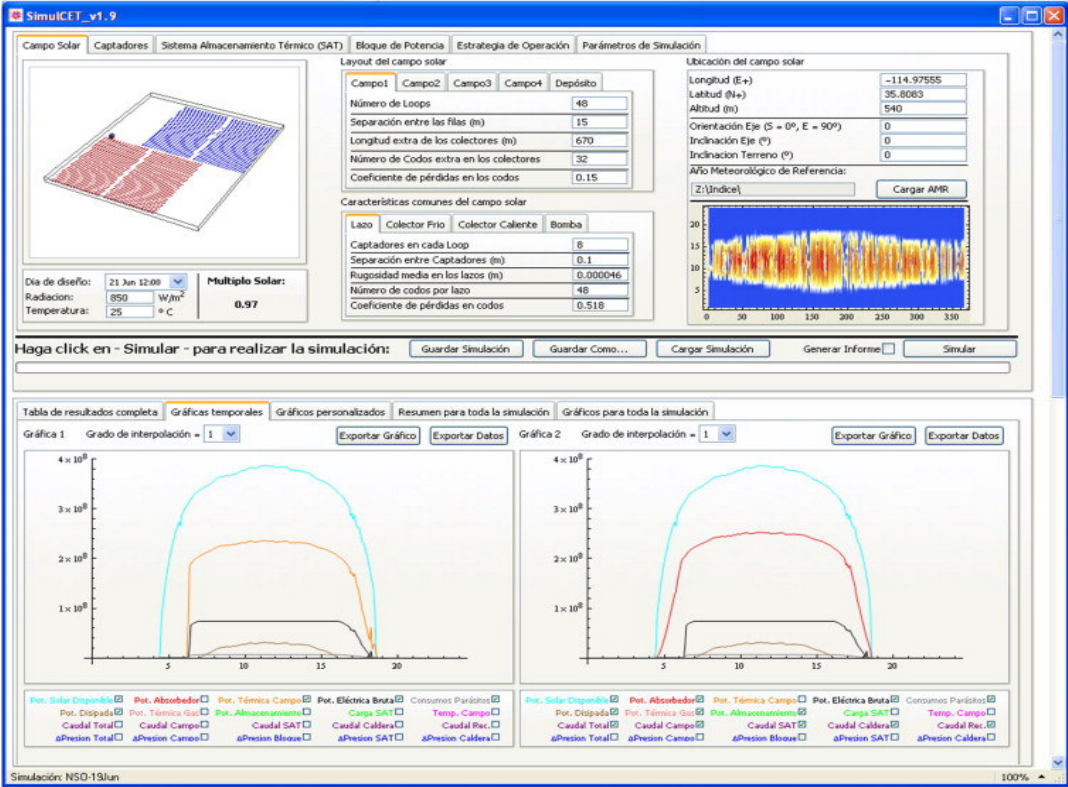


Figure 2.19: The “Solar field” data input tab and the “Time Graphics” results tab [123].

C. DinaCET: DinaCET is a computer tool enabling users to develop stand-alone dynamic programs simulating the performance of parabolic troughs CSPPs. Written in C++, it produces codes in the same language, each of which can simulate only a specific plant. Despite this rigidity, generated models still look attractive as they enable users to model a large set of variables and operational transient alternatives for each specific plant. Last but not least we notice user-friendliness provided by the 3D Graphic User Interface [123]. Having already been validated through its comparison to data gathered from Nevada solar one power plant [124], it is not used exclusively by CENER [120]. Nevertheless, the fact that DinaCET is not publicly available, this short review ends with the following screenshots found in other secondary sources (Figures 2.20 & 2.21).

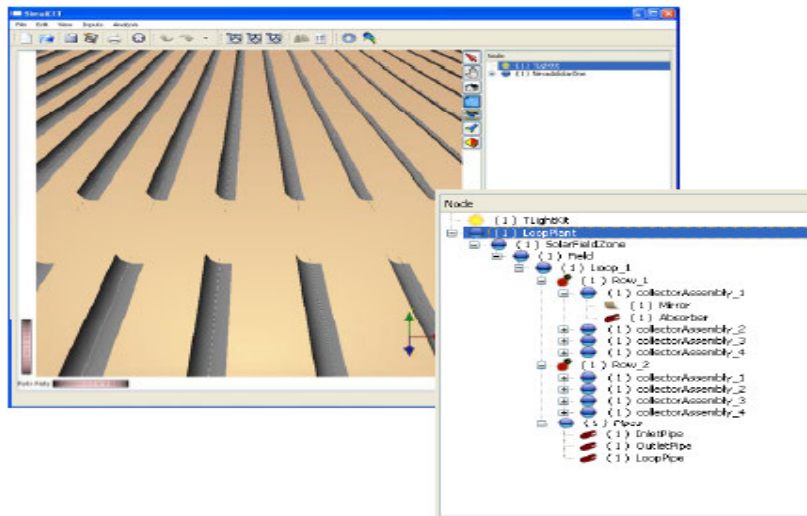


Figure 2.20: DinaCET's solar field simulation sheet [122].

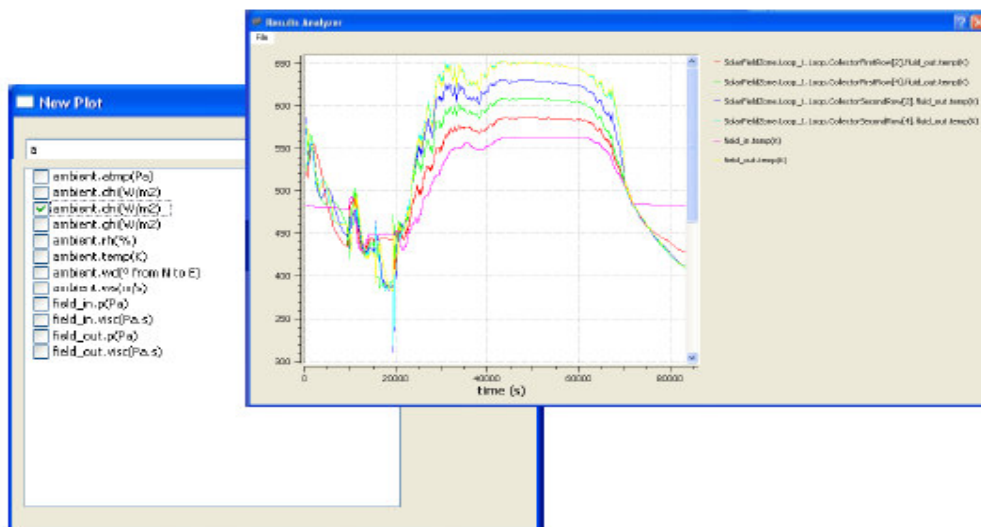


Figure 2.21: DinaCET's simulation of a cloudy day operation [122].

3 Challenges on Modeling a Parabolic Trough CSP Plant

The scope of this section is to illustrate the needs, restrictions and specificities that derive from the input required in the modeling of a parabolic trough CSPP (Figure 2.3). After a clear view on the above is formed, researchers are enabled to choose among modeling tools presented in Chapter 2.

3.1 Introduction

The operation principle of a parabolic trough CSP plant may vary depending on four major factors: a) the coupling of a thermal energy storage system or not, b) the usage of a fossil fuel-fired boiler or not, c) the choice between an intermediate heat transfer fluid (HTF) and the direct production of steam² and d) the objectives of its operation (i.e. performance optimization, LCOE minimization, energy safety etc).

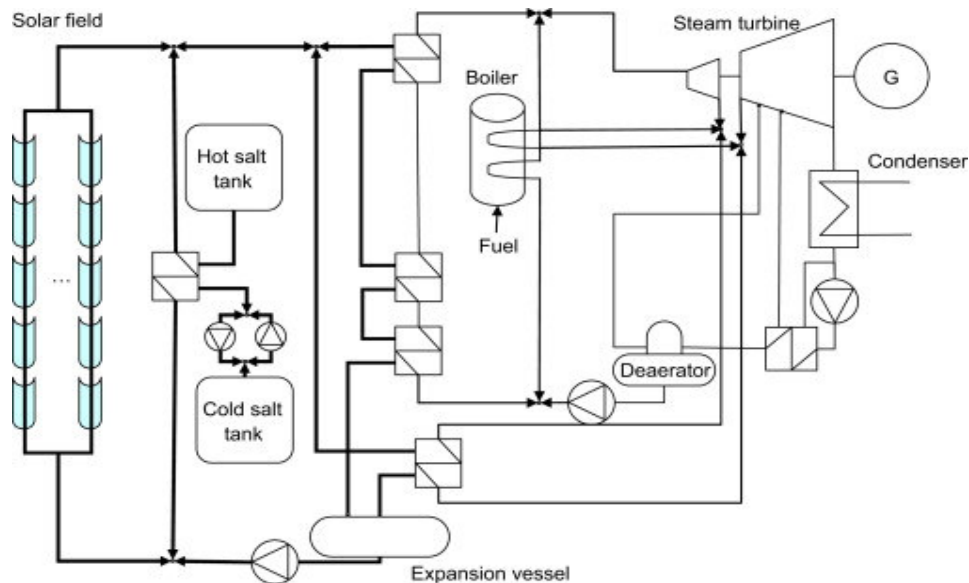


Figure 3.1: Diagram of a hybrid parabolic trough with thermal storage [126].

² Due to the current lack of commercial maturity of the direct steam generation technology [125], dataset determined in this section takes into account only CSPP using an intermediate heat transfer fluid.

As the latter do not necessarily affect a CSPP's components but rather their features and positioning in the respective flow chart, Figure 3.1 shows a typical diagram of probably the most complex combination of these factors, that is a hybrid parabolic trough CSPP with thermal storage and a HTF.

Transforming the above schematic diagram into an power balance flow chart we conclude in Figure 3.2, which in brief determines that a) solar power is reaching the solar field (CSP system) (Q_R); b) this power is partially rejected (Q_{Rj}) and partially further exploited (Q_0); c) Q_0 reaches, reduced due to transfer loses, the power block (Q_1) and/or the energy storage system (Q_2) according to current needs d) power delivered to power block (Q_L), directly from the solar field (Q_1) and/or the energy storage system (Q_3) and/or a fossil fuel supplement (Q_F), is transformed to electric power.

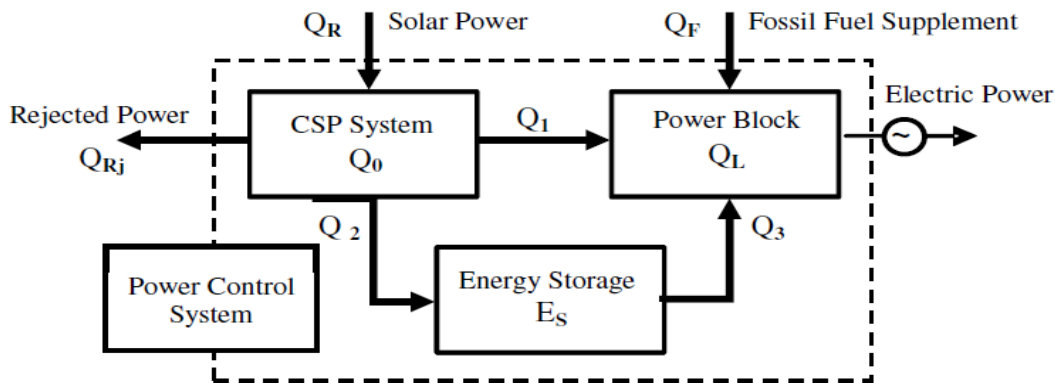


Figure 3.2: Power flow chart of a hybrid parabolic trough with thermal storage [60].

Taking as granted that a CSPP model's objective is to perform calculations based on the power flows and components shown above, we adopt an approach, similar to that proposed by Garcia et al [59], according to which five main categories of data are needed for this process to be executed: a) the geography of the installation site, b) climatic data of the site, c) data and characteristics of the solar field, d) operation principle and features of the thermal energy storage system and e) characteristics of the power cycle and auxiliary equipment. As a result, in the following pages we try to address the most important issues related to the gathering and process of the data mentioned above, partially based on two highly recognized bibliographic works [127] [128]. It should be noted that the following dataset is indicative as it is strongly related to the sophistication level of the model to be built.

3.2 Installation Site

Starting with the calculation of the power reaching the solar field, three main sets of values should be taken into account: a) the relative position of the sun, b) the atmospheric attenuation and c) external shading.

3.2.1 Sun Relative Position

Functions applied in estimating the position of the sun in relation to the installation site require a large set of data, only three pieces of which differ from site to site when both are located on Earth: a) **latitude**, b) **longitude** and c) **time zone**. Obviously values given to the latter cannot be disputed due to its standardization [129], while errors possibly incorporated in the chosen geographical coordinates may easily be considered to be trivial in the case of CSPP modeling [130].

3.2.2 Atmospheric Attenuation

Solar power reaching the earth's surface is partially reduced compared to that entering the atmosphere because some components of the latter tend to scatter, reflect and/or absorb it. These solar power losses depend on a) the ozone layer thickness, b) the distance traveled through the atmosphere before reaching that site, c) the amount of air haze and d) the extent of the cloud cover. As all of these factors could be considered as a function of the site's **elevation**, we determine the latter as another needed input data of a CSPP model. This assumption is partially validated by a research concluding in certainly non-negligible correlations between the annual average direct normal irradiance (DNI) and the aerosol optical depth (AOD) as well as between the latter and the elevation (see Figures 3.3 and 3.4) [131]. It should be noted that uncertainties included in elevation measurements could be treated similarly to that of geographical coordination.

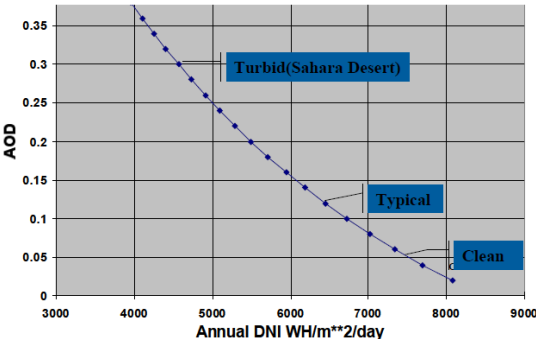


Figure 3.3: DNI as a function of AOD [131].

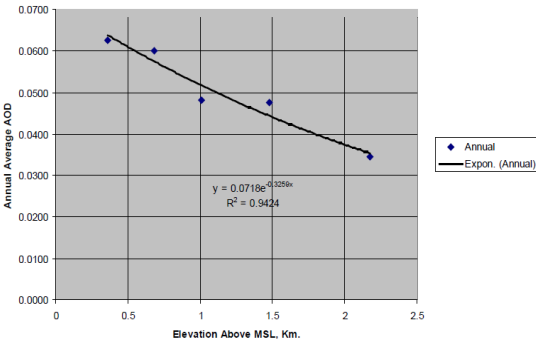


Figure 3.4: AOD as a function of elevation [131].

3.2.3 External Shading

This term is used to describe shading caused to a site by factors other than CSPP's components, such as trees, mountains, buildings etc. Additional data needed, in order to count in solar power losses caused in these cases, include **obstacles'** a) **height** and b) **positioning** compared to the site, c) **length** (its projection to the east-west axis), d) **azimuth** and e) **distance** from the site. Once more, respective values' uncertainty may be considered to be trivial (par. 3.2.1).

3.3 Climate

Another large set of input data required for the modeling of a CSPP concerns weather conditions of the installation site. This data set, usually provided as a Typical Meteorological Year (TMY) [132], enables users to complete the estimation of solar power reaching the solar field while they initiate calculations related to other CSPP power flows. We distinguish related input in a) solar and b) non-solar weather information and, despite the lack of respective bibliographic validation, we feel safe to assume that the former contributes significantly more than the latter in the modeling of a CSPP. This assumption could definitely help researchers in climatic data gathering, assessment and processing as we should not neglect that weather estimations depend on past, either short- or long-term, observations which is likely not to be validated in the years to come due to measurement uncertainties and/or lack of representativeness. The fact that measurement uncertainty analysis has been highly formalized is provided as a piece of related documentation [133].

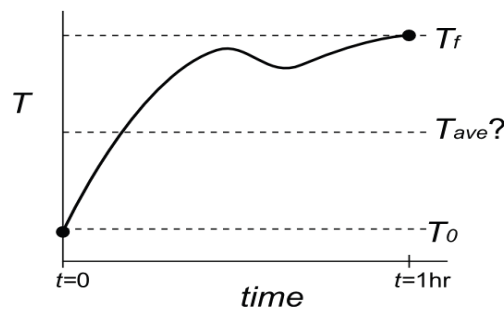


Figure 3.5: An example in which neither the final nor the average of initial and final temperature provides a reliable representation of the temperature over the time step [135].

Furthermore, researchers aiming at accurate CSPP modeling should take into account that a CSPP operates transiently. This makes the temporally stepwise modeling

necessary, while the time step needed is inversely related to accuracy sought (Figure 3.5) [134] [135]. Nowadays climatic data with a temporal resolution of one minute can be found [136], the use of which could enhance results accuracy compared to, the most commonly used, hourly data sets.

3.3.1 Solar Data

The carrier of solar power reaching a CSPP's solar field is the solar radiation which, with regard to solar energy conversion technologies, is distinguished in three fundamental components: a) the **direct normal irradiance (DNI)** being available directly from the solar disc, b) the diffuse horizontal irradiance (DHI) deriving from scattered radiation in the sky dome, DNI excluded, c) the albedo irradiance deriving from ground effects and d) the global horizontal irradiance (GHI) representing the geometric sum (counts in the solar azimuth angle) of the above two components.

CSPPs exploit only DNI which can also be calculated in the case that values of DHI, GHI and albedo ratio are available.

3.3.2 Non-solar Data

Dry-bulb temperature contributes in the calculation of the power losses incurred in the HTF piping system and the thermal energy storage system, and the heat power rejected in a condenser performing either wet or dry cooling. On the other hand **wet-bulb temperature** is used only in the case of wet cooling. Alternatively, wet-bulb temperature can be calculated by psychrometric charts combining dry-bulb temperature, dew-point temperature and relative humidity [137].

Atmospheric pressure is also used in calculations performed in order to calculate power losses incurred in the HTF piping system and power rejected in a wet or dry cooling condenser.

Finally, the contribution of **wind velocity** and **direction** is limited in supporting the more accurate estimations regarding power losses incurred in the HTF piping system.

3.4 Solar Field

Estimating the power output of the solar field requires input of several datasets related to a) its layout, b) the solar collector assemblies (SCAs), c) the heat collection element (HCE) and d) the heat transfer fluid.

3.4.1 Lay-out

A typical solar field is consisted of a, divisible by 2, number of subfields connected in parallel while the latter are formed by a certain number of SCAs loops connected also in parallel. A SCAs loop is derived from SCAs connected in series and SCAs are made from modules also connected in series. As a result, related input data needed is the **number of subfields**, the **number of SCAs loops of each subfield**, the **number of SCAs for each loop** and the **number of solar collector elements (SCEs)** in each SCA (Figure 3.6) [138]. The need of more than one subfield formation is grounded on the objective of minimizing pumping pressure losses [135]. Finally, in order to calculate shading from one row of SCAs to another, the **distance between them** is needed to be determined. Obviously we consider all of the above input data as free of uncertainties.

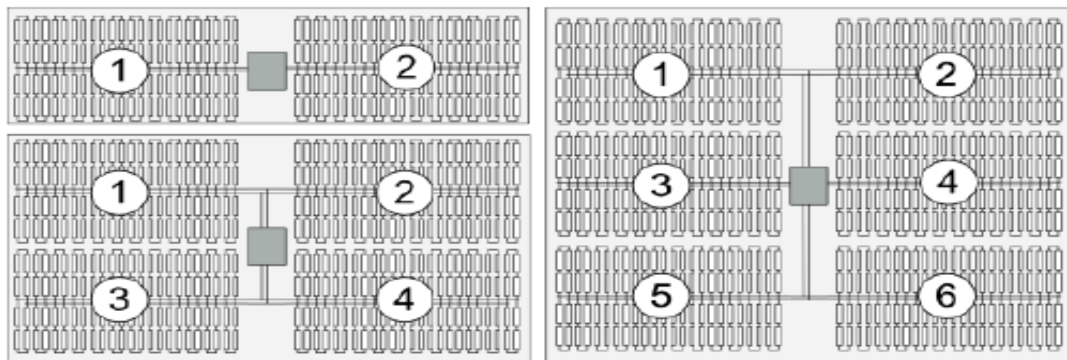


Figure 3.6: Three indicative solar field lay-outs [138].

3.4.2 Solar Collector Assemblies

Solar collector assemblies (Figure 3.7), probably the “heart” of a parabolic trough CSPP are consisted of 3 major components: a) the reflective surface, b) the absorber or receiver or heat collection element (see 3.4.3) and c) the tracking mechanism.

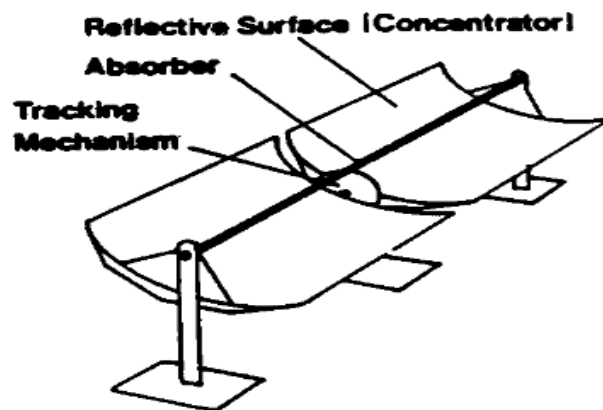


Figure 3.7: Three indicative solar field lay-outs [139]

Starting with their positioning, someone needs to determine their inclination orientation and particularly **collector tilt** and **azimuth**, though they mostly align in either the N-S or the E-W direction exploiting a single-axis tracking mechanism. The latter orientation does not require a tilt, causes almost zero shadowing effects between the rows, and provides a more seamless seasonal production level [140], while the former performs significantly better on an annual basis, especially in its polar mode – SCAs are titled equally to the site’s latitude. Uncertainty inherent in this data is almost zero.

On the other hand, major geometrical input variables required in order to simulate related power flows in a single SCA are its **reflective aperture area** which can roughly be calculated as the product of its length and width (not accounting for spaces, gaps and structural area) and the **average surface-to-focus path length** being calculated knowing the focal length and aperture width. Please note that the total reflective aperture area is estimated taking into account the **irradiation at design** and the desired **solar multiple**, higher values of which typically result in higher investment costs, higher production and higher probability for solar energy losses (Figure 3.8) [141]. Once more data uncertainty is considered as trivial.

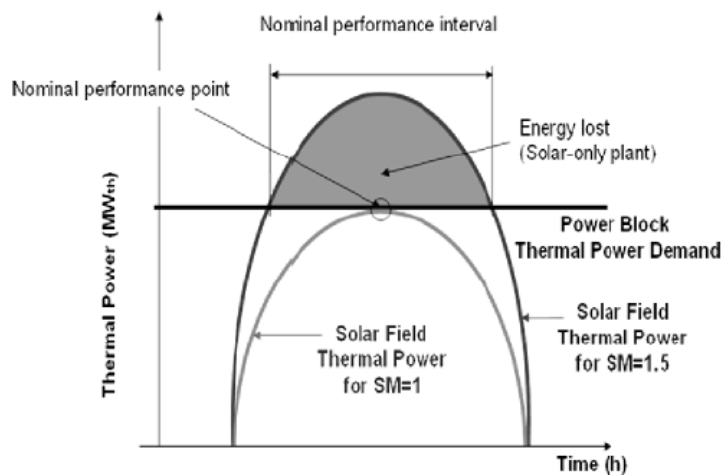


Figure 3.8: Comparison of thermal power production of 2 solar field multiples [141].

As far as their optical performance is concerned, related calculations require the determination of the **clean area reflectance** typically provided by the SCA manufacturer, the **3 incidence angle modifier coefficients** which are rather empirically determined [142] [143] and the reduction of clean area reflectance due to potential **geometry defects, dirt** or **other reasons**. The whole dataset includes uncertainty the characteristics

of which can roughly be standardized apart from related works published on clean area reflectance [144] and dirt effect [128].

Finally, with regard to the tracking mechanism we underline the need to define its ability to **defocus**, if needed, partially or completely the reflectance area, **tracking errors** possibly reducing the optical efficiency. Moreover, the related internal load can be calculated taking into account the **tracking power** per SCA needed and, **stow and deploy angles**. Except from the tracking error which is handled similarly to optical errors mentioned above, the remaining of the dataset could be regarded as uncertainty-free.

Please note that the needed SCA input variables presented in this paragraph can easily derive even if only the respective SCE data is available.

3.4.3 Heat Collection Element

Data required for the modeling of a heat collection element (HCE) is mainly related to its individual parts (Figure 3.9).

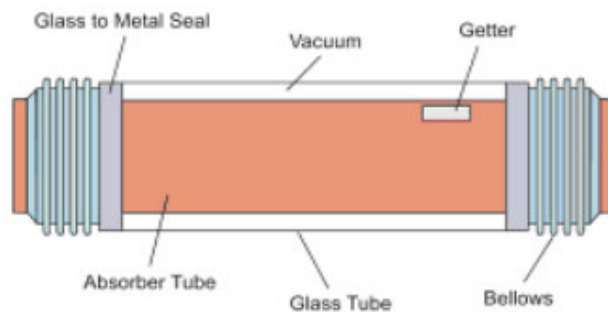


Figure 3.9: A typical HCE for parabolic troughs [145].

Starting with geometrical data, researchers need to determine the **absorber tube's inner and outer diameter**, the corresponding dimensions of **glass tube** as well as the **bracket perimeter, diameter and cross sectional area**. This dataset also includes information on **whether the absorber includes a plug** running it axially and concentrically and the **plug's diameter**. Moreover, the presence of a plug should modify the absorber flow pattern from **tube flow** to **annular flow** [146]. All of this data may safely be represented by single values, although uncertainty of dimensional calibration might not be neglected [147].

In terms of materials, someone should define the **nature of the absorber, the annulus gas and the bracket**. Choice of the former requires the handling of several complex trade-offs, such as (i.e. high solar absorption and low emittance may be mutually

exclusive) [148] while alternatives regarding annulus gas include air, argon and hydrogen among which argon outperforms and hydrogen is the less appropriate choice (Figure 3.10) [149].

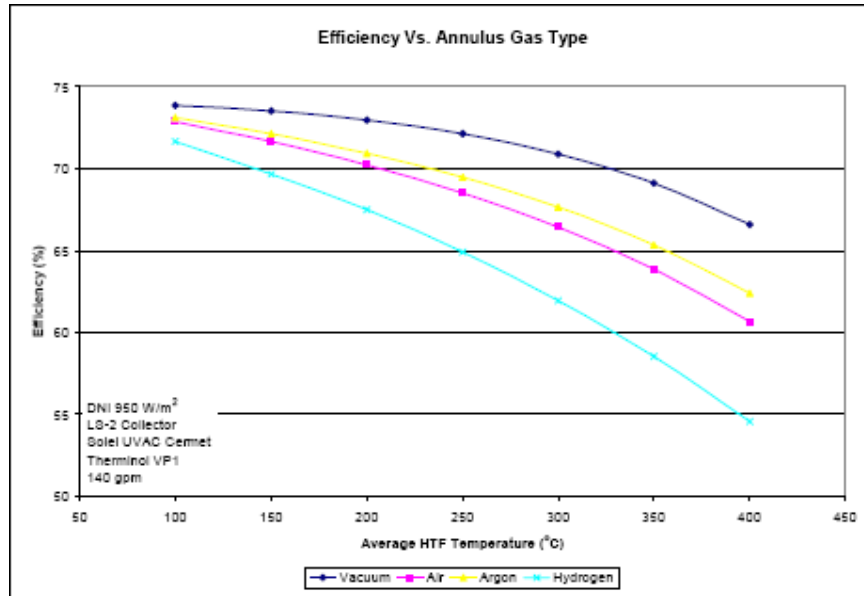


Figure 3.10: Efficiency chart of different annulus gases [149].

Defining the materials/elements used supports the counting in of their major physical properties such as the **absorber absorptance** and **emittance, envelope** (which is typically made of glass) **absorptance, emittance** and **transmittance** and **bracket conduction coefficient** and **base temperature**, the majority of which are typically provided by the manufacturer without lacking uncertainty though [150].

Other related data needed is the **annulus pressure** and quantification of optical losses possibly caused by **bellows shading** and **dirt**. Unless there is a breach on the envelope annulus pressure uncertainty is in line with that of other previously mentioned thermodynamic properties, while optical losses carry inherent uncertainty also similar to these reviewed previously.

3.4.4 Heat Transfer Fluid

Calculating power flows related to the heat transfer fluid (HTF) used in the solar field requires the definition of a dataset regarding its major properties such as its **minimum** and **maximum operation temperature, freeze point** and, with regard to a **specific temperature**, its **specific heat, density, viscosity** and **conductivity**. So far syn-

thetic oil is the HTF typically used in parabolic trough CSPPs although researchers strive to propose new alternatives taking into account HTF's efficiency and other operational aspects, availability and storage safety and, of course, cost [151]. Reliability of this data though stands far from being considered as ideal [152].

3.5 Power Cycle

Next task is to model power flows related to the power cycle. Nowadays the most common power cycle used in parabolic trough CSPPs is the steam Rankine cycle [153] although the organic Rankine cycle emerges as a reasonable alternative especially for small-scale CSPPs [154] [155]. Furthermore someone may choose between the above stand-alone cycles and combined cycles exploiting exhaust gases of fossil fuel-fired power stations [156] [157] or, hybridized cycles being supported by either a fossil fuel-fired boiler [59] [158] or another renewable energy source [159]. Nevertheless, as it was mentioned in the beginning of this section, this study focuses on the mostly used in CSPPs steam Rankine cycle with an auxiliary fossil fuel-fired boiler. In such a power cycle we distinguish a) the fossil fuel-fired boiler, b) the steam generator, c) the set of turbines, d) the electricity generator, e) the condenser, f) the set of feedwater heaters and g) the control systems (Figure 3.11) [160].

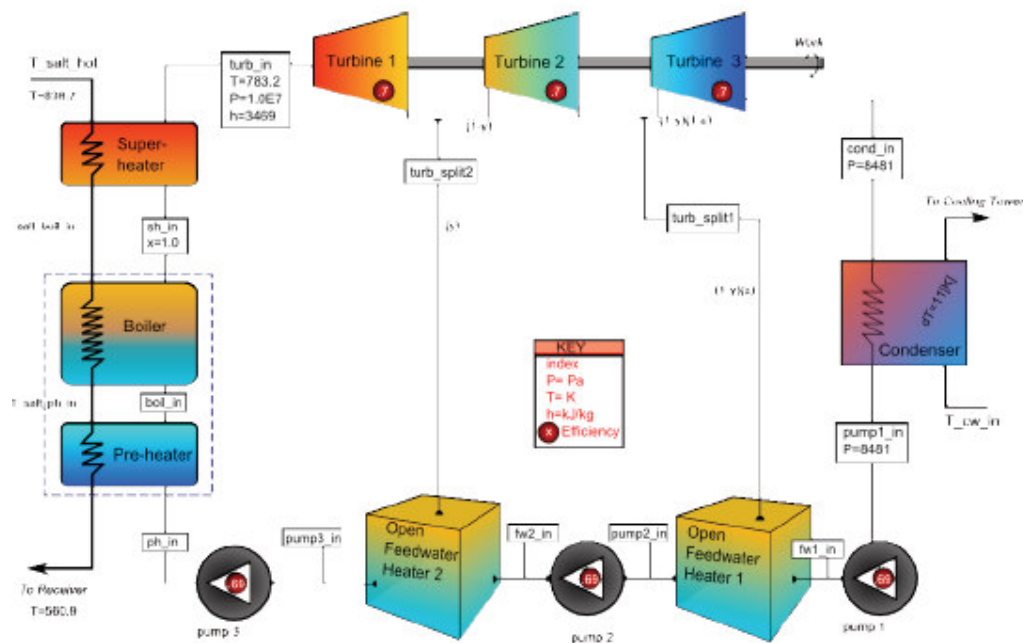


Figure 3.11: An indicative Rankine cycle configuration [160].

Please note that given the complexity related to a power cycle’s modeling, required data mentioned below imply a rather simplified approach of its operation simulation. In any case, the **overall power cycle efficiency under design**³, despite its inherent uncertainty [161], constitutes the corner-stone of further calculations.

3.5.1 Fossil Fuel-fired Boiler

Initially one needs to define the **operational objective** of a fossil-fuel fired boiler which may refer to the supplement of solar power so that a) the power cycle does not stop and/or b) the power cycle maintains its highest possible output even for a shorter time-period (Figure 3.12) [162]. Furthermore, this or another back-up boiler could be used simply in the maintaining of the HTF temperature above its freeze point (minimum HTF operating temperature). Other related input variables are the **heater’s outlet set temperature** which should not exceed the power block’s inlet temperature, its **tank capacity** and **efficiency**, as well as its **lower heating value efficiency**. Cost and availability are probably the two main criteria regarding the choice of fuel, while uncertainty expected in this dataset is limited in the two efficiency factors [150].

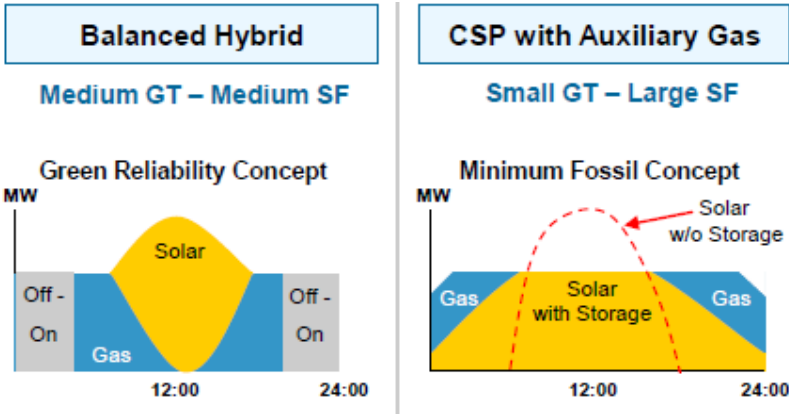


Figure 3.12: Two alternatives of Solar-Fossil Fuel Hybrids [162].

³ In order that a power cycle is analyzed, all related values should refer in a specific condition-point of the cycle. For simplicity reasons we define this status as “the design-point” or “under design”, implying that on that point the power cycle efficiency is optimized. Obviously by this we also take for granted that the power cycle has been previously simulated separately and independently from the fuel used in order for thermal power to be produced. This assumption is made as this study emphasizes in data related to components mostly used in CSPPs, despite that we acknowledge the impact of the power cycle’s configuration on the overall CSPP sizing and performance.

3.5.2 Steam Generator – Feedwater Heaters

Steam generation equipment should definitely include a boiler and optionally a set of pre-heater and/or super-heater. With regard to these components, modelers need to define several data at the design-point such as the **HTF inlet and outlet temperature**, the **boiler steam temperature and operating pressure** and the **preheater, boiler and superheater size**. On the other hand, necessary input describing the operation of the feedwater heaters are their **outlet set temperature, water's mass flow rate and inlet and outlet temperature**. Once more uncertainty of this dataset is not negligible [150].

3.5.3 Steam Turbines - Electricity Generator

Major input variables concerning the steam turbines are their **upper and lower operation limit** (in terms of inserted thermal power), their **isentropic efficiency**, their **mechanical power**, the **steam inlet temperature** and, the **steam extraction fraction and pressure at high and low pressure**. Modelers should also estimate the **amount of steam that is extracted and replaced by fresh water** and to define whether **turbine inlet pressure** is considered to be **constant** or **varies** according to the HTF inlet temperature. In addition to the above implementing a turbine operation strategy requires the control of variables such as the **standby period**, if any, and the **thermal power** needed for **this operation mode**, and the **time**, the **thermal power** and the **minimum temperature** it needs to **start** its operation. Regarding the electricity generator, data needed is its **gross power output** which equals to the nameplate capacity of the CSPP and provided by the manufacturer, and the **gross to net power conversion factor** – a measure of related parasitic loads applied in the whole power cycle (i.e. pumps and feedwater heaters consumption) as well as between the generator and the grid (i.e. transformers and cables losses etc). All of this dataset also includes uncertainty [150] [161].

3.5.4 Condenser

Heat rejection is achieved by the use of a wet-cooling or a dry-cooling system or their combination (hybrid). The major trade-off observed between the first two alternatives, being partially smoothed by the third one, is related to the higher performance achieved and the larger amount of water needed by a wet-cooling system [163]. Considering that sufficient water supply could be a major issue for many potential installation sites, we focus on the dry-cooling model the simulation of which requires the determination of the **ambient temperature** and the **temperature difference between the**

steam at the inlet and the ambient at design, the pressure-drop ratio in the condenser, its minimum operation pressure, its fan isentropic and mechanical efficiency and the condenser ability to operate in part load levels if needed. Apart from the latter, the other data include uncertainty typically met in thermodynamic values and properties [150].

3.6 Thermal Energy Storage System

Utilization of a thermal energy storage system (TESS) in a hybrid solar-fossil CSPP is a rather common and attractive alternative as the solar fraction may surge from 20% up to 70%, while it also improves CSPPs' marketability and dispatchability [60]. The most common arrangement includes a two-tank system although thermocline single-tank systems emerge as an alternative [164]. Focusing on the former arrangement modelers need to determine the **number of hours that a TESS can fully support a CSPP maximum output**, the **number of parallel tank pairs**, the **tank height** and **losses coefficient**, as well as the **minimum allowable height of fluid in the tank**. As both the **cold** and the **hot tank** of a TESS shall maintain a **minimum temperature level**, an **auxiliary heater** with a specific **capacity** and **efficiency** is needed. As far as the **heating transfer fluid** used in a TESS, we meet a variety of options among of which molten salt seems to be the most appropriated one at least with regard to the Rankine cycle [165]. Related input variables needed are **similar to these presented in 3.4.4**, adding its **temperature at the time point that the simulation starts**. Obviously, in case that the TESS HTF is different than the solar field HTF, a heat exchanger is needed which's **both sides (cold and hot) temperature differences** are required. Last but not least stands the **TESS operation strategy** which, similarly to the usage of the auxiliary fossil fuel-fired boiler, is strongly related to the CSPP operation objective. Once more thermodynamic values and properties should not be considered as certain [150].

3.7 Piping System

Simulating the operation of the piping system probably constitutes the most challenging and painful part regarding the building process of an integrated parabolic trough CSPP model as it directly interacts with all of its major parts (solar field, fossil fuel-fired boiler, storage system, power cycle) affecting the respective power flows shown in Figure 3.2 [166]. Simplifying this modeling process, since a detailed approach would

significantly exceed the scope of this study, we distinguish a piping system's main components in two major categories: a) the tubular and b) the non-tubular ones. Below the most important related thermodynamic and dimensional properties and values are presented, pointing out their inherent uncertainty [147] [150].

3.7.1 Tubular Components

This category includes equipment such as a) the runner pipes connecting the solar field, fossil fuel-fired boiler, the storage system and the power cycle, b) the cold and hot header pipes, c) the HCE pipes, d) the power cycle pipes used for the steam and/or water transfer and e) the pipe expansions, contractions and elbows. With regard to the above components modelers need to determine their **dimensions** (length and diameter), **roughness**, **thermal inertia** and, depending on the insulation used, their **heat loss coefficient**.

3.7.2 Non-tubular Components

Not-tubular components are ball joint assemblies and valves. Simulating the performance of the former does not really differ from the process followed to the tubular components. On the other hand, modeling valves, used in each one of the numerous loops of a CSPP, requires two kinds of input data: the first one is related to their controlling tasks while the second to the parasitic loads that they cause. Valves, as controllers of the piping system, manage the fluids (HTF and steam/water mix) **mass flow rate** and **velocity** in order that the latter comply with **minimum and maximum per loop set values**. In parallel, as fluids pass through the valves, determination of the latter's **isentropic efficiency** becomes meaningful. Moreover, as their operation requires a power supply, usually electricity, their **efficiency** and **consumption** should also constitute input data.

3.8 Comments

Ending with this Section, it would be useful to express the notion that simulating the operation of a CSPP is a highly demanding and time-consuming process which makes the use of an already validated model really attractive compared to the alternative of building a new one. On the other hand, keeping in mind that handling so many uncertain variables in a deterministic way could cause a major impact on a model's performance, probabilistic modeling seems to be undoubtedly the most appropriate approach.

4 A 20 MW CSPP Model

In this final section the operation of a 20 MW hybrid parabolic trough CSPP with thermal storage is simulated with the use of the System Advisor Model. Simulation performed includes 3 different locations in Greece while indicative parametric, statistic and financial analysis are also performed.

4.1 Introduction

Keeping in mind comments made in 3.8, we have been looking for a ready-to-use integrated software which a) is available to the public, b) utilizes numerous input data supporting complex calculations and high customization, c) performs probabilistic analysis and d) has already been validated with regard to its output. Being based on the reviews provided in section 2, the only alternative found fulfilling at least the first 3 criteria is the System Advisor Model (SAM). Extending our research and looking for evidence for SAM's validation it became more than clear that this software package emerges as a really attractive alternative (Figures 4.1 and 4.2) [81].

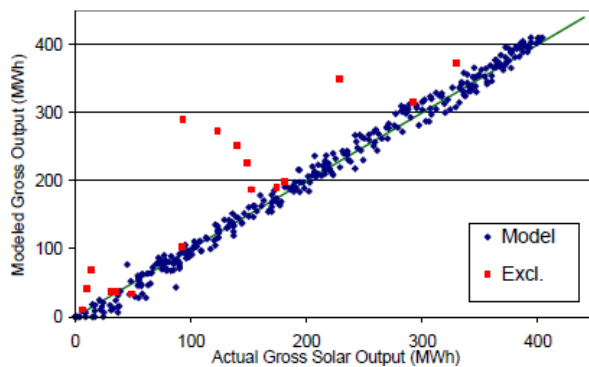


Figure 4.1: Actual and modeled solar output.

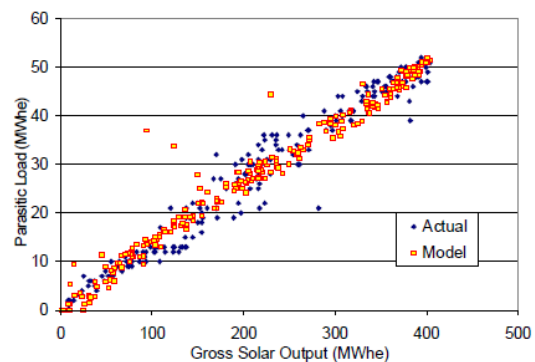


Figure 4.2: Actual and modeled parasitic loads.

As far as further alternatives provided by this software enabling users to choose among a physical and an empirical⁴ model, we have chosen flexibility and further performance uncertainty provided by the former.

⁴ It derived from regression analysis of data collected from the SEGS projects.

4.2 The Objectives

As we had stated in section 3.1, one of the major decisions that has to be reached during a CSPP design process is related to the objectives of its operation. Keeping in mind that a) the LCOE of a CSPP is currently rather high in order to compete, in wholesale market terms, electricity generation using fossil fuels (Figure 1.16), b) RES promotion is mainly accomplished by the establishment of investment-friendly legal frameworks (see 1.1 and 1.5) and c) the CSPP to be modeled will be located in Greece, it becomes explicit that one should take into account the respective Greek legislation. Thorough study of the latter, which consists of a general RES [36] and a specific CSPP legal framework [167], led us to conclude that the most appropriate objective of a CSPP in Greece is the minimization of its LCOE which is achieved by the optimization of the electricity delivered to the Grid⁵ and the minimization of the related investment and O&M costs⁶. The next section this chapter focuses on technical aspects, while cost effects are taken into account in section 4.6.

4.3 Initial Setup

In section 3.1 we had pointed out that designing a CSPP requires the reaching of three additional major decisions. The first one is related to the presence of a thermal storage system or not, but information provided in 3.6 explicitly indicates the attractiveness of the former. Secondly one needs to decide whether the plant will be hybridized. This dilemma is answered by the Greek legal framework [167] which clearly promotes hybrid CSPPs as it allows the utilization of thermal energy produced by auxiliary sources up to the 15% of this produced by the solar field. Finally, choosing between the use of an intermediate HTF and the direct production of steam, nowadays seems to be a rather easy process as direct steam production technology, despite its individual advantages, needs time in order to reach its maturity [168] [169]. As a result, we consider the hybrid parabolic trough CSPP with thermal storage as the most appropriate design among all other alternatives related to the respective technology. Right below a simplified schematic view of that plant is provided (Figure 4.3). Please note that since SAM has been chosen for the modeling of such a plant and complying with its simulation

⁵ Electricity is sold to a public entity under a specific PPA lasting for 25 years.

⁶ For simplicity reasons, potential capital and land constraints are discarded.

principles is a necessity, this figure as well as other individual schematic views presented afterwards, come from the respective SAM’s technical manual [135].

The following subparagraphs particularize the modeling of the plant in the individual data sets as they were presented in section 3. Nevertheless, as SAM’s interface architecture slightly differs from the structure presented in section 3, we decided to conform to the former possibly facilitating the reader’s understanding.

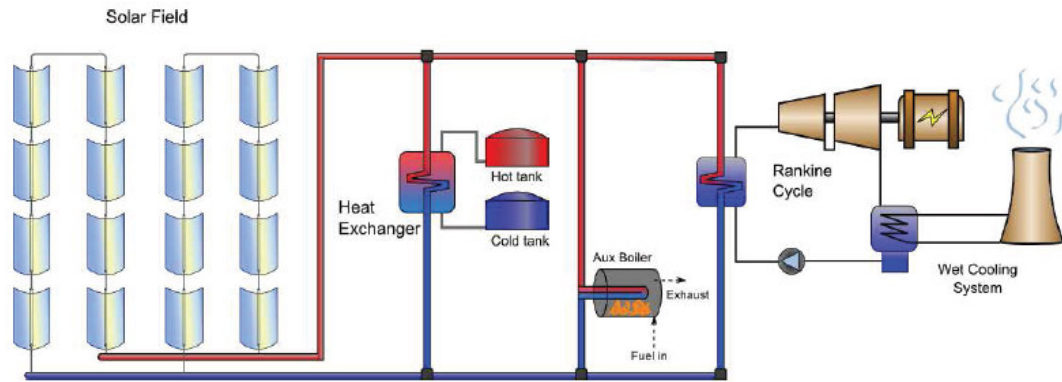


Figure 4.3: Schematic view of a hybrid parabolic trough CSPP with thermal storage [135].

4.3.1 Climate

The first data set that needs to be defined is included in the “climate” tab. With regard to insertion of hourly climate data, the program enables users a) to choose an already existing file corresponding to a specific location (Figure 4.5) or b) to insert any other related file in a TMY2, TMY3 or EPW format found in other sources some of which are also suggested by SAM (Figure 4.6) or c) to build a TMY3 (Figure 4.7) or a SMW⁷ file. Although SAM’s weather library is adequately rich regarding the USA, it does not contain any location in Greece. For this we had to look for in other related sources finding 3 EPW files concerning Thessaloniki, Athens and Andravida (Figure 4.4) [170]. Although we do not consider the installation of a CSPP next to the two cities as feasible, we keep utilizing data concerning **Thessaloniki** assuming that nearby locations’ climate does not significantly differ.



Figure 4.4: The 3 locations.

⁷ It refers to Sam Weather File being used in the case of sub-hourly steps.

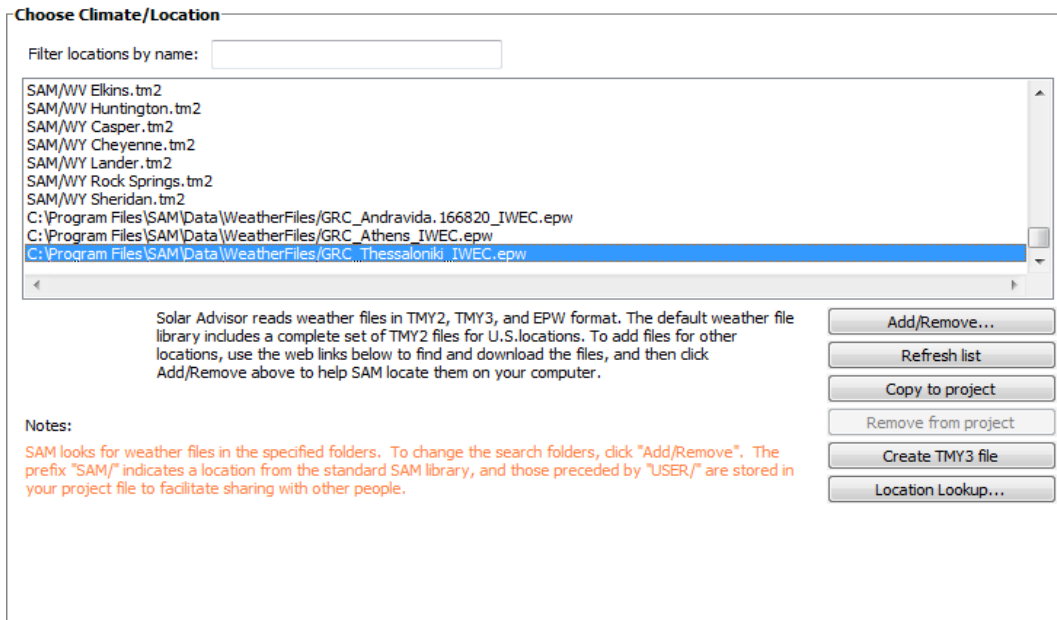


Figure 4.5: SAM weather file library.

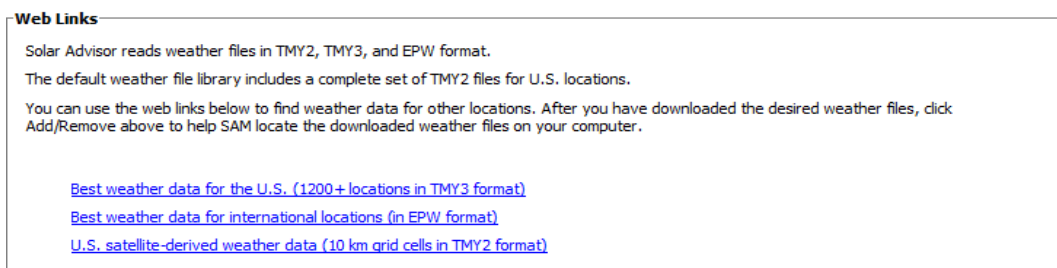


Figure 4.6: SAM suggested weather file web links.

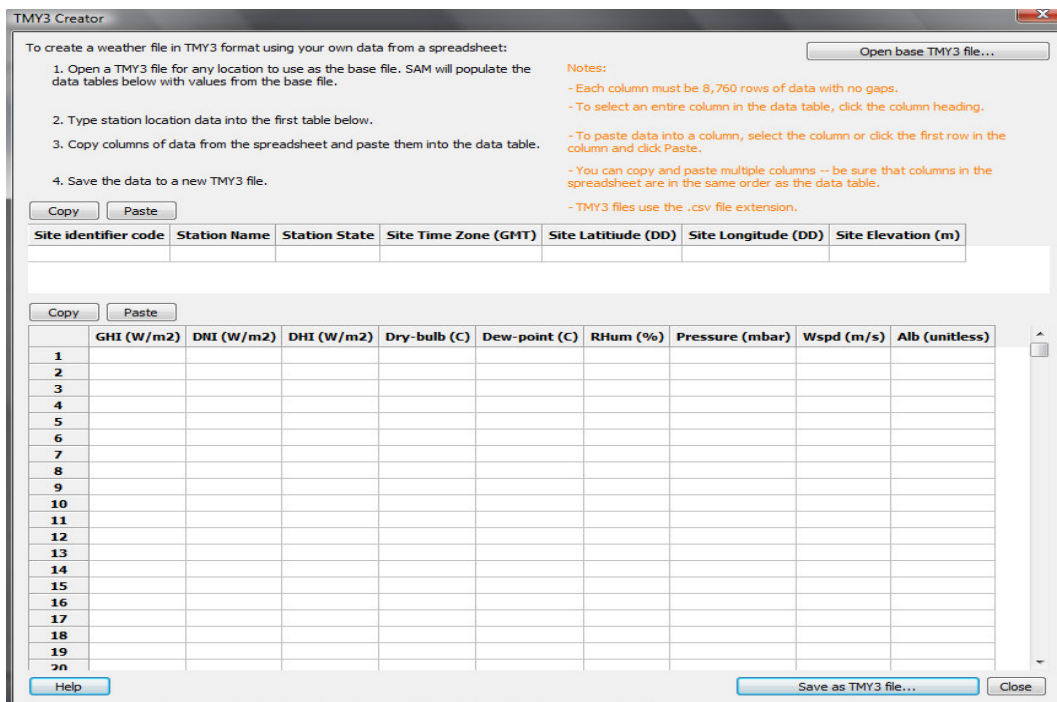


Figure 4.7: SAM TMY3 creator.

Based on data included in the weather file, SAM provides a short summary of it (Figure 4.8) while it also allows its thorough examination (Figure 4.9).

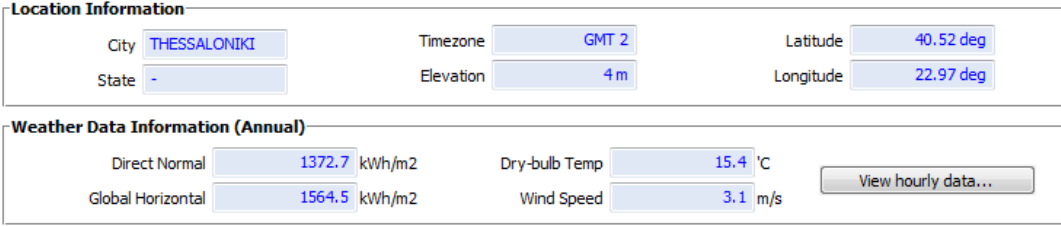


Figure 4.8: SAM weather and location data summary.

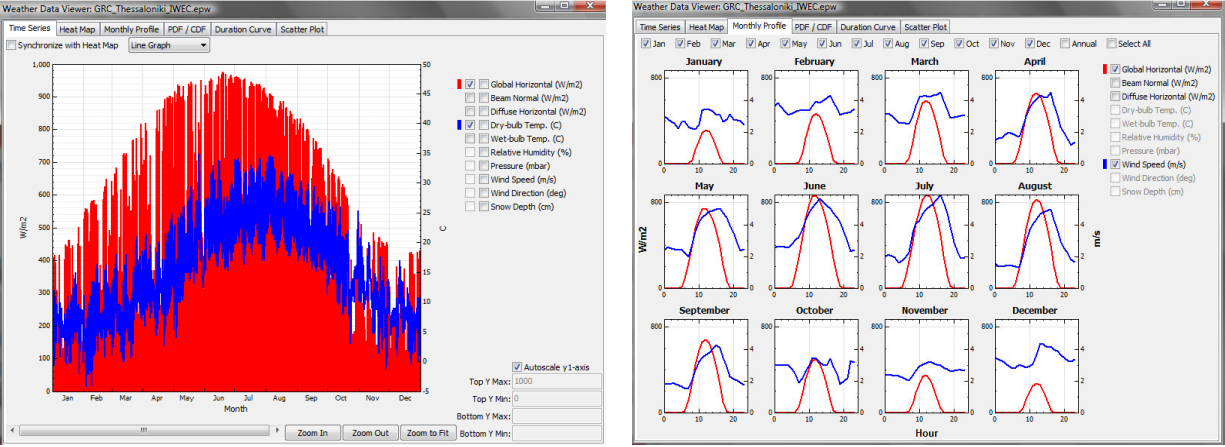


Figure 4.9: Two indicative levels of weather data analysis.

4.3.2 Annual Performance

The second tab requires the provision of estimations regarding the CSPP’s annual degradation rate, mainly caused by systems aging, and availability. Although extensive research has taken place in the degradation rate of individual CSPP components [171], little literature was found with regard to overall system degradation [172]. Based on the latter though, we assume that this factor equals to **1%**. On the other hand SAM proposes that a typical availability rate, mostly related to maintenance tasks, of a parabolic trough CSPP equals to **96%**. As we lack confronting data, except from the 94% provided by the Greek Regulatory Authority of Energy (RAE) [167], we adopt SAM’s proposal.

Please note that SAM enables users to define the above factors either in an average annual form (Figure 4.10), or a variable one for each year (Figure 4.11).

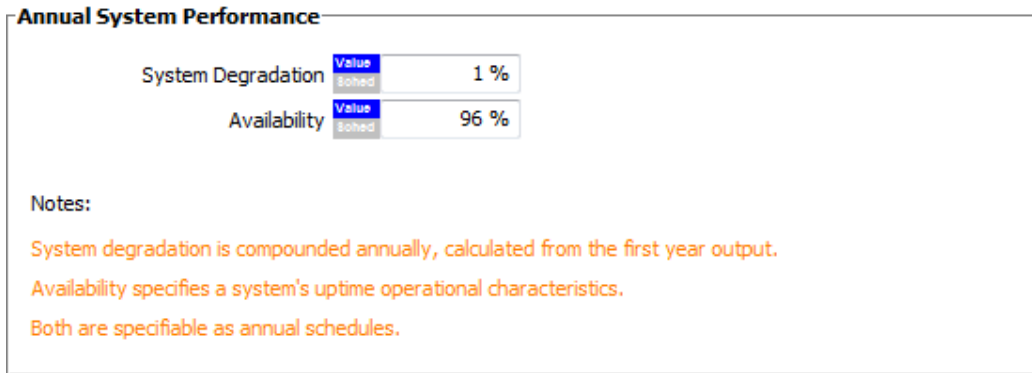


Figure 4.10: The annual system performance tab in average form.

4.3.3 Solar Field

The solar field tab could easily be considered as the “heart” of the model. Initially needed input data concerns the **collector orientation**⁸. As it was explicitly mentioned in 3.4.2, the **polar N-S axis with W-E tracking** arrangement typically outperforms compared to other arrangements using non-adjustable tilt⁹. As such we adopt the former, assuming a careful installation so that azimuth remains equal to **0°** and preserving our intention to perform parametric analysis with regard to the collector tilt which initially is considered to be equal to the latitude (its negative value = -40,52°) (Figure 4.12).

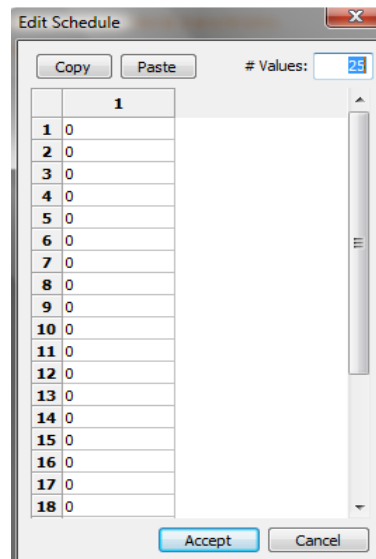


Figure 4.11: The module for the definition of variable system performance factors for each year.



Figure 4.12: The solar collector arrangement.

Secondly users need to define the **solar multiple** (SM) which refers to the field aperture area compared to that needed in order that the power cycle operates at its design

⁸ SAM assumes that all collectors are moved by the use of a single-axis mechanism.

⁹ We discard regularly adjusted tilts due to unknown effects on installation and operation costs.

capacity. Obviously this figure should receive values larger than 1 (Figure 4.13). On the other hand, precise sizing of the field requires the simultaneous comparison of the solar thermal energy produced with the respective a) installation and operating costs and b) the utilization of an auxiliary fossil fuel-fired boiler and a thermal energy storage system. In other words, the optimum solar field multiple derives from the minimization of the LCOE (Figure 4.14)¹⁰. Given that this optimization requires the completion of the CSPSP modeling, in terms of initial setup, at this point we consider a SM equal to 2, relying on indicative values provided in SAM’s manual (Figure 4.14) and the full load hours (5) of thermal storage capacity defined hereinafter. By the time that this initial setup is finished, the “financing”, “tax credit incentives”, “payment incentives” and “trough system costs” tabs are also filled in so that the abovementioned optimization is executable.

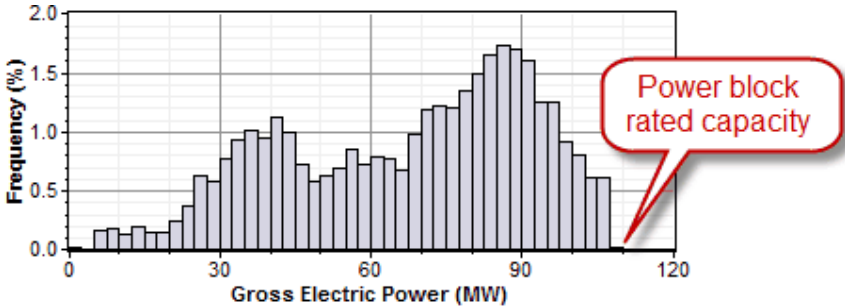


Figure 4.13: The probability of a CSPSP with SM=1 to operate at its rated capacity [135].

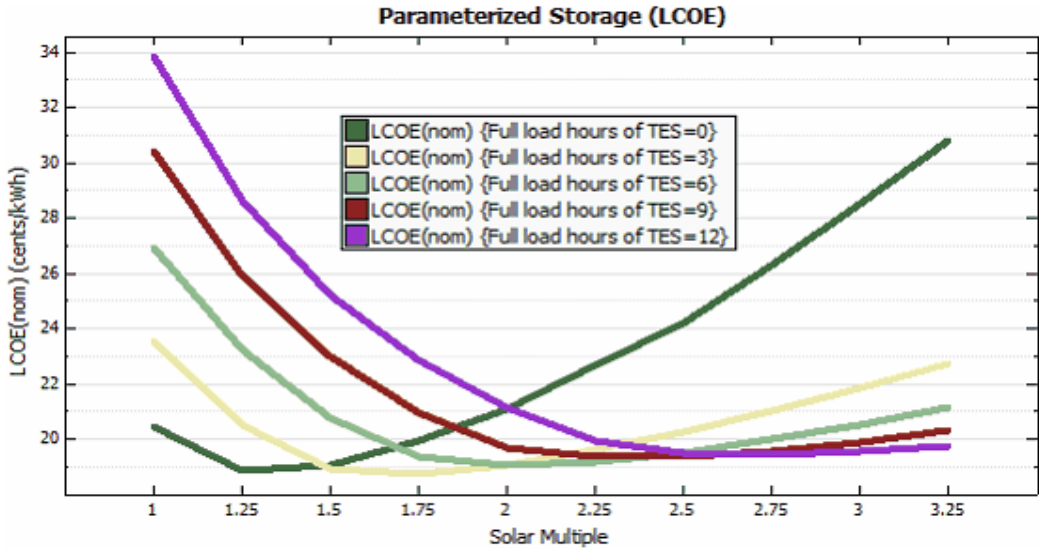


Figure 4.14: An example of LCOE as a function of SM and full hours of thermal storage [135].

¹⁰ Once more land constraints are neglected.

Another highly important variable is the **irradiation at design** used in sizing of both the aperture area needed to drive the power cycle at its nominal capacity and the mass flow rate of the HTF for header pipes. In general its value should approximate the maximum actual DNI on the installation site [135]. Setting as an objective to maximize cosine-adjusted DNI and determining the capacity of the power cycle and the thermal storage, the CSPP is simulated resulting in a maximum DNI value of **873 W/m²** (Figure 4.15). Cross-checking this estimation, we also count in dumped thermal energy which seem to vary in a rather acceptable level – approximately 34 MWh (Figure 4.16).

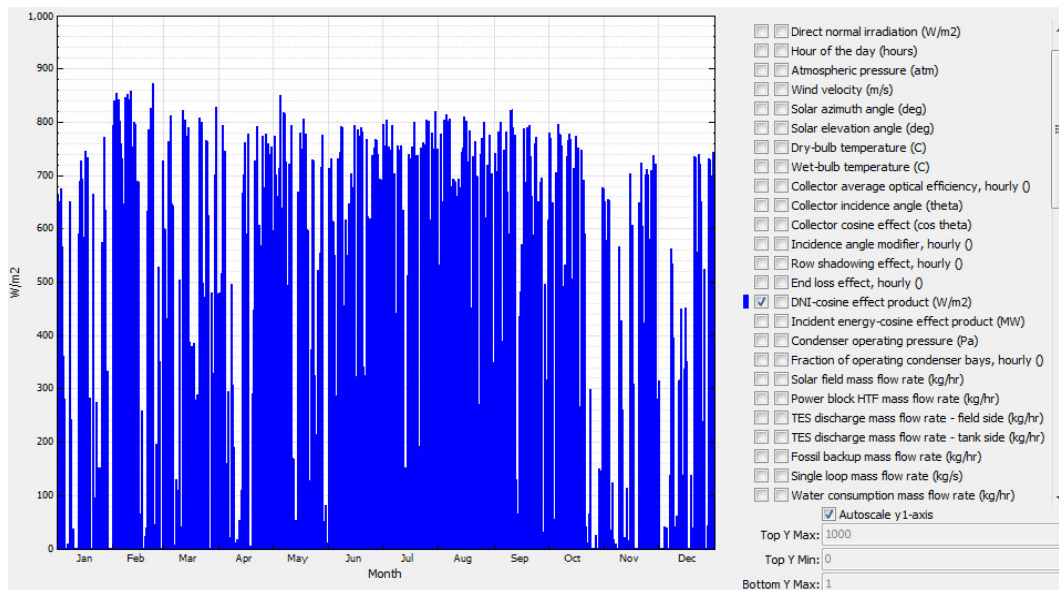


Figure 4.15: The maximum DNI-cosine effect product.

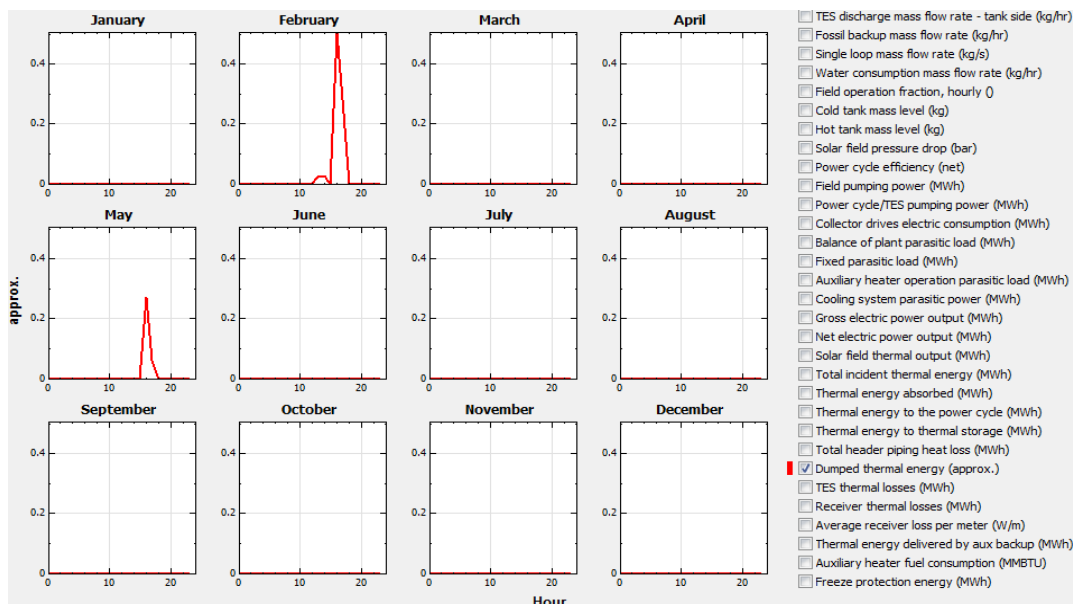


Figure 4.16: The monthly profile of the dumped thermal energy.

Row spacing is estimated by the use of a rule of thumb according to which main concern is to avoid shadowing caused by front rows to subsequent ones during the noon on the winter solstice. Taking into account a) that the installation site has no inclination, b) the location's latitude and c) the row height¹¹ and applying the appropriate equations [127] we conclude that row spacing should be equal to **11,79 m**.

With regard to the plant **lay-out**, we propose a **two-subsection field** (Figure 3.6), as the modeled CSPP is rather small and advantages deriving from the minimization of pumping pressure losses could easily be counter-balanced by the use of more and less effective pumps (see 3.4.1). As far as the **number of SCAs per loop** is concerned, we define it equal to **4** (Figure 4.17), mainly based in former practices [173]. In parallel we discard the ability provided by SAM for up to 4 different configurations of SCAs, HCE and defocus orders. Nevertheless the fact that we do not define different defocus orders implies that sequenced defocusing is not an option any more. On the other hand, as defocusing advantages are more than obvious, we define the ability of **simultaneous defocusing** meaning that all SCAs defocus at the same time by the same angle.

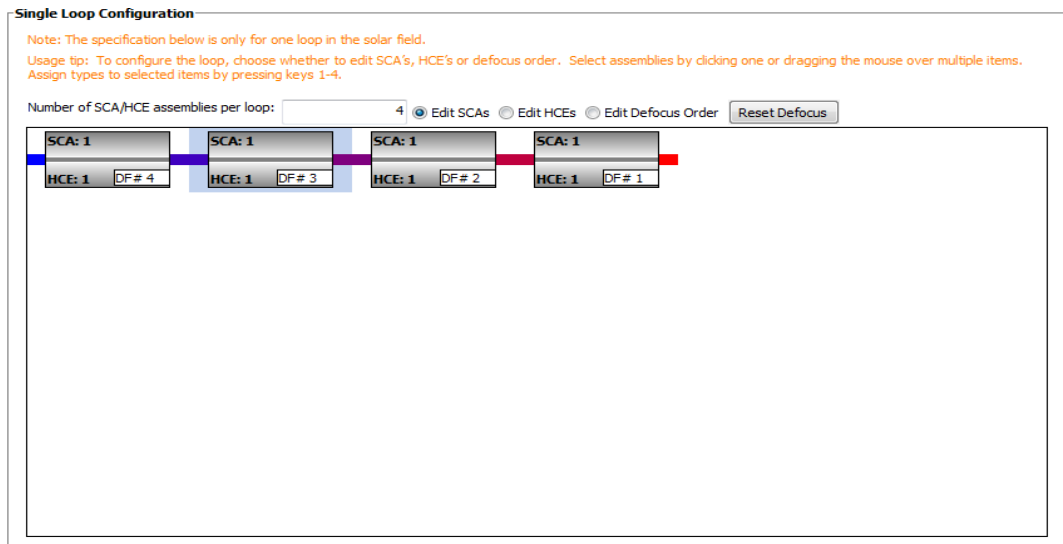


Figure 4.17: The arrangement of SCA's per loop.

In any case, this CSPP layout combined to a **non-solar field land area multiplier**, which may be assumed to equal **1,4** – SAM's default value, results in the need of 121 acres (489.670 m²) of land (Figure 4.18).

¹¹ It is provided in the next tab.

Land Area

Solar Field Area acres Non-Solar Field Land Area Multiplier Total Land Area acres

Figure 4.18: Land requirements.

Choosing **stow** and **deploy angles** is rather tough to be precisely determined at this stage. As such we adopt SAM's default values, **170°** and **10°** respectively, and we consider performing parametric analysis afterwards. **Header** and **runner pipe roughness** as well as **pump efficiency** also equal to SAM's default values, **0,0000457 m** and **0,85** respectively, as we lack reliable data to document an alternative option.

Another dataset required in this tab is related to the HTF. SAM enables users to select one among various fluids included in its library while it also allows them to define their own (Figure 4.19). Utilizing the first option and taking into account information provided in 3.4.4, the **Therminol VP-1** is selected. As its minimum operation temperature is 50 °C, significantly higher than its freeze point – 12 °C, we define the **freeze protection temperature** also equal to **50 °C**.

Edit Material Properties

Number of data points: Import... Export...

	Temperature (°C)	Specific Heat (kJ/kg-K)	Density (kg/m3)	Viscosity (Pa-s)	Kinematic Viscosity (m2-s)	Conductivity (W/m-K)	Enthalpy (J/kg)
1	<input type="text" value="0"/>	0	0	0	0	0	0

OK Cancel

Figure 4.19: Defining an alternative HTF.

Another task is the determination of the **HTF temperature inlet and outlet under design conditions** at **293 °C** and **391 °C** respectively. This choice is made due to the fact that these values equal to the power cycle outlet and inlet HTF temperature respectively, and SAM power cycle model has been built based on these [135]. Besides they perfectly comply with the properties of VP-1 ($50\text{ °C} < T_{op} < 400\text{ °C}$) and the selected collector (max outlet temperature = 400 °C) [174]. Finally users are called to determine the **minimum** and **maximum** allowable **HTF mass flow rate through a single loop**, as well as its **min** and **max velocity through the header pipes**. Lacking pieces of evidence to counter SAM's default values we adopt them – **1 kg/s, 12 kg/s, 2 m/s** and **3 m/s** respectively. Besides 1-12 kg/s is considered as an adequately wide range while the second dataset is utilized exclusively in the sizing of header pipes. Figure 4.20 summarizes input related to the solar field and the HTF.

The figure shows two panels from the SAM software interface. The left panel, titled 'Solar Field Parameters', includes options for 'Option 1' and 'Option 2'. Under 'Option 1', parameters are: Solar multiple (2), Field aperture (861590 m²), Row spacing (11.79 m), Stow angle (170 deg), Deploy angle (10 deg), Number of field subsections (2), Header pipe roughness (4.57e-005 m), HTF pump efficiency (0.85), Freeze protection temp (50 °C), Irradiation at design (610 W/m²), and Allow partial defocusing (checked, Simultaneous). The right panel, titled 'Heat Transfer Fluid', shows: Field HTF fluid (VP-1), User-defined HTF fluid (Edit...), Design loop inlet temp (293 °C), Design loop outlet temp (391 °C), Min single loop flow rate (1 kg/s), Max single loop flow rate (12 kg/s), Min field flow velocity (0.356106 m/s), Max field flow velocity (4.9655 m/s), Header design min flow velocity (2 m/s), and Header design max flow velocity (3 m/s).

Figure 4.20: Summary of the solar field parameters and HTF properties.

Finally users are enabled to specify the plant heat capacity by estimating values for the **thermal inertia** of **hot, cold and field loop piping**. As literature was found to be rather poor regarding these components, especially when it comes to their adjustment in CSPPs, once more we adopt SAM's default values, that is 0,2 kWh/K-MWt, 0,2 kWh/K-MWt and 4,5 Wh/K-m respectively (Figure 4.21). Moreover, since modelers aim also at the estimation of water needed so that the plant is washed, they may define the **amount of water used per wash** as well as the **number of washes per year**. For the purposes of this study we do not proceed in related estimations.

The figure shows two panels from the SAM software interface. The left panel, titled 'Mirror Washing', includes: Water usage per wash (0.1 L/m², aper.) and Washes per year (1). The right panel, titled 'Plant Heat Capacity', includes: Hot piping thermal inertia (0.2 kWh/K-MWt), Cold piping thermal inertia (0.2 kWh/K-MWt), and Field loop piping thermal inertia (4.5 Wh/K-m).

Figure 4.21: Water needs and plant heat capacity.

4.3.4 Collectors

As it was mentioned in 4.3.3, in order that row spacing is calculated, a SCA type has to be selected first. Having decided to choose an option among these provided in the SAM's library, we selected the **EuroTrough ET 150** (Figure 4.22) to be the modeled **parabolic trough collector**,

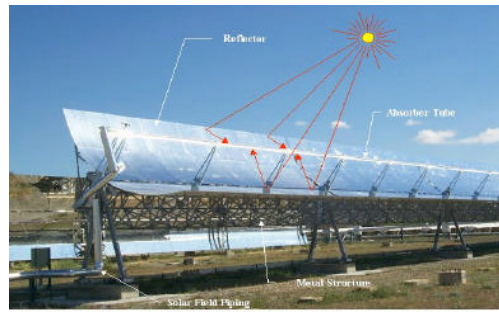


Figure 4.22: The EuroTrough collector [175].

possibly expressing an emotionally derived preference¹² rather than reaching a firmly grounded decision. Nevertheless EuroTrough indeed seems to outperform in several aspects compared to at least LS-2 and LS-3 [174] [175]. SAM's library includes all related input variables that are its **reflective aperture area**, its **length** and **width**, the **number of modules per assembly**, the **average surface-to-focus path length** and the **pipng distance between assemblies**. Additionally, SAM automatically fills EuroTrough optical parameters, such as the **incidence angle modifier coefficients** and several **factors indicating optical losses** (tracking error, geometry effects, mirror reflectance, dirt and general optical error) (Figure 4.23).

Collector (SCA) Type 1

Configuration name: SAM/CSP Physical Trough SCAs/EuroTrough ET150 Choose collector from library...

Collector Geometry

Reflective aperture area	817.5 m ²	Number of modules per assembly	12
Aperture width, total structure	5.75 m	Average surface-to-focus path length	2.11 m
Length of collector assembly	150 m	Piping distance between assemblies	1 m

Optical Parameters

Incidence angle modifier coeff 1	1	Geometry effects	0.98
Incidence angle modifier coeff 2	0.0506	Mirror reflectance	0.935
Incidence angle modifier coeff 3	-0.1763	Dirt on mirror	0.95
Tracking error	0.99	General optical error	0.99

Optical Calculations

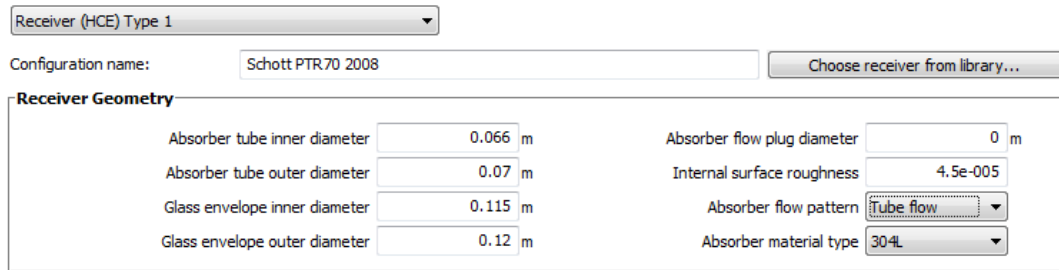
Length of single module	12.5 m	End loss at design	0.999171
Incidence angle modifier	0.968692	Optical efficiency at design	0.853162

Figure 4.23: The SAM collectors tab.

¹² It is a European product partially developed in the Greek Center of Renewable Energy Sources.

4.3.5 Receivers

As a heat collector element the Schott PTR 70 2008 is selected. This choice is mostly based on the compatibility of this HCE with the EuroTrough [176] while there is evidence of its outperformance compared to other alternatives [177]. As NREL has already simulated the performance of this receiver, we gather required **geometry variables** from the respective study [178]. Given that no **absorber flow plug** is foreseen to be added, this variable equals to **0** and the flow follows **the tube pattern**. On the other hand the **internal surface roughness** of a HCE, made from **304L stainless steel** [179] and with a 0,066 m inner diameter, is estimated to be **0,000045 m** [135] (Figure 4.24).



Receiver (HCE) Type 1

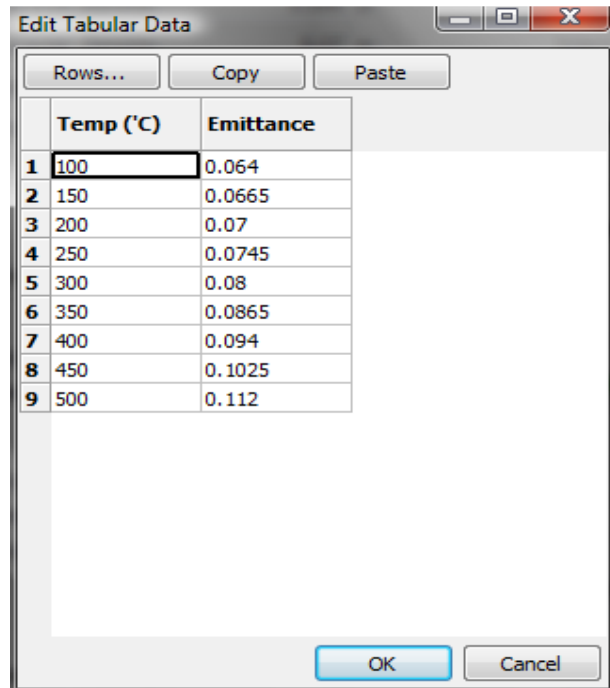
Configuration name: Schott PTR.70 2008

Receiver Geometry

Absorber tube inner diameter	0.066 m	Absorber flow plug diameter	0 m
Absorber tube outer diameter	0.07 m	Internal surface roughness	4.5e-005
Glass envelope inner diameter	0.115 m	Absorber flow pattern	Tube flow
Glass envelope outer diameter	0.12 m	Absorber material type	304L

Figure 4.24: The HCE geometrical parameters.

Hereinafter, SAM enables users to specify up to 4 types of receiver conditions. The motive for providing such an option is probably related to several reasons for which a receiver may underperform [180]. However, as spotting a corresponding fault and repairing it is not that difficult and SAM does not enable the definition of the time for which the deficient receivers keep operating, we feel safe to discard this option and assume that all receivers operate perfectly, considering that minor divergences from the reality are incorporated in the total system availability factor (4.3.2). As such in this single condition type of HCE, we



	Temp (°C)	Emittance
1	100	0.064
2	150	0.0665
3	200	0.07
4	250	0.0745
5	300	0.08
6	350	0.0865
7	400	0.094
8	450	0.1025
9	500	0.112

Figure 4.25: The module enabling the definition of emittance for different temperature values.

set the value **1** to the **variant weighting factor** and define **argon** as the **annulus gas**. The latter was selected as it constitutes the optimal solution as mentioned in 3.4.3. Other parameters presented in Figure 4.25, such as the absorber and envelope absorptance and emittance, are set by SAM's library and correspond to the specific HCE. Please note that if users prefer to define a receiver other than these included in SAM's library, they are enabled to modify these parameters while the absorber emittance may be defined either as a single value or a set of different values corresponding to different temperatures (Figure 4.26).

Parameters and Variations				
	Variation 1	Variation 2	Variation 3	Variation 4*
Variant weighting fraction*	1	0	0	0
Absorber Parameters:				
Absorber absorptance	0.96	0.96	0.8	0
Absorber emittance	Value Table... Table...	Value Table... 0.65	Value Table... 0.65	Value Table... 0
Envelope Parameters:				
Envelope absorptance	0.02	0.02	0	0
Envelope emittance	0.86	0.86	1	0
Envelope transmittance	0.963	0.963	1	0
	<input type="checkbox"/> Broken Glass	<input type="checkbox"/> Broken Glass	<input checked="" type="checkbox"/> Broken Glass	<input type="checkbox"/> Broken Glass
Gas Parameters:				
Annulus gas type	Argon	Air	Air	Hydrogen
Annulus pressure (torr)	0.0001	750	750	0
Heat Loss at Design:				
Estimated avg. heat loss (W/m)	150	1100	1500	0
Optical Effects:				
Bellows shadowing	0.96	0.96	0.96	0.963
Dirt on receiver	0.98	0.98	1	0.98
<small>Note: * The variant weighting fractions and Variation 4 inputs are not part of the library.</small>				
Total Weighted Losses				
Heat loss at design	150 W/m			
Optical derate	0.869751			

Figure 4.26: Various HCE parameters and variations.

4.3.6 Power Cycle

The next tab is used for the entering of data related to the simulation of the power cycle. Initially we set the plant **gross output** equal to **20 MWe**, being partially motivated by a rule of thumb set by Abengoa Solar SA representatives stating the minimum capacity of a CSPP for which this company would be interested in negotiating an engineering, procurement and construction (EPC) contract in Greece. Adopting the **90% gross-to-net conversion factor** suggested by SAM, we estimate that **net output capac-**

ity equals to **18MWe** (Figure 4.27). Typical causes of gross-to-net losses are cables and transformers used.

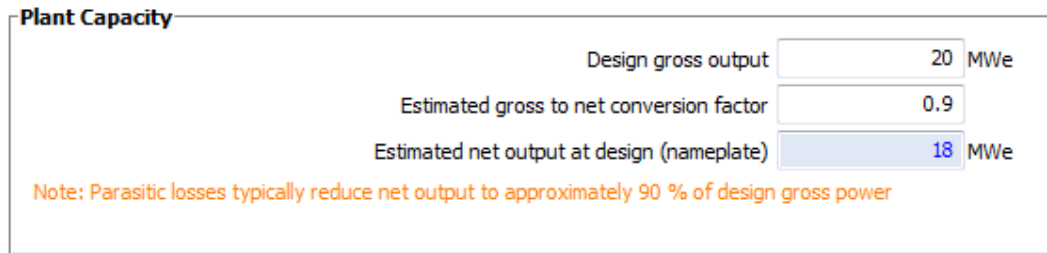


Figure 4.27: Estimating the plant capacity.

Going on with the modeling of the power cycle we point out that the cycle type adopted is the Rankine cycle both because of information provided in 3.5 and mostly due the fact that this kind of power cycle is the only that SAM simulates [135]. Providing more details on the second condition, we report that developers of this program preferred not to add major complexity by incorporating a detailed power cycle model in SAM but to utilize the “design of experiments” statistical approach.

According to the latter a 10 MWe Rankine cycle (Figure 3.11) was previously modeled under a certain dataset (Figure 4.28) and a respective regression model was built so that the operation of the power cycle is simulated taking into account varying impact coming only from HTF inlet temperature, condenser pressure, HTF mass flow rate and heat input. As a result the **rated cycle conversion efficiency** and the **boiler operating pressure** equal to the default values, **0,3774** and **100 bar** respectively, while **inlet** and **outlet temperature** equal to the outlet and inlet temperature of the solar field respectively (see 4.3.3). An average value for **steam cycle blowdown fraction** for a typical dry-cooled condenser, like that defined afterwards, is

Item	Value	Units
HTF inlet temperature	393	°C
HTF outlet temperature	293	°C
Steam temperature at turbine inlet	373	°C
Boiler steam temperature	311.1	°C
Boiler pressure	100	bar
Condenser pressure	0.085	bar
Steam extraction fraction, high pressure	0.13	-
Steam extraction pressure, high pressure	23.9	bar
Steam extraction fraction, low pressure	0.16	-
Steam extraction pressure, low pressure	2.9	bar
Turbine isentropic efficiencies (all)	0.7	-
Pump isentropic efficiencies (all)	.695	-
Turbine mechanical power	10.0	MW
Calculated heat exchanger sizes:		
Preheater size (UA)	267.6	$\frac{MW}{K}$
Boiler size (UA)	691.1	$\frac{MW}{K}$
Superheater size (UA)	115.6	$\frac{MW}{K}$

Figure 4.28: Conditions at design point for the basis Rankine cycle.

As a result the **rated cycle conversion efficiency** and the **boiler operating pressure** equal to the default values, **0,3774** and **100 bar** respectively, while **inlet** and **outlet temperature** equal to the outlet and inlet temperature of the solar field respectively (see 4.3.3). An average value for **steam cycle blowdown fraction** for a typical dry-cooled condenser, like that defined afterwards, is

0,016 [135], while users need to determine the **fossil fuel-fired boiler**¹³ **LHV efficiency** too. Counting in SAM's suggestion and information gathered from other sources [181], the latter is estimated at **90%** (Figure 4.29).

Power Block Design Point	
Rated cycle conversion efficiency	0.3774
Design inlet temperature	391 °C
Design outlet temperature	293 °C
Boiler operating pressure	100 bar
Fossil backup boiler LHV efficiency	0.9
Steam cycle blowdown fraction	0.016

Figure 4.29: Power block variables at the design point.

With regard to the way that the power cycle is implemented, SAM considers up to 3 different modes: the operation, the standby and the shutdown. Two further options regarding the former are defined in the next tab. On the other hand, at this point users are enabled to choose whether the CSPP will remain in a standby mode, when thermal energy available reaches low levels, or it passes directly in the shutdown mode. The tradeoff of this choice is related to the energy consumed in the standby mode and the longer time needed for the cold startup of the turbine.

Plant Control	
Low resource standby period	0 hrs
Fraction of thermal power needed for standby	0.2
Power block startup time	0.5 hr
Fraction of thermal power needed for startup	0.2
Minimum required startup temp	300 °C
Max turbine over design operation	1.05
Min turbine operation	0.25
Turbine Inlet Pressure Control	Fixed pressure

Figure 4.30: Plant control dataset.

For simplicity reasons we initially consider that no standby mode is applied, although this configuration will be parametrically analyzed afterwards. Other variables

¹³ Detailed description of this auxiliary heater is provided in the thermal storage section.

regarding the plant control, such as the **power block start time from shutdown mode**, the **fraction of thermal power** and the **minimum temperature needed for this process** and the **minimum** and **maximum over design turbine operation**, are considered equal to the values proposed by the model. Last variable of this data set is the type of **turbine inlet pressure** allowing either **fixed** or **floating pressure**. As the CSPP operates under a PPA with no load constraints and variations, we choose the **first option** (Figure 4.30).

This tab ends with the definition of the cooling system. Discarding the higher efficiency possible achieved by a wet-cooled or hybrid condenser, we secure our model from potential water shortage selecting a dry-cooled one (see 3.5.4). Similarly to these mentioned above, SAM has simulated the condenser under specific conditions, such as the **ambient temperature**, the **initial temperature difference** of the steam at the turbine outlet and the ambient temperature, and the **condenser pressure ratio**, which we set at design (Figure 4.31).

Cooling System

Condenser type	Air-cooled	Hybrid Dispatch
Ambient temp at design	20 °C	Period 1: 0
Ref. Condenser Water dT	10 °C	Period 2: 0
Approach temperature	5 °C	Period 3: 0
ITD at design point	16 °C	Period 4: 0
Condenser pressure ratio	1.0028	Period 5: 0
Min condenser pressure	2 inHg	Period 6: 0
Cooling system part load levels	2	Period 7: 0
		Period 8: 0
		Period 9: 0

Note: Hybrid dispatch control parameters refer to the dispatch periods defined on the thermal storage page.

Figure 4.31: Parameters and variables conceding the cooling system.

In parallel the model assumes 4 more variables (Figure 4.32). Finally, users shall define the **minimum condenser pressure**, which's fair value equals to **2 inches of mercury**, and the **number of levels on which heat may be rejected under part load conditions**. The latter is initially assumed to be **2** indicating that the cooling system may perform either at 100% or 50% rejection, while a related parametric analysis follows hereinafter.

Variable	Description	Units	Value
<i>User-supplied inputs</i>			
$T_{ITD,des}$	The initial temperature difference (steam-to-ambient)	°C	16
$r_{p,cond}$	The condenser air pressure ratio	-	1.0028
<i>Inherited inputs</i>			
\dot{W}_{des}	Power output at design	MW	-
η_{des}	Power cycle efficiency at design	-	-
T_{db}	Dry bulb temperature	°C	-
P_{amb}	Atmospheric pressure	Pa	-
<i>Assumed values</i>			
ΔT_{out}	Temperature difference at the hot side of the condenser	°C	3
$\eta_{fan,s}$	Fan isentropic efficiency	-	0.80
η_{fan}	Fan mechanical efficiency	-	0.94
$c_{p,air}$	Specific heat of air	$\frac{J}{kg.K}$	1005

Figure 4.32: Input data to the SAM dry cooling model.

4.3.7 Thermal Storage

Setting data required in the thermal energy storage (TES) tab starts with the **system capacity** in terms of full load hours of TES. As it was mentioned in 4.3.3, we consider this value equal to **5 hours**, counting in motives provided by the Greek government for a value equal to or greater than 2 [36] [167] and achieving an acceptable level of dumped thermal energy – 4h configuration results in 15 times more losses (472 MWh). In any case further calculations should be made, this time taking into account installation and O&M costs too. The number of used **pair of tanks**¹⁴ remains at its minimum value – **1**, so that related thermal losses are also minimized. Other related input data is the **tank height** and **thermal loss coefficient**, the **minimum height of the fluid inside the tank** and the **temperature of the TES fluid just before the simulation starts**, for which values proposed by SAM are adopted – **20 m, 0,4, 1 m** and **391 °C** respectively.

Another major choice to be made in the thermal storage tab is related to whether the HTF used in the solar field is used in the TES system too. As explicitly mentioned in 3.6, currently **solar salt** is considered to be far the most appropriated alternative, especially regarding the Rankine cycle. Nevertheless SAM includes a ready-to-use library of various TES HTFs while it also enables users to define their own through a module similar to this presented in Figure 4.19. What is important to know is that because of the

¹⁴ SAM utilizes only paired-tank TES systems discarding the emerging technology of thermocline single-tank ones (see 3.6).

utilization of a different HTF circuit than the solar field's, a heat exchanger (HX) is added to the system for which users need to estimate the temperature derate that the HX causes by defining the **temperature difference of its cold and hot side compared to the respective sides of the solar field**. SAM proposed related values remain unchanged at **5 °C** and **7 °C** respectively.

Furthermore, since SAM considers the presence of an auxiliary electric heater, used exclusively for the supplementary heating of the storage tank, users need to size it in terms of **cold** and **hot tank set point**, its **outlet temperature**, its **capacity** and **efficiency**. The former value is set at **260 °C** taking into account solar salt's minimum operating temperature while the second variable equals to SAM's proposal – **365 °C**. Its outlet temperature cannot be different than the turbine inlet temperature - **391 °C**, its capacity is considered to be **5 MW**, reserving our intention to analyze further this assumption afterwards, and its efficiency may safely to be assumed at **98%** just like SAM proposes. A summary of the values mentioned above is provided in Figure 4.33.

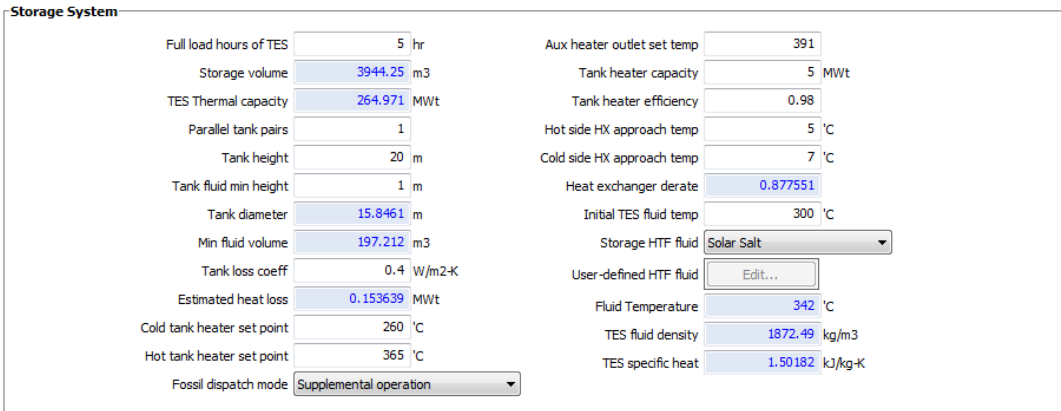


Figure 4.33: Input data to the SAM TES system.

As mentioned before, in this tab the fossil fuel-fired boiler is being also defined. Typically SAM assumes that this auxiliary component operates combusting natural gas, although this does not really affect related calculations and lack of this fuel type could be easily countered by the use of a LPG or diesel boiler, with minor performance effect but potentially with major financial impact. At this point users need to decide between two fossil dispatch modes: a) the minimum backup level and b) the supplemental operation. Scope of the former mode is to define the power level below which the auxiliary boiler starts supplying energy to the HTF so that the power cycle runs at its design gross output. This mode represents the alternative shown at the right in Figure 3.12. On the

hand, the supplemental operation defines a maximum level of fossil energy added in the HTF as a fraction of power cycle running at its design gross output. This mode is shown at the left in the same Figure while it explicitly indicates the maximum capacity of the auxiliary boiler. Serving the scope of this initial setup we choose the **latter mode**.

The last dataset needed to be defined in this tab is related to the thermal storage and fossil dispatch control. As shown in Figure 4.34, SAM allows the definition of up to 9 different dispatching periods based on different fractions regarding a) the reservation of a minimum storage level when solar field keeps producing energy, b) the reservation of a minimum storage level when solar field does not produce energy, c) the energy required in the turbine inlet at the design point, d) the auxiliary boiler operation as it was described above and e) differentiation in the pricing of sold energy. At this point we have formed **2 scheduling periods**. In both of them there is **no need to reserve thermal energy** and we consider **no pricing volatility**, while, taking into account intermediate thermal losses, we define a **fraction of 1.05 compared to the energy required in the turbine inlet so that the power cycle runs at its design output**. The difference of these scheduling periods is the **production of up to 5 MW of fossil power** in the second one, being applied during the whole day-time solely in June and July. This choice was made aiming at both avoiding potential shutdowns during a crucial period in terms of production and providing the grid operator a solid base for the daily scheduling.

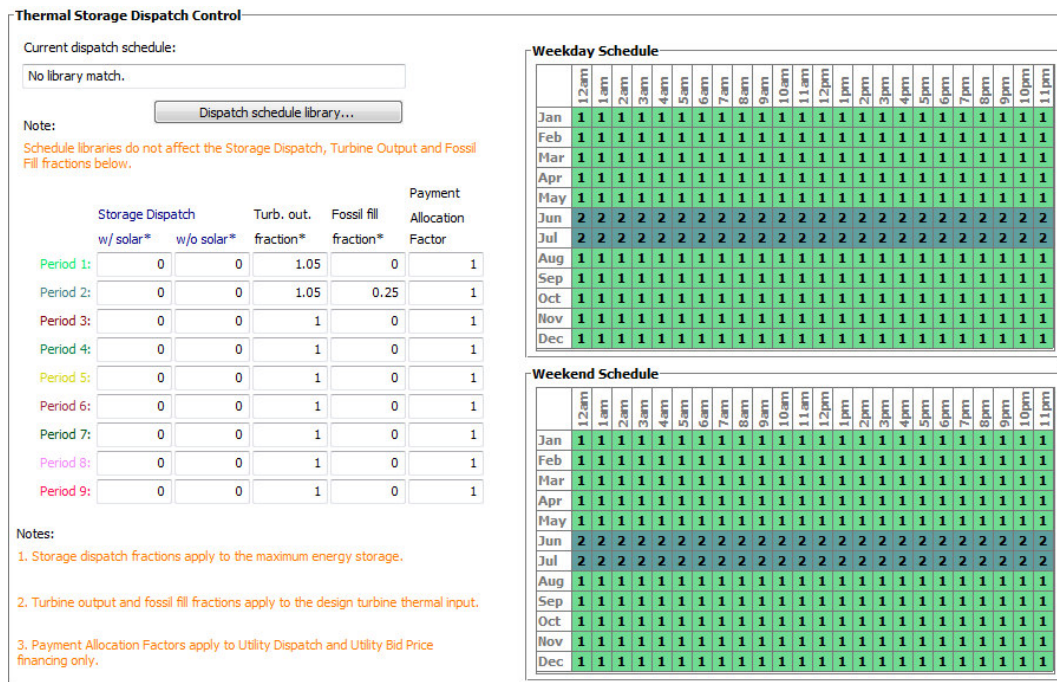


Figure 4.34: The thermal storage and fossil energy dispatch schedule.

4.3.8 Parasitics

The last dataset needed in order that this initial simulation is performed refers to the parasitic loads. These are a) the **piping thermal loss coefficient**, b) the **power consumed by the tracking mechanism**, c) the **cycle pumps** and the d) **storage pumps**, e) a fixed load applied at all times as a fraction of rated gross power, and parasitics applied f) **to the overall plant operation as a function of thermal input to the power cycle** and g) to the **auxiliary heaters as a function of their thermal output**. These variables are combined with data already inserted in the previous tabs or assumed by the model. I.e. with regard to the piping model, SAM makes assumptions shown in Figure 4.35.

Nominal pipe size (in)	Schedule	Internal diameter (in)	Internal diameter (m)	Wall thickness (m)
2.5	A	2.71	0.0688	0.0013
3	A	3.33	0.0847	0.0016
4	B	4.26	0.1082	0.0021
6	B	6.36	0.1615	0.0031
8	C	8.13	0.2064	0.0040
10	D	10.25	0.2604	0.0051
12	C	12.25	0.3112	0.0060
14	C	13.38	0.3398	0.0066
16	C	15.38	0.3906	0.0076
18	D	17.25	0.4382	0.0085
20	C	19.25	0.4890	0.0095
22	C	21.00	0.5334	0.0104
24	C	23.00	0.5842	0.0113
26	C	25.00	0.6350	0.0123
28	D	26.75	0.6795	0.0132
30	D	28.75	0.7303	0.0142
32	D	30.75	0.7811	0.0152
34	E	32.62	0.8286	0.0161
36	E	34.50	0.8763	0.0170
42	D*	40.50	1.0287	0.0200
48	D*	46.00	1.1684	0.0227
54	D*	52.00	1.3208	0.0256
60	D*	58.00	1.4732	0.0286
66	D*	64.00	1.6256	0.0316
72	D*	70.00	1.7780	0.0345

Line	Description	Length (ft)
1	Pump suction header to pump inlet	45
2	Pump discharge to discharge header	45
3	Pump discharge header	100
4	Collector field to expansion vessel/TES	120
5	Steam generator supply header	80
6	Inter-steam-generator piping	120
7	Steam generator exit to exp. vessel/TES	80

Item	$k_{\Delta P}$	IOCop	Receivers	Runners		Headers	
				Hot	Cold	Hot	Cold
Length of pipe Eq.	-	[2.94]	[2.95]	[2.96]	[2.96]	[2.97]	[2.97]
Eval. mass flow	-	\dot{m}_{loop}	\dot{m}_{loop}	\dot{m}_{run}	\dot{m}_{run}	\dot{m}_{hdr}	\dot{m}_{hdr}
Eval. temperature	-	$T_{sf,ave}$	T_i	$T_{sf,out}$	$T_{sf,in}$	$T_{sf,out}$	$T_{sf,in}$
Tube diameter	-	D_2	D_2	D_{run}	D_{run}	$D_{hdr,i}$	$D_{hdr,i}$
Expansions	0.50	0	0	[2.98]	[2.98]	N_{hgrp}	0
Contractions	0.50	0	0	0	0	0	N_{hgrp}
Standard elbows	0.9	2	10/loop	0	0	0	0
Medium elbows	0.75	0	0	0	0	0	0
Long elbows	0.6	0	0	[2.99]	[2.99]	1	1
Gate valves	0.19	2	0	1	1	0	0
Globe valves	10	0	0	0	0	0	0
Check valves	2.5	0	0	0	0	0	0
Loop weldolets	1.8	2	0	0	0	0	0
Loop control valves	10	1	0	0	0	0	0
Ball joint assemblies	8.69	0	$3 + N_{sca}$	0	0	0	0

Figure 4.35: Assumed values for a) Pipe sizing schedules (up left), b) Piping lengths (up right), c) Various configurations regarding the piping equipment (down).

Due to the lack of solid data for the documentation of different values than these proposed by SAM, we adopt the latter (Figure 4.36).

Parasitics					Design Point Totals	
Piping thermal loss coefficient	0.45	W/m ² -K			Tracking	37500 W
Tracking power	125	W/sca			Fixed	0.11 MWe
Required pumping power for HTF through power block	0.55	kJ/kg				
Required pumping power for HTF through storage	0.15	kJ/kg				
Fraction of rated gross power consumed at all times	0.0055					
			Factor	Coeff 0	Coeff 1	Coeff 2
Balance of plant parasitic	0	MWe/MWcap	1	0.483	0.517	0
Aux heater, boiler parasitic	0.02273	MWe/MWcap	1	0.483	0.517	0
					BOP	0 MWe
					Aux	0.4546 MWe

Figure 4.36: The assumed parasitic coefficients.

4.4 Deterministic Modeling

Having completed the initial setup of the model, in this paragraph a series of parametric analysis will take place, either in its typical form (a set of calculated values for a given range of input values) or in a direct optimization mode (minimization or maximization of a function for a given range of input values).

4.4.1 Alternative Locations

Our initial concern has been the selection of the most appropriate installation location. As mentioned in 4.3.1, hourly climate data were found for the regions of Thessaloniki, Andravida and Athens. Preserving most of the initial model setup unchanged, we simulated its performance modifying solely the weather file, the collectors tilt, the solar irradiation at design and the row spacing (Table 4.37). Setting the annually produced thermal energy by the solar field as the solely criteria of determining the most suitable location, Athens emerges as the undoubted best choice. This also confirms the relationship between the annual DNI and the solar field production while it prevents modelers from assuming that lower latitude always results in higher DNI (Figure 4.38).

Location	DNI (kWh/m ²)	Tilt (°)	Row Spacing (m)	Solar Irradiation at Design (W/m ²)	Annual Solar Field Energy (MWh)
Thessaloniki	1.372,70	-37,92	10,55	864	102,283.00
Andravida	1.151,70	-40,52	11,79	873	130,205.00
Athens	1.519,80	-37,9	10,55	860	138,131.00

Figure 4.37: The assumed parasitic coefficients.

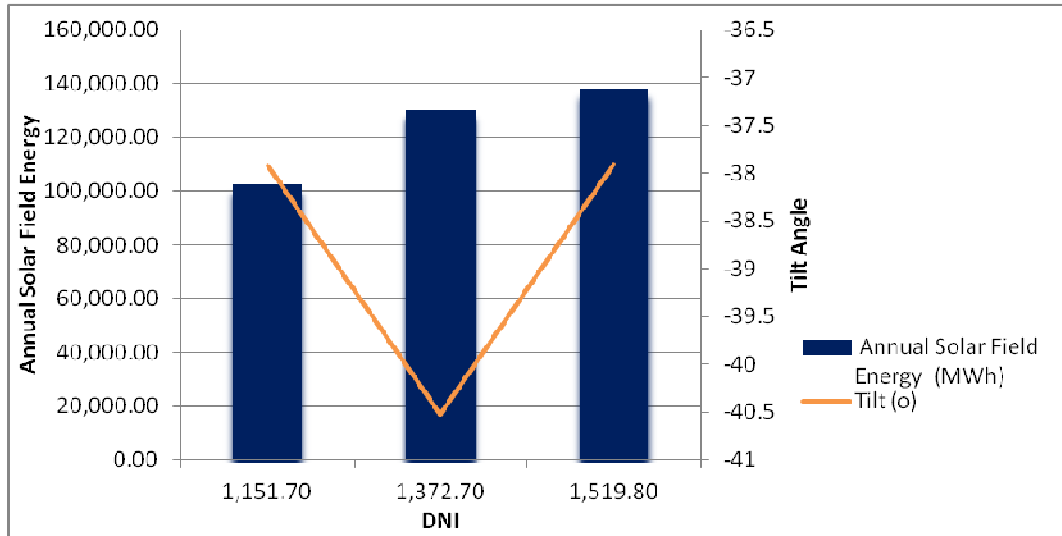


Figure 4.38: The correlation of annual solar field energy and, the DNI and collectors tilt.

4.4.2 Output of the Initial Setup

Having determined the most appropriate location for the installation of the CSPP, this study goes on with the review of the output calculated based on the initial setup of that CSPP located in Athens. Starting with the gross and net electricity output we realize that the CSPP remains net producer of electric energy during the whole year, outweighing fully parasitic loads deducted from the gross electric output (Figure 4.39). Estimated annual values are 50.691.000 kWh and 44.971.173 kWh respectively.

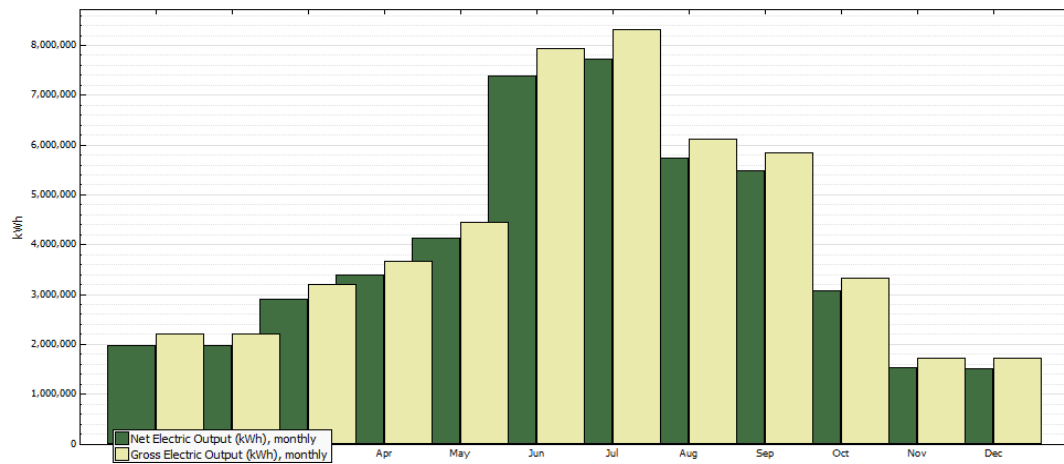


Figure 4.39: The monthly distribution of gross and net electric output.

Looking for major sources causing this energy reduction, we notice a remarkable compliance among the net electric output and the tank freeze protection energy. The latter indicates the energy consumed so that the TES HTF does not freeze (Figure 4.40).

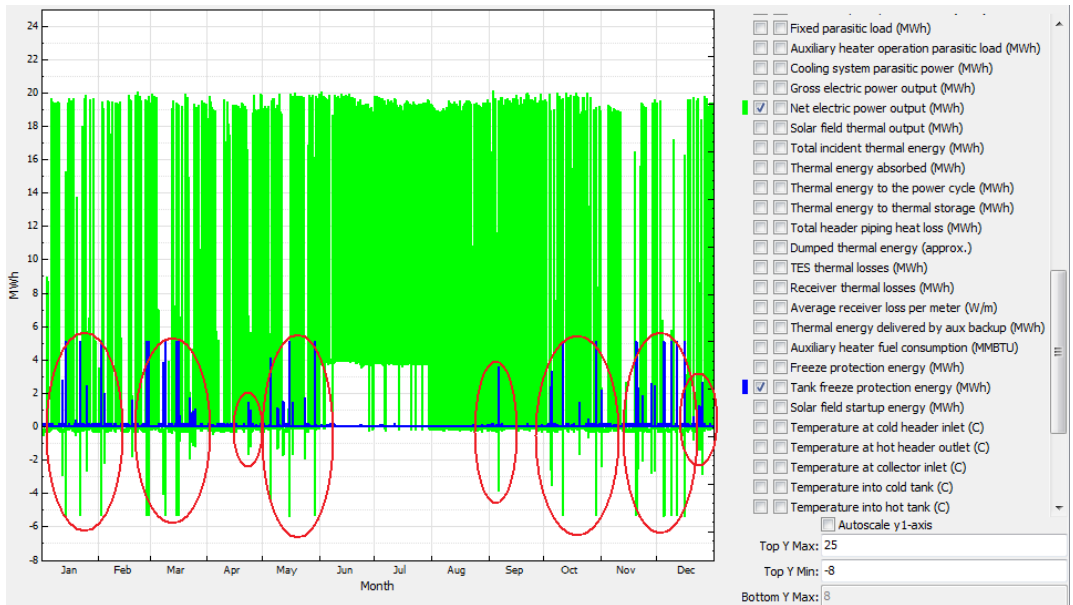


Figure 4.40: Net electric power output and freeze protection energy.

Additionally, having set the goal of utilizing thermal energy produced by auxiliary sources up to 15% of this produced by the solar field, we calculate the respective fraction at 7,65%. This was derived by the sum of energy produced by the fossil fuel-fired boiler and the electrical heaters used to protect the HTFs from being frozen and its division to the solar field thermal output (Figure 4.41). Please note that this auxiliary energy comes at 0,024%, 2,41% and 97,567% from the solar field HTF freeze protection, TES HTF freeze protection and fossil fuel-fired boiler operation respectively.

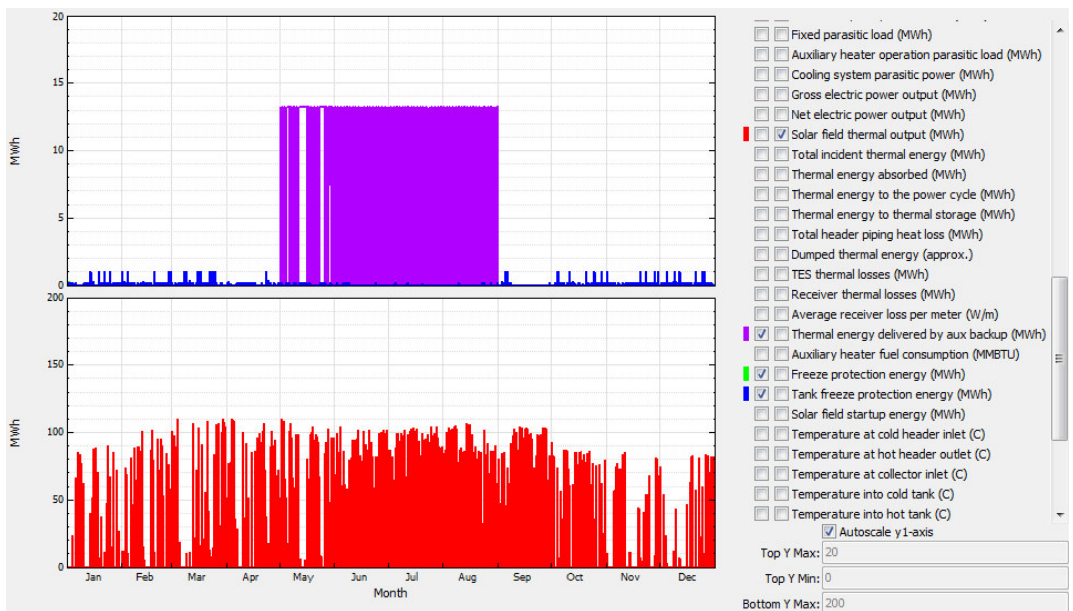


Figure 4.41: Solar thermal output and thermal energy produced by the auxiliary heaters.

Finally we point out that changing the location of the CSPP caused variations in two more output values. The first one is the land required as the same CSPP needed approximately 121 acres of land in Thessaloniki but only 108 (437.060 m²) in Athens. The second change does not really delights like the former, as dumped thermal energy surged at 548,7 MWh (Figure 4.42)

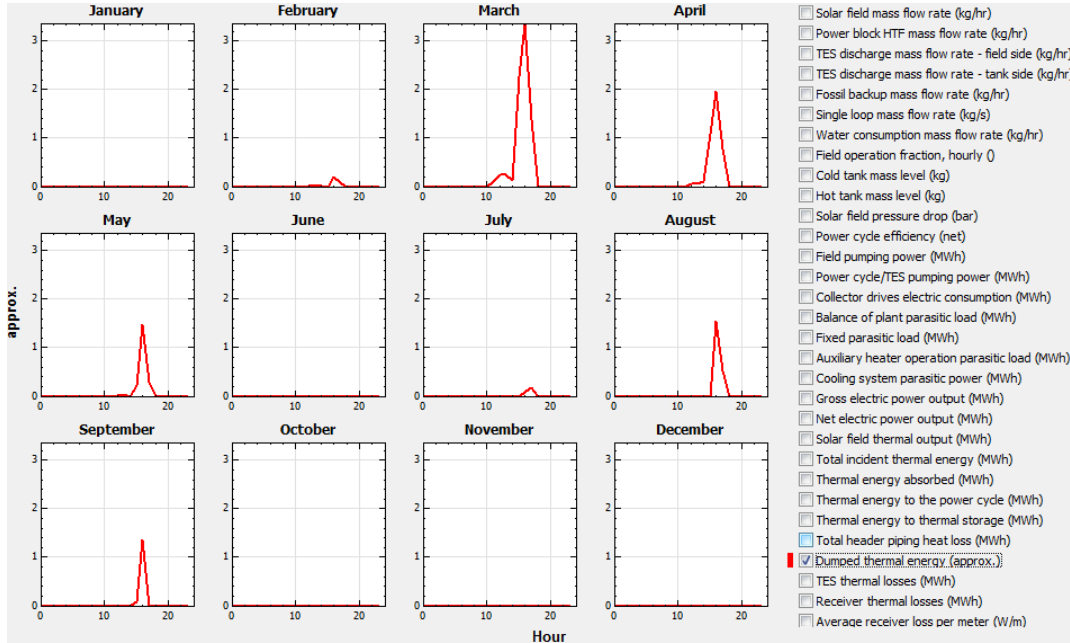


Figure 4.42: The monthly profile of the dumped thermal energy.

4.4.3 Parametric Analysis

After this short but critical review of the initial set up we utilize SAM's ability to perform parametric analysis of data inserted into the model, starting with the solar field and specifically with probably the only two variables that do not affect the installation and O&M costs: the tilt and azimuth angle¹⁵. Figure 4.43 shows the first step of parametric analysis performed regarding the collectors tilt. After this, several levels of analysis took place, finally defining a value range between -31° and -30.5° and the increment at $0,1^{\circ}$. This simulation set indicates a rather clear system outperformance, in terms of net annual energy, when the tilt equals to $-30,5^{\circ}$. The reduction of the tilt, com-

¹⁵ Parametric analysis requires the definition of a starting and ending value, as well as the increment size. This means that large value range and small increments increases significantly the simulation time. For this reason all parametric analysis presented hereinafter were performed in multiple steps, utilizing initially large value ranges and increments which shrink when the value range containing the optimal option becomes clear.

pared to the initial polar arrangement, is obviously caused by the system performance profile shown in Figure 4.39 which indicates the need of a lower tilt between May and September harvesting larger amounts of DNI. This change rises the gross and net electric output from 50.605.900 kWh and 44.884.621 kWh to 52.419.700 kWh and 46.509.054 kWh respectively. Similarly working for the azimuth angle, it is proven that the initial configuration (0°) is the optimal one.

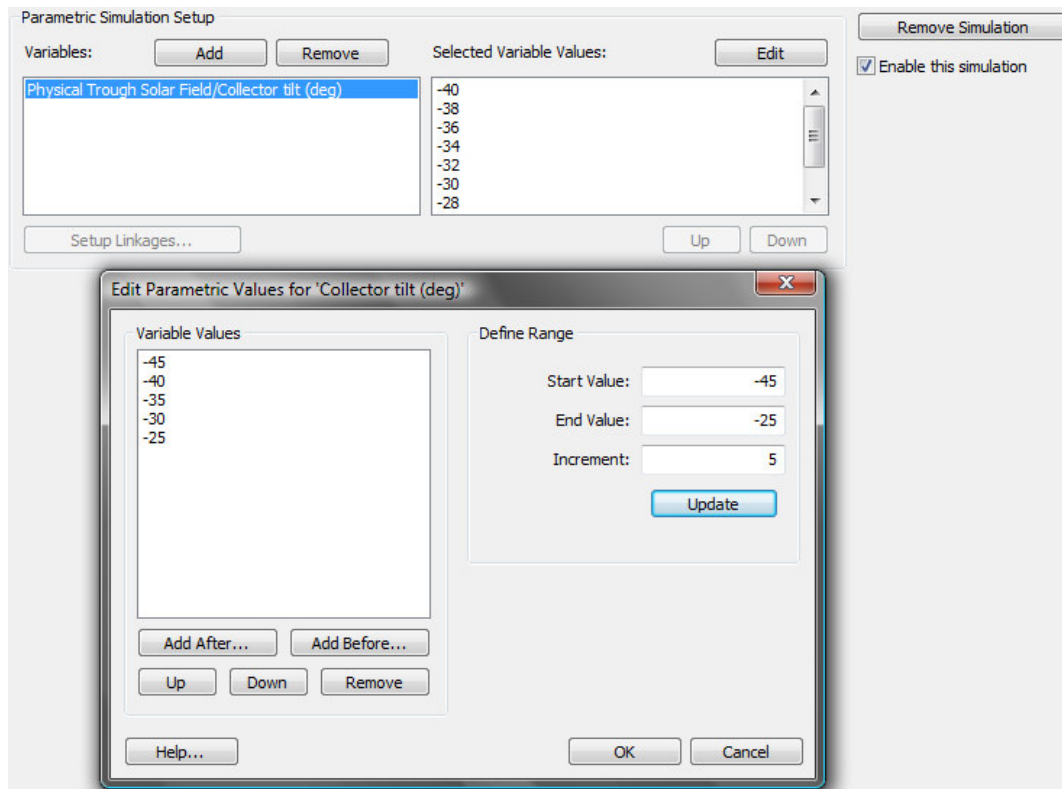


Figure 4.43: The SAM parametric analysis module.

On the other hand, looking for the optimal stow and deploy angle, we utilize SAM's optimization module. The range of values, within simulation is performed, is also defined but this time no increment determination is needed. Instead users are enabled to fill in a series of values setting their controlling preferences on the optimization process. Initially set values are found to be optimal again (Figure 4.44). The same conclusion is reached in the case of the number of subfields and the number of SCA assemblies per loop.

Ending with the optimization of the solar field, we distinguish the used HTF (Therminol VP-1) performance as its temperature operation range allows it to fully car-

ry out the assigned task while its relatively low minimum operation temperature result in trivial needs in auxiliary heating. Under the latest configuration this amount of energy equals to 4,35 MWh. As a result, searching for an alternative does not seem to be highly important.

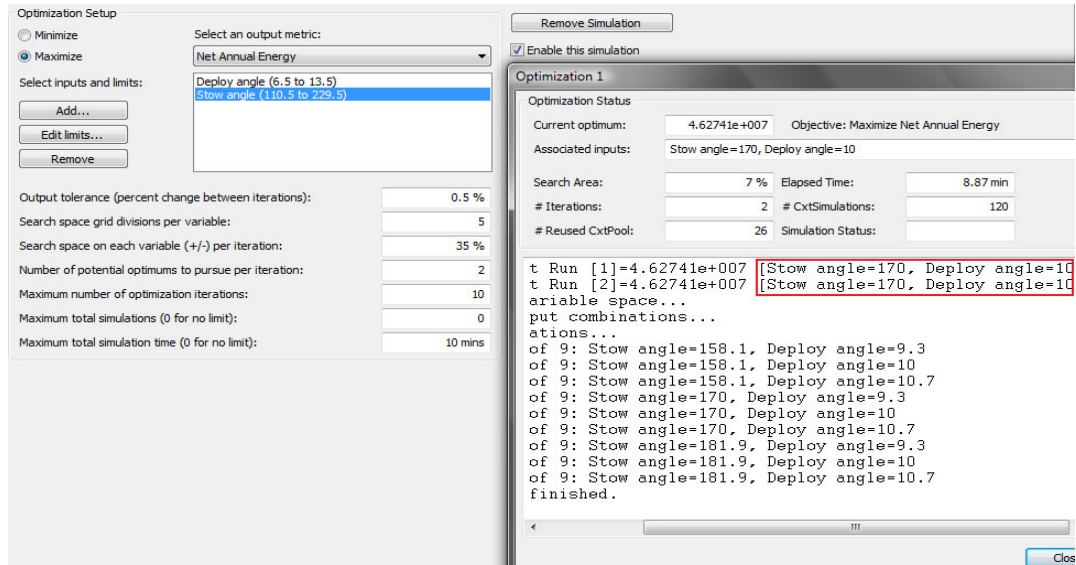


Figure 4.44: The optimal stow and deploy angles.

At this point we remind that the optimal solar multiple is estimated in paragraph 4.6.4, having completed before finance-related datasets included in the respective tabs. Moreover SAM allows a similar optimization of the row spacing too, the rise of which simultaneously increases the collected solar energy, the required land and the installation and O&M costs related to the piping and HTF. However further analysis on the latter is not performed, considering the related bibliography used reliable enough.

Moving to the collectors and receivers tabs, the only variable that could be parametrically analyzed is the type of the annular gas. Once more initial choice seems to be the most suitable (Figure 4.45).

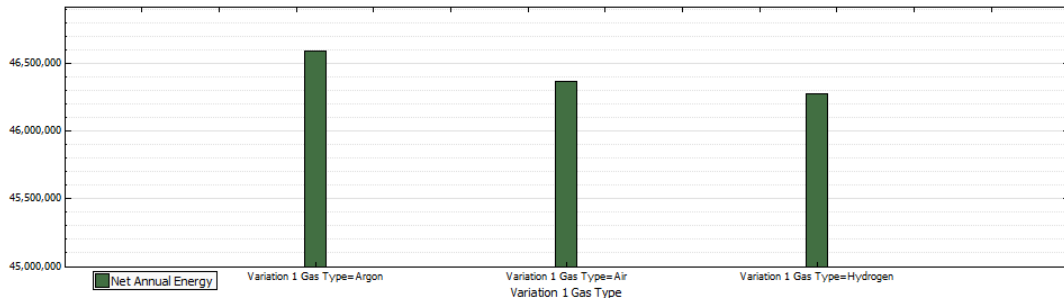


Figure 4.45: The optimal annular gas type used in the receivers.

Similarly in the power cycle tab, having settled on the CSPP’s gross output and type of cooling system (see 4.3.6), parametric analysis is considered meaningless for other parameters than the low resource standby period. Nevertheless, Figure 4.46 proves the appropriateness of the initial choice not to foresee such an operating mode.

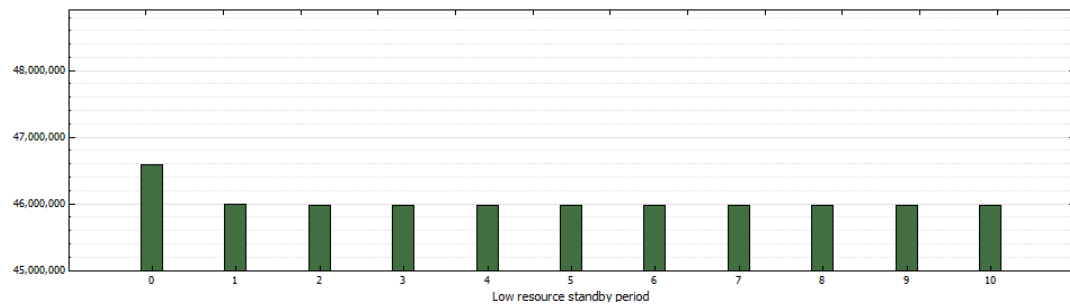


Figure 4.46: No low resource standby period is proposed.

In the thermal storage tab though, plenty of work has to be done. Starting with the full hours of TES someone is tempted to increase the TES system capacity, as the modification of the collectors tilt led the annually dumped thermal energy increase at 974 MWh. Nevertheless, watching the mitigation of the energy saved by the storage capacity increase (Figure 4.47) and counting in the rise of the installation and O&M costs that it causes, we prefer to preserve this figure unmodified (5h). Besides, this measure is being further optimized, taking into account cost effects too, in paragraph 4.6.4.

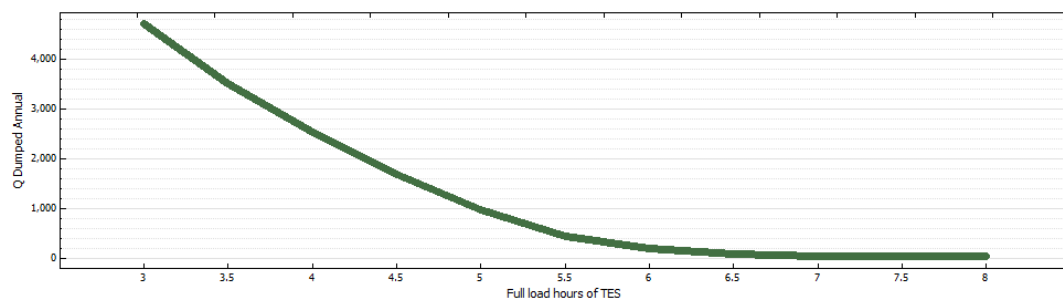


Figure 4.47: Mitigation of benefits leads to the preservation of the current TES capacity.

With regard to the number of parallel tank pairs it is found that current configuration outperforms compared to alternatives, while the tank heater capacity, after a multi-level parametric analysis is found to be optimized at the value of 1.9 MW. A change is proposed in the case of the HTF used in the TES system, as utilizing the same HTF with this used in the solar field (Therminol VP-1) seems as the most appropriate alternative.

Since SAM does not allow the simultaneous optimization taking into account various HTFs and the tank heater capacity, the latter is parametrically analyzed again. Indeed, this time the optimal tank heater capacity is reduced at 1 MW while dumped thermal energy also drops at 675 MWh.

Finally, remaining focused on the objective for full coverage of the allowable 15% of auxiliary thermal energy, compared to this produced by the solar field, as well as on the operation strategy set and documented in 4.3.7, we recalculate the current fraction at approximately 7% (detailed description of this calculation is provided in 4.4.2) and partially add the second scheduling period in a radical way (see 4.3.7). By the time that this configuration is applied to all of the days, both weekdays and weekends, of May and August, the fossil fraction equals to 15,11%. For nonce this fraction is considered to be acceptable, while the advanced reliability achieved between May and August is clearly illustrated in Figure 4.48. Under the optimal configuration, net electricity output raises at 51.082.341 kWh, while dumped energy falls at 666 MWh.

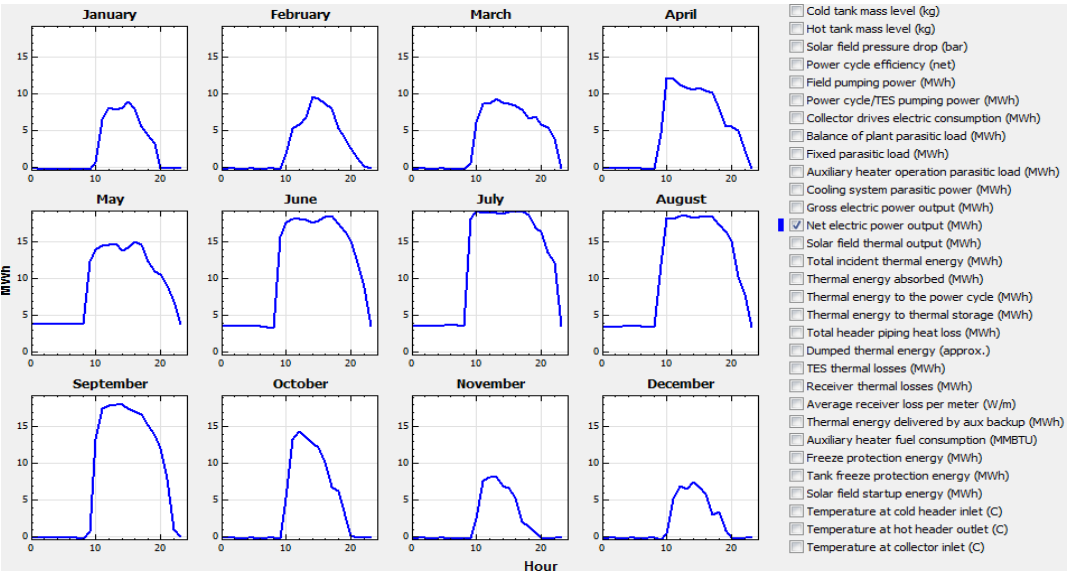


Figure 4.48: The monthly profile of the net electric output corresponding to the optimal setup.

Reaching the last tab of the SAM model - parasitics, we consider parametric analysis as meaningless because the variance of these figures does not necessarily correspond to different configurations.

4.5 Probabilistic Modeling

Ending paragraph 4.4.3, parametric analysis of parasitic loads was discarded. However, since variations in their values may significantly affect the CSPP performance, users should further analyze them. Performing sensitivity analysis, of crucial output variables based on the potential volatility of certain input data, allows modelers to determine the level on which the latter affect the former. This supports decision-making regarding the impactful selection of input variables that will be further analyzed in terms of probabilistic modeling. Utilizing results shown in Figure 4.49 we consider that the top 14 of them and the piping thermal loss coefficient should be used in a probabilistic modeling approach. Please note that this result counters our initial hypothesis that any of the parasitic loads significantly affects the energy produced, while it makes clear that estimating accurately performance coefficients of several components emerges as a high priority.

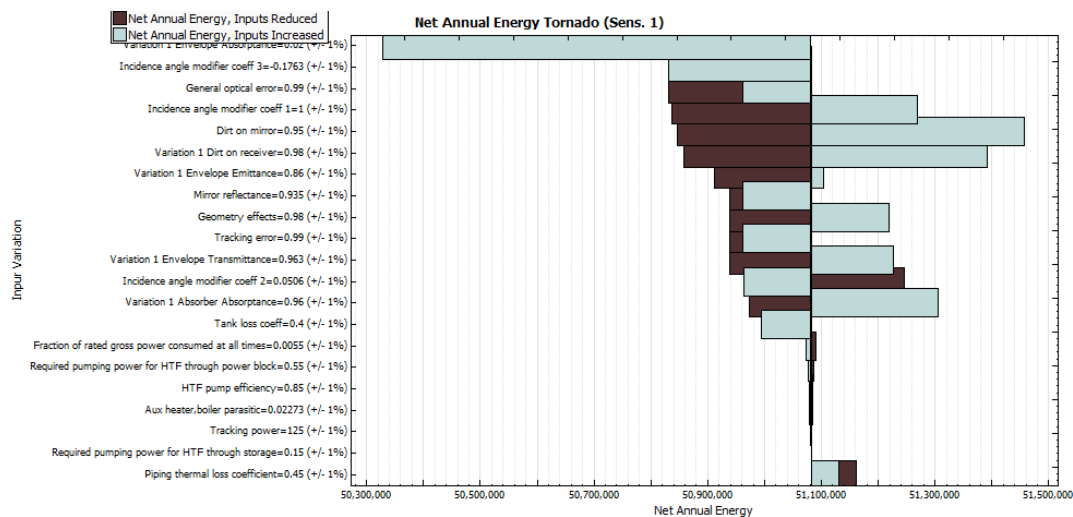


Figure 4.49: Sensitivity analysis of net electric output to selected parasitic loads.

Having selected the input data distinguished for its inherent uncertainty and major impact on net electric output, SAM enables users to perform probabilistic modeling by defining to each one of them a specific probability distribution and its characteristic values. Since the two distributions mainly assumed for related values are the uniform and the normal one, these characteristic values are the range of values, and the mean value and the deviation respectively (Figure 4.50). Furthermore users are enabled to indicate any potential correlations among the variables that are to be probabilistically modeled as well as the number of sampled values per variable.

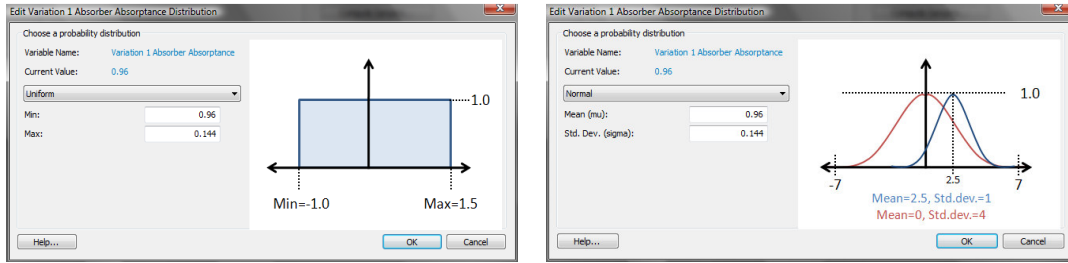


Figure 4.50: Defining whether an input variable follows a uniform or a normal distribution.

The major challenge faced at this stage by the modelers is making a choice among known distributions and determining their characteristic values. This comes from the lack of related data accompanying technical properties of installed equipment. This has been the reason for which related researching efforts were based on either, hypothetical distributions and characteristic values, or limited past experience which could definitely not document a well-grounded related setting [40]. Since this study has not been able to override these challenges, probabilistic modeling performed obtains a rather exhibition rather than a substantial meaning. As such, with regard to the 15 variables selected above, we assume that they follow a normal distribution with a mean value equal to this defined in the deterministic modeling process and a deviation equal to the 15% of the mean value. The number of sampled values per variable was set at 50 which clearly meets the request for at least $4k/3^{16}$ sampled values ($=20$). Indeed, random cross-checking of the distribution followed by the general optical error proves the appropriateness of the variable sampling (Figure 4.51).

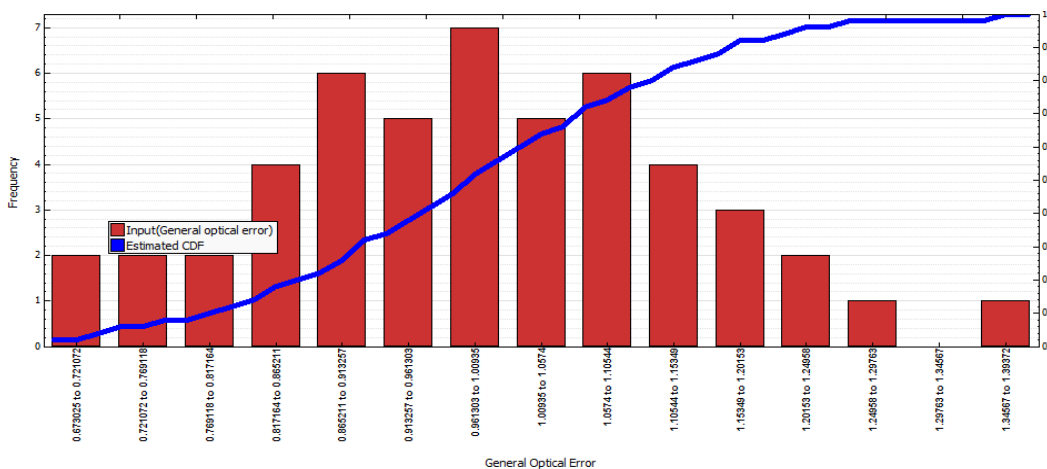


Figure 4.51: The histogram/cumulative distribution function of the general optical error.

¹⁶ k corresponds to the number of variables.

The diagram, corresponding to the annual net electric output, is shown in Figure 4.52 indicating a probability of 50% so that the CSPP produces annual net electric output equal to or more than 50.550.099 kWh.

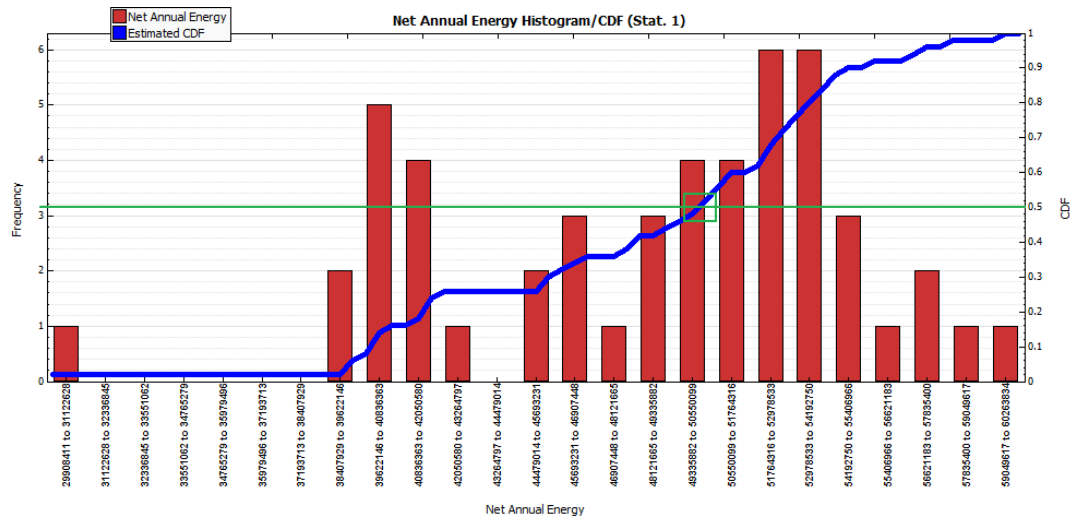


Figure 4.52: The histogram/cumulative distribution function of the net annual energy.

Finally, since during the probabilistic modeling process SAM performs a step-wise regression analysis too, below we present the estimated correlation factors. Figure 4.53 definitely imposes a different impact ranking of each variable compared to this estimated in the sensitivity analysis in the beginning of this paragraph. Nevertheless this should not cause any confusion as it relies on the limited explanatory variables used in the probabilistic approach and the size of each one of them.

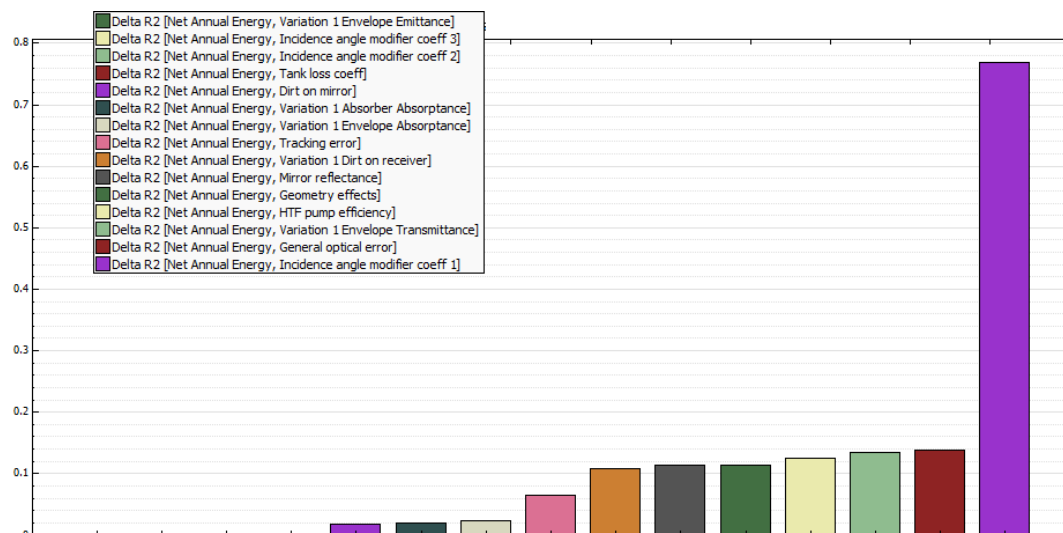


Figure 4.53: Estimated δR^2 s of the uncertain variables.

4.6 Financial Modeling

When related costs are included in the analysis, the optimal design of a CSP plant may change significantly. Therefore, in this section the previously modeled 20 MW CSPP is being redesigned aiming this time at the optimal LCOE for each one of the three locations. The parameters that are not altered are a) the plant capacity, b) its hybridization, c) its ability to store energy capable of preserving the plant operation at its nominal capacity for at least 2 hours and d) the absence of land and capital constraints. This section ends with a short review of the feasibility of such an investment in the 3 locations through the parametric analysis of the respective internal rates of return (IRR).

4.6.1 Trough System Costs

Starting with the investment and O&M cost, assumptions shown in Figure 4.54 rely strongly on a previous study highly adjusted to the SAM configuration [182]. Moreover we assumed that¹⁷ a) the cost of the **fossil backup system**, regardless of the fuel burned (natural gas, LPG or diesel), equals to **130\$/kWe**, based on information gathered directly from the market, b) the **balance of the plant does not really require the provision of additional costs**, c) **no contingency costs should be counted in** as parametric analysis is performed afterwards, d) the **land** is being bought for **5.260 \$/acre**, e) **no sales tax** (value added tax) **is applied on the investment costs** as they are fully deducted from the sales tax collected by the company in the future, a condition that SAM cannot model, f) **no fixed annual cost is considered to be applied** as we estimate a fixed cost by capacity, g) **no variable cost by generation** is applied considering that only the fuel cost really varies with the generation, h) the cost of **natural gas, LPG and diesel** are **24** [183], **42** [184]¹⁸ and **57** [184] \$/MMBTU¹⁹ respectively – or 0,08, 0,14 and 0,19 \$/kWh and i) **the escalation rate above inflation is 0%** considering the successful estimation of such a figure rather utopic. Finally due to the extensive uncertainty of this dataset, exploiting SAM's ability to count in an annual schedule regarding the individual O&M costs was considered to be rather meaningless.

¹⁷ The Euro/US-dollar exchange rate was taken equal to 1,33.

¹⁸ Due to the lack of official LPG prices this value was estimated by taking into account Slovakia's prices which are similar to these of Greece.

¹⁹ This measure is the only one for which SAM utilizes the imperial and not the metric system.

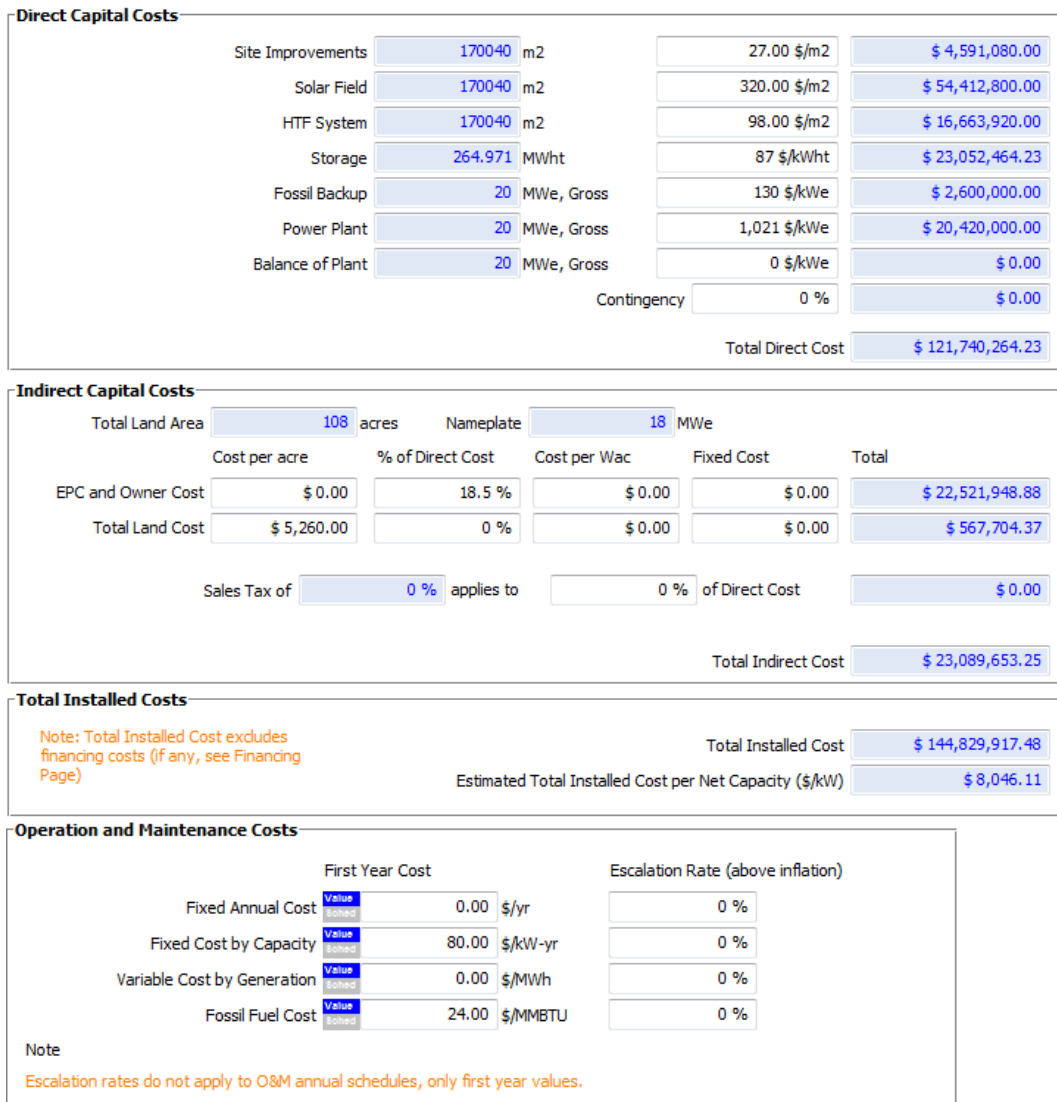


Figure 4.54: Trough system costs.

4.6.2 Financing

With regard to the financing scheme (Figure 4.55), we consider that the **analysis period** extends up to **25 years** based on the duration of the Power Purchase Agreement (PPA). The **inflation rate** is estimated at **2%** while the **real discount rate** is considered to be **10%**²⁰. The **federal tax** – corresponds to the Greek profit tax, is assumed to be **25%** mostly based on the historical trend rather than adopting the current legislation,

²⁰ This estimation mostly relies on a rather arbitrary assumption according to which investors would demand a return rate greater by 100 base points compared to this of loans provided by domestic banks. The alternative of using a related model in order to calculate the real discount rate has been neglected as the notion of the, widely used in the past, risk-free investment has recently collapsed.

while the **sales tax** is set at **0%** as it deducts fully from the sales tax collected by the company. **Insurance** will annually cost approximately **0,4%** of the installed cost, while the **net salvage value** is set at **0,4%** of the initial investment so that we count in the value of the land and discard any equipment salvage value potentially countered by dismantling and recycling costs. Finally **no property tax** is applied.

General Analysis Period <input type="text" value="25"/> years Inflation Rate <input type="text" value="2.00"/> % Real Discount Rate <input type="text" value="10.00"/> % Nominal Discount Rate <input type="text" value="12.20"/> %		Taxes and Insurance Federal Tax <input type="text" value="25.00"/> %/year State Tax <input type="text" value="0.00"/> %/year Sales Tax <input type="text" value="0.00"/> % Insurance <input type="text" value="0.40"/> % of installed cost																																																													
Salvage Value Net Salvage Value <input type="text" value="0.40"/> % of installed cost End of Analysis Period Value <input type="text" value="\$ 579,319.67"/>		Property Tax Assessed Percent <input type="text" value="0.00"/> % of installed cost Assessed Value <input type="text" value="\$ 0.00"/> Assessed Value Decline <input type="text" value="0.00"/> %/year Property Tax <input type="text" value="0.00"/> %/year																																																													
Construction Period <table border="1"> <thead> <tr> <th>Loan</th> <th>Percent of Installed Costs</th> <th>Up-front Fee (%)</th> <th>Months Prior to Operation</th> <th>Interest Rate (Annual)</th> <th>Principal Amount</th> <th>Interest</th> <th>Total Construction Financing Cost</th> </tr> </thead> <tbody> <tr> <td>Loan 1</td> <td><input type="text" value="0"/></td> <td><input type="text" value="0"/></td> <td><input type="text" value="0"/></td> <td><input type="text" value="0"/></td> <td><input type="text" value="\$ 0.00"/></td> <td><input type="text" value="\$ 0.00"/></td> <td><input type="text" value="\$ 0.00"/></td> </tr> <tr> <td>Loan 2</td> <td><input type="text" value="0"/></td> <td><input type="text" value="0"/></td> <td><input type="text" value="0"/></td> <td><input type="text" value="0"/></td> <td><input type="text" value="\$ 0.00"/></td> <td><input type="text" value="\$ 0.00"/></td> <td><input type="text" value="\$ 0.00"/></td> </tr> <tr> <td>Loan 3</td> <td><input type="text" value="0"/></td> <td><input type="text" value="0"/></td> <td><input type="text" value="0"/></td> <td><input type="text" value="0"/></td> <td><input type="text" value="\$ 0.00"/></td> <td><input type="text" value="\$ 0.00"/></td> <td><input type="text" value="\$ 0.00"/></td> </tr> <tr> <td>Loan 4</td> <td><input type="text" value="0"/></td> <td><input type="text" value="0"/></td> <td><input type="text" value="0"/></td> <td><input type="text" value="0"/></td> <td><input type="text" value="\$ 0.00"/></td> <td><input type="text" value="\$ 0.00"/></td> <td><input type="text" value="\$ 0.00"/></td> </tr> <tr> <td>Loan 5</td> <td><input type="text" value="0"/></td> <td><input type="text" value="0"/></td> <td><input type="text" value="0"/></td> <td><input type="text" value="0"/></td> <td><input type="text" value="\$ 0.00"/></td> <td><input type="text" value="\$ 0.00"/></td> <td><input type="text" value="\$ 0.00"/></td> </tr> <tr> <td>Totals:</td> <td><input type="text" value="0"/></td> <td><input type="text" value="0"/></td> <td><input type="text" value="0"/></td> <td><input type="text" value="0"/></td> <td><input type="text" value="\$ 0.00"/></td> <td><input type="text" value="\$ 0.00"/></td> <td><input type="text" value="\$ 0.00"/></td> </tr> </tbody> </table> <p>Note: If you specify construction period loans, the sum of percentages in the Percent of Installed Costs column must equal 100.</p>								Loan	Percent of Installed Costs	Up-front Fee (%)	Months Prior to Operation	Interest Rate (Annual)	Principal Amount	Interest	Total Construction Financing Cost	Loan 1	<input type="text" value="0"/>	<input type="text" value="0"/>	<input type="text" value="0"/>	<input type="text" value="0"/>	<input type="text" value="\$ 0.00"/>	<input type="text" value="\$ 0.00"/>	<input type="text" value="\$ 0.00"/>	Loan 2	<input type="text" value="0"/>	<input type="text" value="0"/>	<input type="text" value="0"/>	<input type="text" value="0"/>	<input type="text" value="\$ 0.00"/>	<input type="text" value="\$ 0.00"/>	<input type="text" value="\$ 0.00"/>	Loan 3	<input type="text" value="0"/>	<input type="text" value="0"/>	<input type="text" value="0"/>	<input type="text" value="0"/>	<input type="text" value="\$ 0.00"/>	<input type="text" value="\$ 0.00"/>	<input type="text" value="\$ 0.00"/>	Loan 4	<input type="text" value="0"/>	<input type="text" value="0"/>	<input type="text" value="0"/>	<input type="text" value="0"/>	<input type="text" value="\$ 0.00"/>	<input type="text" value="\$ 0.00"/>	<input type="text" value="\$ 0.00"/>	Loan 5	<input type="text" value="0"/>	<input type="text" value="0"/>	<input type="text" value="0"/>	<input type="text" value="0"/>	<input type="text" value="\$ 0.00"/>	<input type="text" value="\$ 0.00"/>	<input type="text" value="\$ 0.00"/>	Totals:	<input type="text" value="0"/>	<input type="text" value="0"/>	<input type="text" value="0"/>	<input type="text" value="0"/>	<input type="text" value="\$ 0.00"/>	<input type="text" value="\$ 0.00"/>	<input type="text" value="\$ 0.00"/>
Loan	Percent of Installed Costs	Up-front Fee (%)	Months Prior to Operation	Interest Rate (Annual)	Principal Amount	Interest	Total Construction Financing Cost																																																								
Loan 1	<input type="text" value="0"/>	<input type="text" value="0"/>	<input type="text" value="0"/>	<input type="text" value="0"/>	<input type="text" value="\$ 0.00"/>	<input type="text" value="\$ 0.00"/>	<input type="text" value="\$ 0.00"/>																																																								
Loan 2	<input type="text" value="0"/>	<input type="text" value="0"/>	<input type="text" value="0"/>	<input type="text" value="0"/>	<input type="text" value="\$ 0.00"/>	<input type="text" value="\$ 0.00"/>	<input type="text" value="\$ 0.00"/>																																																								
Loan 3	<input type="text" value="0"/>	<input type="text" value="0"/>	<input type="text" value="0"/>	<input type="text" value="0"/>	<input type="text" value="\$ 0.00"/>	<input type="text" value="\$ 0.00"/>	<input type="text" value="\$ 0.00"/>																																																								
Loan 4	<input type="text" value="0"/>	<input type="text" value="0"/>	<input type="text" value="0"/>	<input type="text" value="0"/>	<input type="text" value="\$ 0.00"/>	<input type="text" value="\$ 0.00"/>	<input type="text" value="\$ 0.00"/>																																																								
Loan 5	<input type="text" value="0"/>	<input type="text" value="0"/>	<input type="text" value="0"/>	<input type="text" value="0"/>	<input type="text" value="\$ 0.00"/>	<input type="text" value="\$ 0.00"/>	<input type="text" value="\$ 0.00"/>																																																								
Totals:	<input type="text" value="0"/>	<input type="text" value="0"/>	<input type="text" value="0"/>	<input type="text" value="0"/>	<input type="text" value="\$ 0.00"/>	<input type="text" value="\$ 0.00"/>	<input type="text" value="\$ 0.00"/>																																																								
Loan Parameters Installed Cost <input type="text" value="\$ 144,829,917.48"/> Construction Financing Cost <input type="text" value="\$ 0.00"/> Principal Amount <input type="text" value="\$ 101,380,942.24"/>				Loan Term <input type="text" value="15"/> years Loan Rate <input type="text" value="9"/> %/year Debt Fraction <input type="text" value="70"/> % WACC <input type="text" value="8.39"/> %																																																											
Solution Mode <input checked="" type="radio"/> Specify IRR Target <input type="radio"/> Specify PPA Price <p style="color: orange; font-size: small;">Choose Specify IRR Target when you know the minimum IRR and want SAM to calculate a PPA price to meet the target. Choose Specify PPA Price when you know the PPA price and want SAM to calculate the resulting IRR. Note that you can specify an optional annual power price escalation rate. See help for details.</p>																																																															
Specify IRR Target Minimum Required IRR <input type="text" value="12.2"/> % PPA Escalation Rate <input type="text" value="1.6"/> %				Specify PPA Price PPA Price <input type="text" value="0.38434"/> \$/kWh PPA Escalation Rate <input type="text" value="1.6"/> %																																																											
Financial Optimization <input type="checkbox"/> Allow SAM to pick a debt fraction to minimize the LCOE <input type="checkbox"/> Allow SAM to pick a PPA escalation rate to minimize the LCOE																																																															
Federal Depreciation <input type="radio"/> No Depreciation <input type="radio"/> 5-yr MACRS <input checked="" type="radio"/> Straight Line (specify years) <input type="text" value="20"/> <input type="radio"/> Custom (specify percentages) <input type="button" value="Edit..."/>				State Depreciation <input checked="" type="radio"/> No Depreciation <input type="radio"/> 5-yr MACRS <input type="radio"/> Straight Line (specify years) <input type="text" value="7"/> <input type="radio"/> Custom (specify percentages) <input type="button" value="Edit..."/>																																																											

Figure 4.55: The financing dataset of the investment.

As far as the used capital mix is concerned, we assume that the investment will be funded by **equity** and **loan** at **30%** and **70%** respectively. **Equity will be used during**

the construction period, which will last approximately 12 months, while the **loan will repay the rest of the investment cost by the time the CSPP is completed**. The **loan term** is set at **15 years** and its **annual interest rate at 9%**.

With regard to the solution mode that SAM will adopt, we select the “**Specify IRR target**” as initially we need to size the solar field and the storage system for a certain value of IRR. The latter is considered to be equal to the **nominal discount rate** (=12,2%). According to the Greek legislation [36], this CSPP’s PPA price is currently set at 397,25 \$/MWh, escalating annually by the 80% of the variation of the Consumer Price Index as it is published by the Bank of Greece. The latter condition results to an estimated **price escalation rate** of **1,6%** (= estimated inflation rate x 80%) while the initial **PPA price** is reduced by 3%, being modified at **384,34 \$/MWh**, due to a special tax applied on the 3% of the gross sales of such a company [36].

Finally we set the financial model so that it counts in a **straight line depreciation method** for **20 years** based on the related Greek legislation [185].

4.6.3 Tax Credit and Payment Incentives

In order to eliminate uncertain factors that could significantly and incorrectly prettify the related outcomes, this financial analysis does not count in any potential tax credit and payment incentives that can be simulated by the model and Greek Government has occasionally provided to companies producing energy from RES.

4.6.4 Sizing the Solar Field

Based on the results provided in 4.4.3, concerning the technical optimization of the CSPP located in Athens for a solar multiple of 2, and the financial assumptions made in 4.6.1, 4.6.2 and 4.6.3, the plant operation is simulated multiple times for each one of the three different locations, a storage capacity of 2-8 hours (by an 1-hour step) and a solar multiple of 1-3 (by a 0,25 step). Please note that, due to SAM’s inability to take into account the objective set in paragraph 4.3, according to which energy delivered by fossil fuels is approximately the 15% of the energy produced by the solar field, parametric analysis performed afterwards considers no fossil fuel-fired boiler, as the related calculations would be highly time-consuming. This simplification does not really affect the purpose of this comparison since it discards minor reductions of the LCOE caused almost exclusively by the increase of the solar multiple.

Figure 4.56 shows the outcome of the parametric analysis mentioned above regarding Athens. Since graphically it is hard to say the conditions under which the LCOE is optimized, we examined the related values reaching the conclusion that the **optimal LCOE (41.611 \$/kWh)** is achieved for a **s.m. of 2.5** and a **thermal capacity of 7 hours of full load**. An alternative combination could be that of a s.m. of 1,75 and a thermal capacity of 2,5 hours of full load, resulting a LCOE of 41.6359 \$/kWh. Given that we consider no land constraints and keeping in mind that the financial benefit of counting in energy produced by the auxiliary boiler is larger in the first option, we adopt the former configuration.

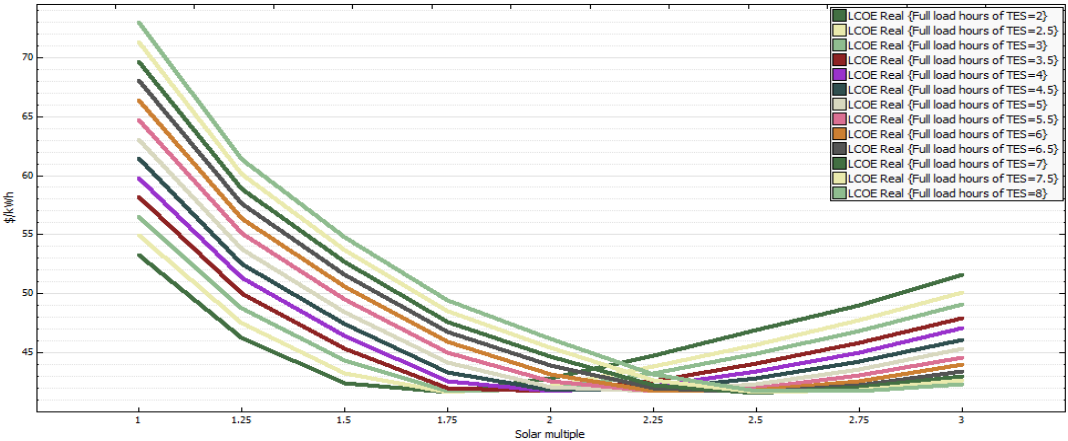


Figure 4.56: The optimal solar multiple-storage capacity combination for Athens.

Similarly working for Thessaloniki, we calculate the **optimal LCOE at 45.0331 \$/kWh** for a **s.m. of 2,5** and a **thermal capacity of 6,5 hours of full load** (Figure 4.57). The respective values for Andravida are **58,2501 \$/kWh, 2,5** and **5,5 hours** (Figure 4.58).

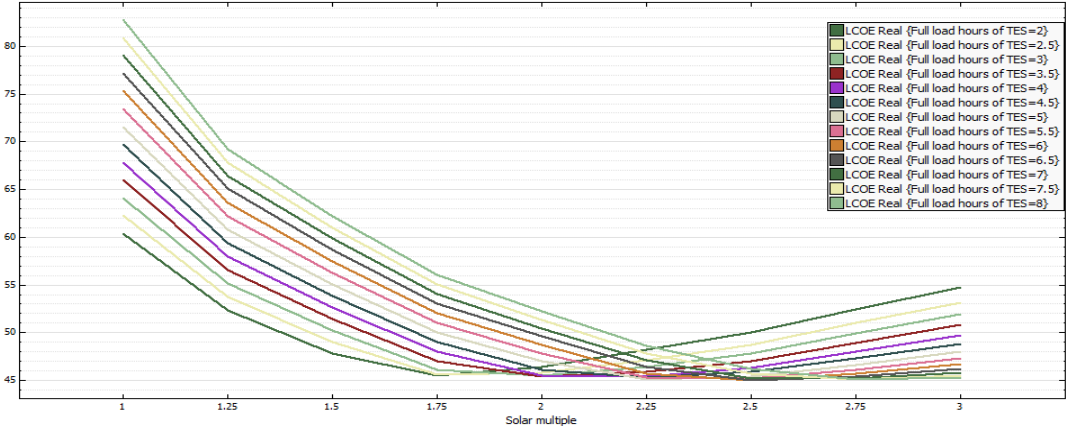


Figure 4.57: The optimal solar multiple-storage capacity combination for Thessaloniki.

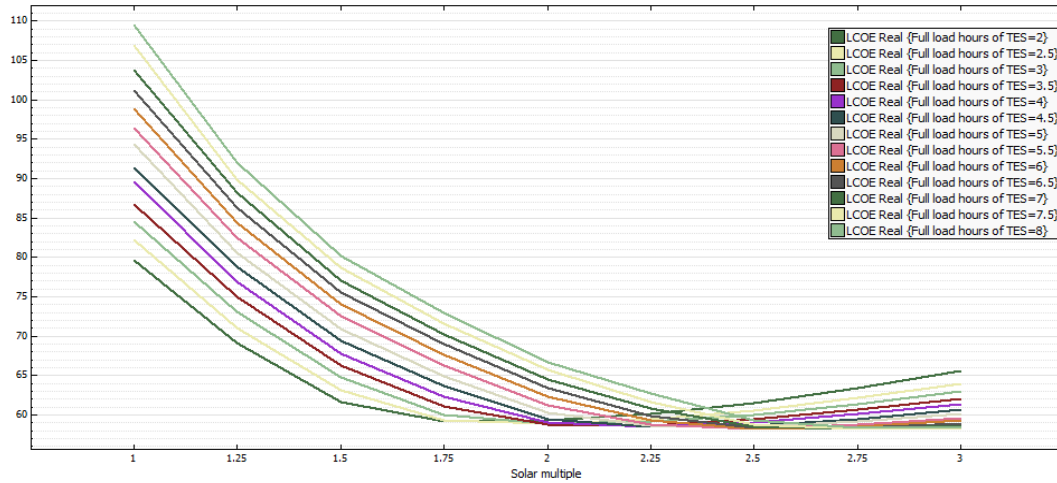


Figure 4.58: The optimal solar multiple-storage capacity combination for Andravida.

4.6.5 Technical Optimization

Due to the technical redesign imposed by the sizing of the solar field and the adjustment of the thermal storage capacity, the three CSPPs have to be technically optimized again.

In the case of Athens, initially we determine the period for which the fossil fuel-fired boiler operates (see Figure 4.34). This time we assume that the respective period is April-August. Indeed, based on this assumption the estimated energy produced by fossil fuels constitutes the 13.5% of the energy delivered by the solar field. The only figure left to be further analyzed is the tank heater capacity. Figure 4.59 clearly shows that the optimal value is 0,6 MWt – values larger than 3 MW tend to reduce the energy produced annually. Furthermore, rechecking the ratio of fossil/solar energy, we realize that the limit of 15% is still not exceeded (13.8%).

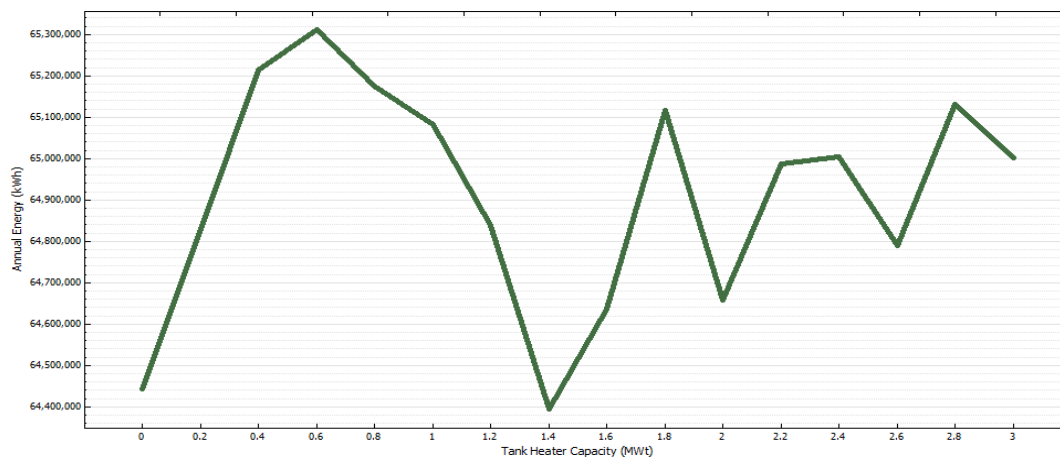


Figure 4.59: The optimal tank heater capacity for Athens.

With regard to the city of Thessaloniki, technical optimization will start with the collectors tilt. Working in a similar way to this presented in paragraph 4.4.3, we find out that the optimal value is $-31,7^\circ$. Afterwards we configure the period for which the fossil fuel-fired boiler operates. Setting values similar to these for the case of Athens, we notice that the ratio of fossil/solar energy is $15,7\% > 15\%$. This forces us to limit the boiler operation by excluding its contribution during April's weekends. The new scheduling results an acceptable ratio of fossil/solar energy equal to $14,5\%$. Finally, looking for the optimal tank heater capacity, we conclude that the value of $0,6$ MWt constitutes the optimal one, just like in the case of Athens. The ratio of fossil/solar energy is not further analyzed since the calculation made above took into account a tank heater capacity of $0,6$ MWt.

Finally, in the case of Andravida analysis performed does not really differ from this of Thessaloniki. The optimal collectors tilt is $-36,9^\circ$ while, for a schedule similar to this applied in the case of Thessaloniki, the ratio of fossil/solar energy is estimated at $20,1\%$, far beyond the limit of 15% . This condition is fulfilled²¹ when the fossil boiler operates only during the period May-August ($15,08\%$), excluding May's weekends. The optimal value of the tank heater capacity is $0,6$ MWt for this case too.

The final form of the three models may be found in the related SAM files accompanying this study.

4.6.6 Feasibility Analysis

In order that the feasibility of the three CSPPs is determined, the solution mode shown in Figure 4.55 (see paragraph 4.6.2) is changed into "Specify PPA Price". By this adjustment SAM is being set to calculate the Net Present Value (NPV) and the IRR of the equity invested.

a. Andravida

Starting with Andravida, based on the initial financial assumptions (see paragraphs 4.6.1 to 4.6.3) and the optimal technical configuration (see paragraphs 4.6.4 and 4.6.5), the estimated NPV and IRR are $\$-44.971.692,69$ and 2.81% respectively. Obviously such results can by no means document a wise suggestion for the realization of the investment. Having performed sensitivity analysis on the direct and indirect costs of this

²¹ For the scope of this study we consider $15,08\%$ as an acceptable value.

investing plan (Figure 4.60), the former conclusion does not really change as even if the investment cost drops by 25% - a rather extreme divergence from the mean estimation, the NPV remains negative – or the IRR stands lower than the nominal discount rate. This conclusion remains unchanged even if the O&M cost is also reduced by 25%.

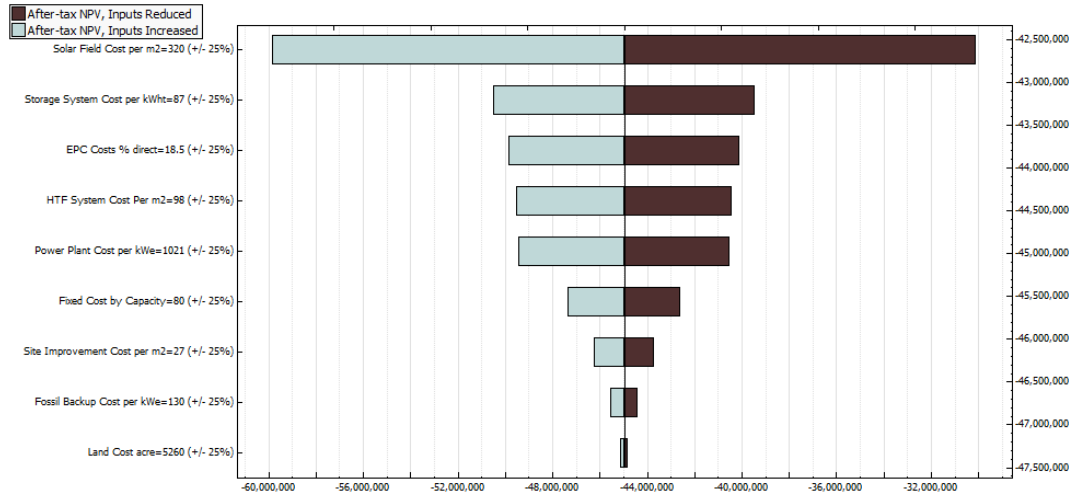


Figure 4.60: Sensitivity analysis between the NPV and the trough system costs (Andravid).

NPV remains negative, even if solely loan is used, a rather unusual capital mix for large energy investments (Figure 4.61).

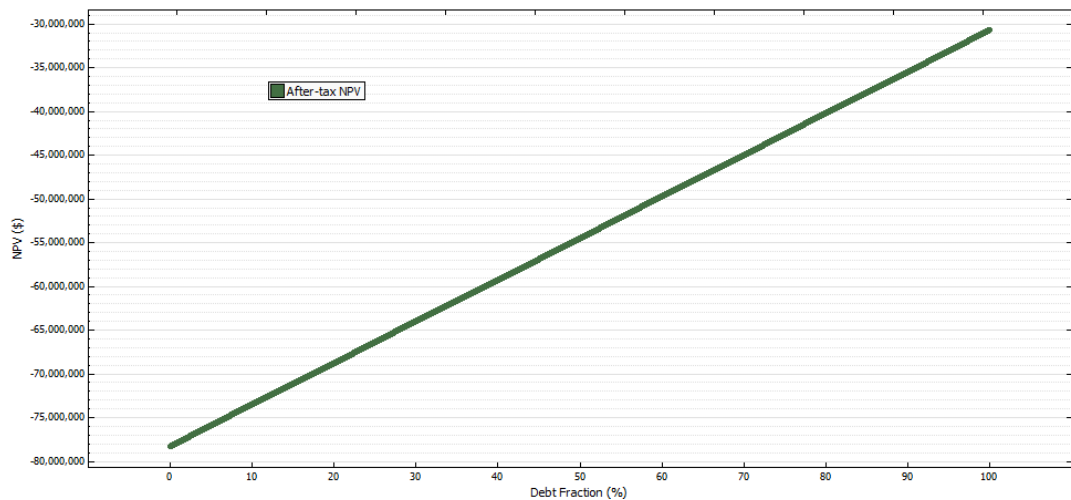


Figure 4.61: Parametric analysis concerning the investment capital mix (Andravid).

On the other hand examining the impact of the loan and the real discount rate, under the assumption that the latter will always be greater than the former by 1% (the blues line on Figure 4.62), a hope for the feasibility of that investment arises, since in a

euphoric financial environment, similar to that during 2003-2007 when the loan rate is limited to 3%, investing in the particular CSPP becomes meaningful.

Financial analysis of Andravida CSPP ends with the quantification of the impact that the fuel usage causes. Based on data forming the lines of the Figure 4.63, the increase of the fossil fuel cost per 1\$/MMBTU reduced the NPV by approximately \$500.000. This practically means that the results presented above could be considered as optimistic, given the absence of natural gas supply in the region and the much higher cost of the alternative fuels – LPG and diesel cost 18 and 33 \$/MMBTU respectively more than the natural gas does (see paragraph 4.6.1).

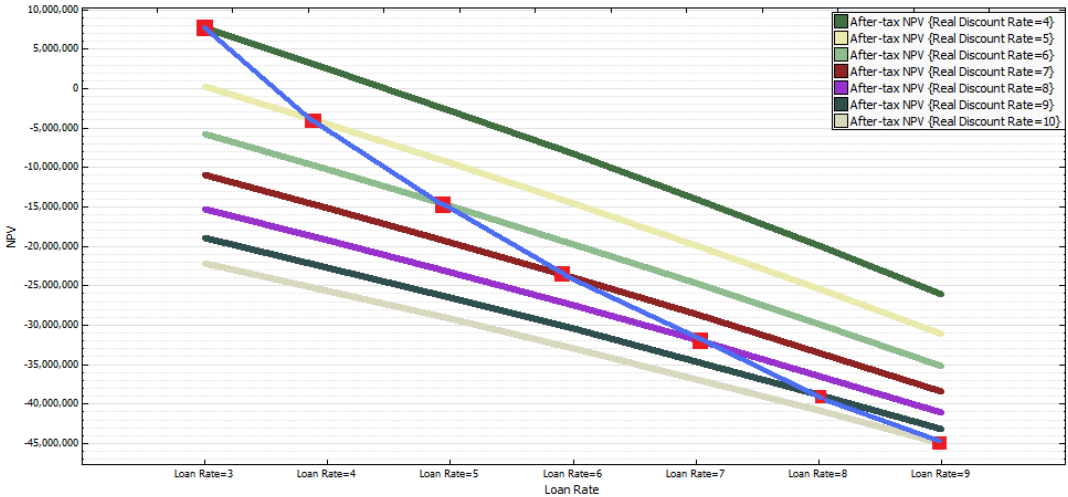


Figure 4.62: Parametric analysis concerning the cost of capital (Andravida).

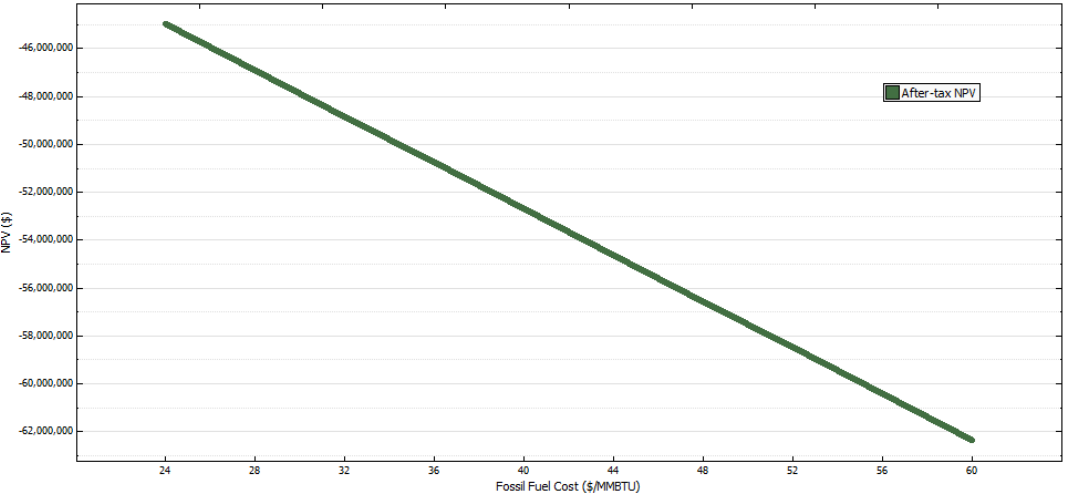


Figure 4.63: Parametric analysis concerning the fossil fuel cost (Andravida).

b. Thessaloniki

Working in a similar way for the case of Thessaloniki, estimated NPV and IRR are \$-20.185.877,15 and 8.09% respectively, proposing the rejection of the investment. In this case however, a drop of 10% in the sum of the direct and indirect investment costs or the reduction of just the solar field and the storage system costs by 25%, invert the initial assessment making the investment seem feasible (Figure 4.64).

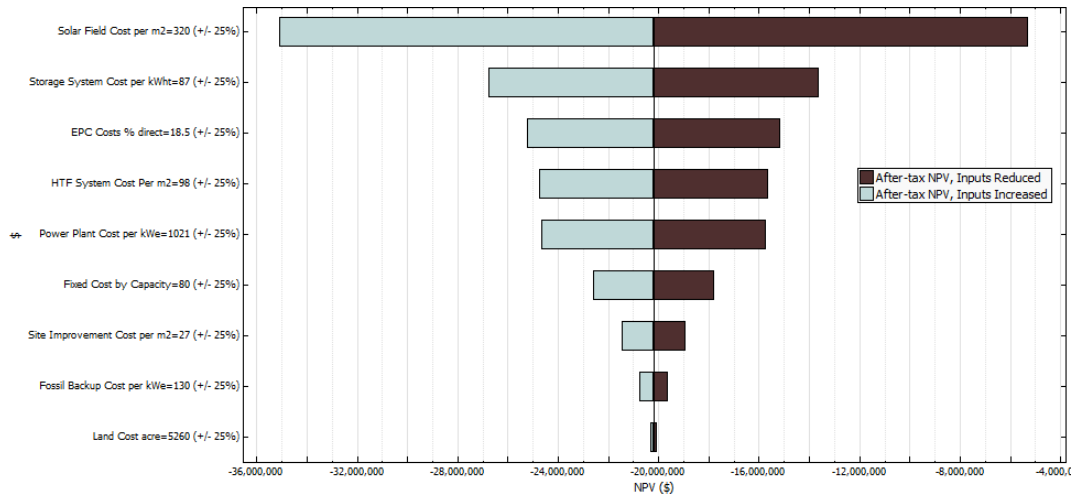


Figure 4.64: Sensitivity analysis between the NPV and the trough system costs (Thessaloniki).

Once more, the variation of the capital mix by itself cannot lead the NPV to a positive value (Figure 4.65).

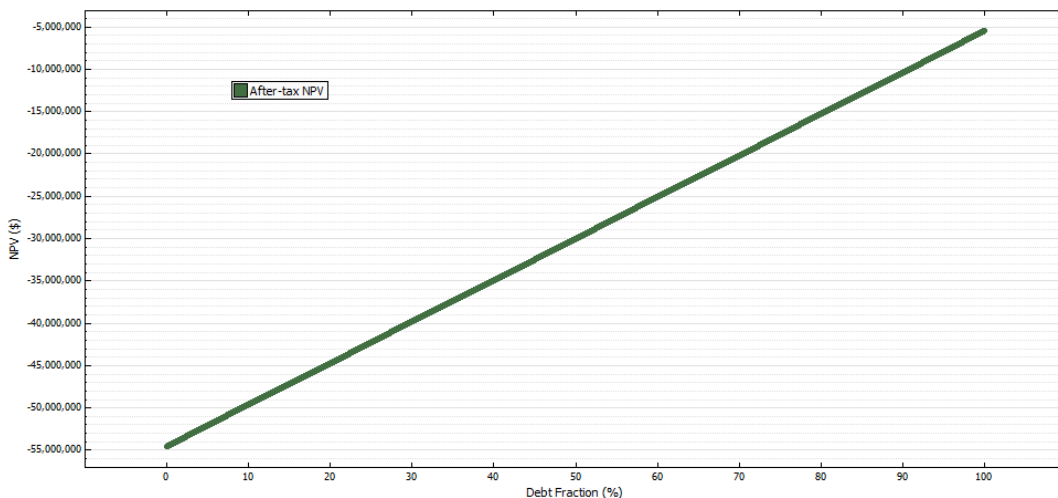


Figure 4.65: Parametric analysis concerning the investment capital mix (Thessaloniki).

Nevertheless, the improvement that might be observed in the next few years in the Greek economy, could definitely affect the feasibility of the investment in Thessaloniki

in a highly positive way. Figure 4.66 shows that a loan rate of 5% - and a corresponding real discount rate of 6%, is enough to result a positive NPV. The impact of fossil fuel cost is not analyzed as the usage of other fuel than the natural gas, which is currently provided in the region for industrial purposes too, seems meaningless.

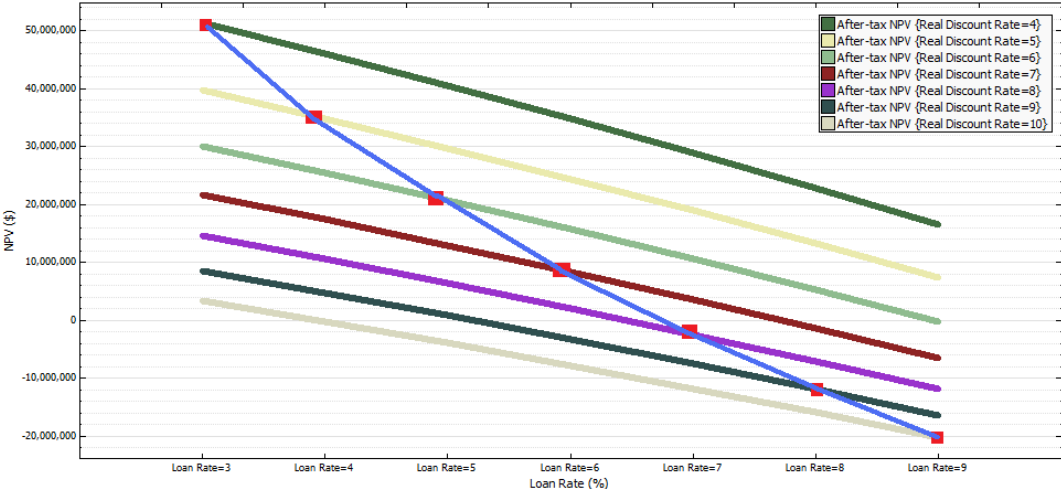


Figure 4.66: Parametric analysis concerning the cost of capital (Thessaloniki).

c. Athens

Although for the region of Athens IRR and NPV are even better than these of Thessaloniki (9,77% and \$-12.168.928,89), they still cannot financially document the implementation of the investment. Nevertheless in this case the CSPP becomes feasible by the drop of solely the solar field cost by 20% or the reduction of the general investment cost by approx. 8% (Figure 4.67).

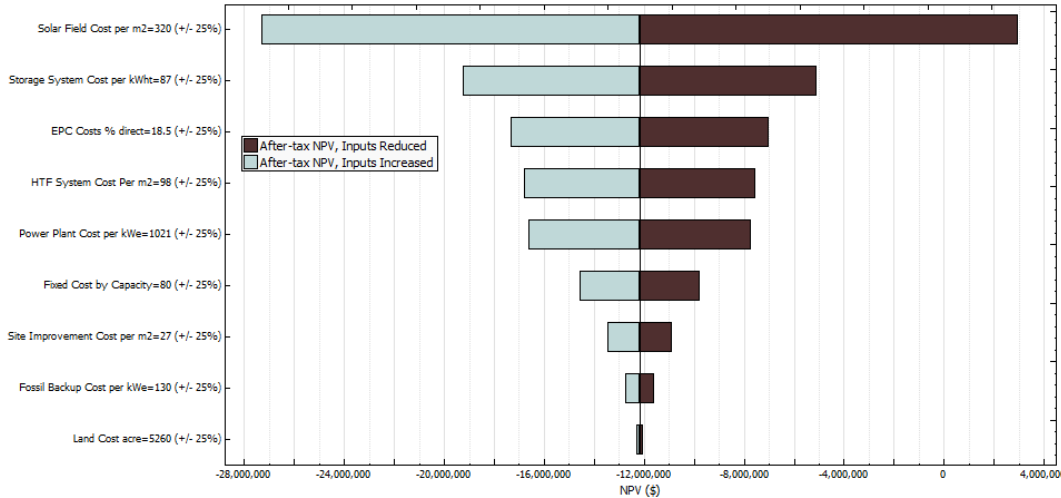


Figure 4.67: Sensitivity analysis between the NPV and the trough system costs (Athens).

A CSPP in Athens becomes also feasible in the rather utopic scenario according to which 95% of the total investment cost is funded by loans (Figure 4.68).

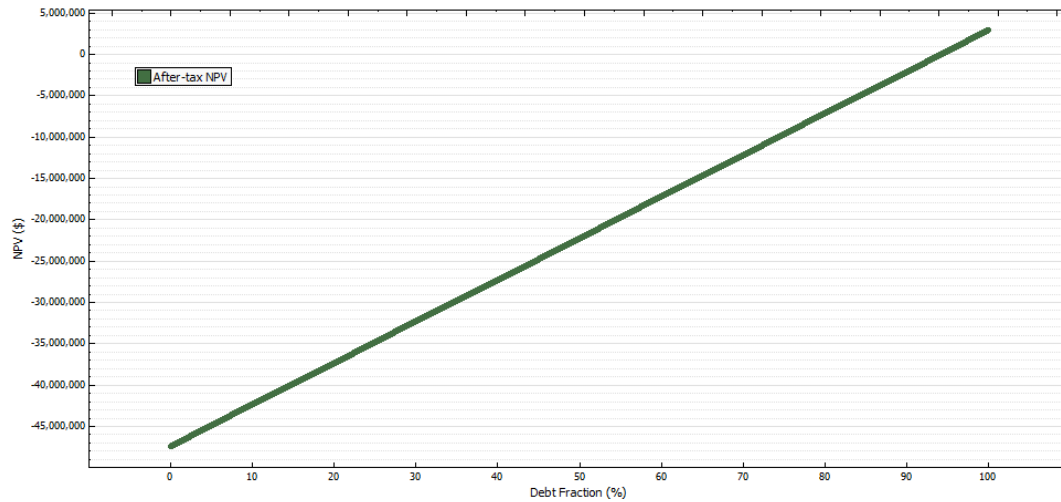


Figure 4.68: Parametric analysis concerning the investment capital mix (Athens).

Finally, once more the cost of capital seem to constitute a highly important factor regarding the feasibility of the CSPP as a drop of 1% of the loan and the real discount rates cause the increase of the NPV by more than \$8.000.000. In the case of Athens this investment seems worthwhile when the loan rate is no larger than approximately 7% and the real discount rate 8% (Figure 4.69).

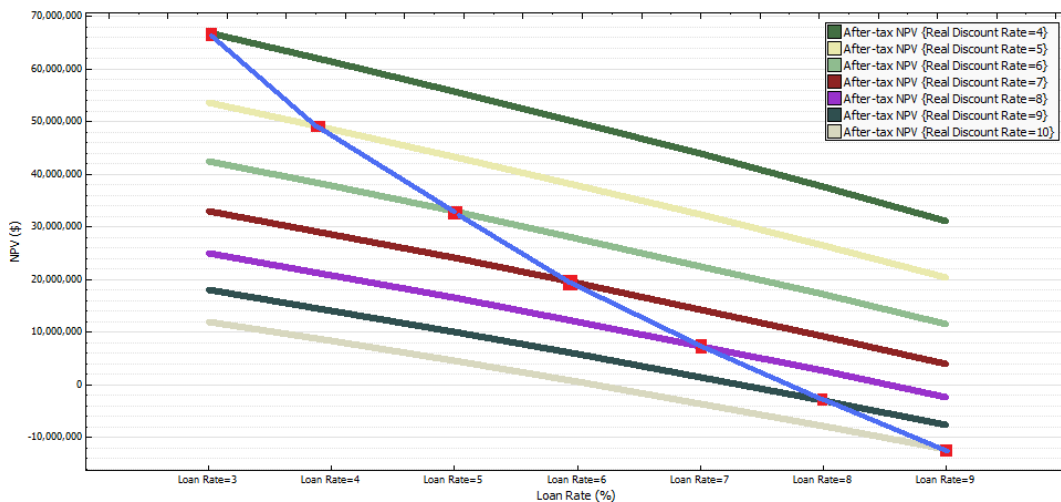


Figure 4.69: Parametric analysis concerning the cost of capital (Athens).

The table shown below (Figure 4.70) summarizes the major calculations made above.

FIGURES	VALUES		
	Andravidia	Thessaloniki	Athens
Location			
Total Investment Cost (\$)	170.203.553	175.583.580	180.050.568
Base Case NPV (\$)	-44.971.693	-20.185.877	-12.168.929
Base Case IRR (%)	2,81%	8,09%	9,77%
Sensitivity to Inv. Cost (\$/1%)	-1.452.942	-1.297.084	-1.537.168
Sensitivity to Fuel Cost [\$/(\$/MMBTU)]	-482.607	-591.500	-624.971
Sensitivity to Debt Fraction (\$/1%)	475.400	490.400	502.929
Sensitivity to LoanRate (\$/100 base points)	-5.430.607	-7.369.623	8.134.371

Figure 4.70: The values of the 3 locations' major calculations.

5 Conclusions

Observing the undoubted climate change taking place nowadays and accusing mostly CO₂ emissions for this, many governments have focused on the reduction of the latter. Within this frame utilization of RES technologies has been promoted through the provision of several incentives. Electricity production exploiting concentrated solar power stands among these technologies, being especially distinguished for its low CO₂ emissions during its life-cycle and the on-going reduction observed in the respective LCOE. For this we assume that investments made in this field will preserve and even reinforce their upward momentum, making CSPP modeling appear as a highly important process. The latter is based on the meeting of demands set by the governments providing incentives, the grid operators scheduling the plants dispatchability and the investors looking to maximize their return on investment.

Starting the modeling process, researchers need to define whether they acknowledge or not uncertainty inherent to the input variables used in such a model. This choice will facilitate them reaching a decision on which ready-to-use simulating program will they use or which programming tools will they utilize in order that they build a new CSPP model. Nowadays, the System Advisor System seems to be the most comprehensive, widely available, integrated software capable of simulating the operation of CSPPs, having been successfully validated in terms of its related output.

Therefore, this study utilized SAM so that a 20 MW hybrid parabolic trough with thermal storage to be modeled. This arrangement was chosen so that advantages, from the technological maturity of parabolic troughs and the performance improvements and financial incentives, being derived from the usage of thermal storage and a fossil fuel-fired auxiliary boiler, to be taken. The modeling process started with an initial setup concerning climate data of Thessaloniki, Greece. Estimated solar field thermal output was compared to this of two other Greek regions, Andravida and Athens, making the latter's suitability explicit. Moreover the frequently assumed correlation between a CSPP's performance and the location latitude has been strongly disputed. During this modeling process, the only variable that SAM did not allow us to utilize it the shading

caused to the collectors aperture by external factors (mountains, trees, buildings etc). The model, considering Athens as the installation site, has been further optimized utilizing SAM's ability to perform parametric analysis and process optimization. The thermal storage was set at 5 MW, leading the estimated annual net electricity output and dumped energy at 51.082 MWh and 666 MWh respectively.

Furthermore, lacking actual data concerning the distribution, and its characteristic values, that many of the uncertain input variables have, probabilistic modeling of the optimized CSPP was performed relying on hypothetical distributions and characteristic values. Unfortunately poor documentation of the assumptions mentioned above makes, further analysis of the results coming from the probabilistic modeling, seem meaningless. Nevertheless, during this process appeared a rather significant weakness of SAM, as it does not allow the probabilistic modeling of maybe the most uncertain variable, the DNI. In any case the reason of this shortage is fully anticipated as this process would require the modeling of 8.760 variables²² and the setting of at least 8.760×2 distribution characteristic values. Besides we are looking forward to reviewing SAM's new features since, by the time that this study was reaching to its end, NREL had already released a new version of this program.

Finally, given that stand-alone technical values are definitely not enough the feasibility of the CSPP to be determined, a comprehensive financing plan as well as estimations on investment and O&M costs were made. For this process SAM performs in an adequately acceptable way, although it is reasonably inferior to custom-made financial models, i.e. discarding the working capital possibly needed and not being able to adjust the size – and thus the cost, of the auxiliary boiler to this specified in the respective schedule. Under this framework the three CSPPs were technically optimized once more, this time taking into account cost effects as well. Initial calculations set the appropriateness of the three investments under doubt due to their negative NPV – or an IRR lower than the discount rate. This view is hardly inversed when the debt fraction is increased while related prospects really improve by the reduction of the investment and O&M costs. What we distinguish as the most important factor though is the cost of capital – equity and debt, since small variations of its value cause dramatic changes in the way that potential investors assess these investments.

²² We assume an hourly step modeling process.

Bibliography

1. J. Hansen, R. Ruedy, M. Sato, and K. Lo, 2012, *Global Temperature in 2011, Trends, and Prospects*, Goddard Institute for Space Studies, National Aeronautics and Space Administration
2. S. Solomon, D. Qin, M. Manning, Z. Chen, M. Marquis, K. B. Averyt, M. Tignor and H. L. Miller, 2007, *Contribution of Working Group I to the Fourth Assessment Report of the Intergovernmental Panel on Climate Change*, Cambridge University Press, Cambridge, United Kingdom and New York, NY, USA
3. WIKIPEDIA, retrieved on June 26 2012, from http://en.wikipedia.org/wiki/Milankovitch_cycles
4. CLIMAP, 1981, *Seasonal reconstructions of the Earth's surface at the last glacial maximum in Map Series, Technical Report MC-36*, Boulder, Colorado: Geological Society of America
5. WIKIPEDIA, retrieved on July 02 2012, from http://en.wikipedia.org/wiki/Milutin_Milankovic
6. WIKIPEDIA, retrieved on July 02 2012, from <http://en.wikipedia.org/wiki/SPECMAP>
7. SOFTPEDIA, retrieved on June 26 2012, <http://news.softpedia.com/news/Ice-Age-Theory-Turned-On-Its-Head-30889.shtml>
8. J. R. Petit et al., 1999, *Climate and atmospheric history of the past 420,000 years from the Vostok ice core, Antarctica*, Nature 399, pages 429-436
9. W. F. Ruddiman, 2006, *Orbital changes and climate*, Quaternary Science Reviews, Volume 25, pages 3092-3112
10. WIKIPEDIA, retrieved on July 02 2012, from http://en.wikipedia.org/wiki/United_Nations_Framework_Convention_on_Climate_Change

11. International Institute for Sustainable Development, 2009, *Summary of the Copenhagen Climate Change Conference*, Earth Negotiations Bulletin, Vol. 12 No. 459
12. WIKIPEDIA, retrieved on July 02 2012, from http://en.wikipedia.org/wiki/Kyoto_Protocol
13. International Energy Agency, 2011, *Key World Energy Statistics*
14. International Energy Agency, 2011, *CO₂ Emissions from Fuel Combustion*
15. National Renewable Energy Laboratory, 2011, retrieved on July 02 2012, from http://www.nrel.gov/analysis/sustain_lca_results.html
16. J. Sathaye, O. Lucon, A. Rahman, J. Christensen, F. Denton, J. Fujino, G. Heath, S. Kadner, M. Mirza, H. Rudnick, A. Schlaepfer, A. Shmakin, 2011, *Renewable Energy in the Context of Sustainable Energy*, National Renewable Energy Laboratory
17. O. Edenhofer, R. Pichs-Madruga, Y. Sokona, K. Seyboth, P. Matschoss, S. Kadner, . Zwickel, P. Eickemeier, G. Hansen, S. Schlömer, C. von Stechow, 2011, *IPCC Special Report on Renewable Energy Sources and Climate Change Mitigation*, Cambridge University Press
18. C. Cleveland, 2008, *Energy transitions past and future*, Encyclopedia of Earth, retrieved on July 06 2012, from http://www.eoearth.org/article/Energy_transitions_past_and_future
19. British Petroleum, 2012, Statistical Review of World Energy, retrieved on July 06 2012, from <http://www.bp.com/statisticalreview>
20. A. Smith, 1776, *The Wealth of Nations*, Random House Inc, London
21. Macrotrends, retrieved on July 07 2012, from <http://www.macrotrends.org/1380/gold-to-oil-ratio-heading-back-up>
22. H. Koh, C. Magee, 2008, *A functional approach for studying technological progress: Extension to energy technology*, Technological Forecasting and Social Change, Volume 75
23. DG ENER, 2010, *Energy Trends 2030*
24. EURELECTRIC, 2010, *Power Choices*
25. WIKIPEDIA, retrieved on July 08 2012, from http://en.wikipedia.org/wiki/Cost_of_electricity_by_source

26. International Energy Agency, 2010, *Projected Costs of Generating Electricity*
27. I. Roth, L. Ambs, 2004, *Incorporating externalities into a full cost approach to electric power generation life-cycle costing*, Energy, Volume 29, Pages 12–15
28. B. Prior, 2011, *Concentrating Solar Power 2011: Technology, Costs and Markets*, GTM Research
29. National Renewable Energy Laboratory, retrieved on July 09 2012, from <http://www.nrel.gov/csp/projects.html>
30. European Commission, retrieved on July 09 2012, from http://ec.europa.eu/research/energy/eu/research/csp/support/index_en.htm
31. J. Hernández-Moro, J. M. Martínez-Duart, 2012, *CSP electricity cost evolution and grid parities based on the IEA roadmaps*, Energy Policy, Volume 41
32. Solar Millennium AG, The Solar Thermal Power Plant Market, retrieved on July 09 2012, from <http://www.solarmillennium.de/english/archiv/energy-market/market-development/index.html>
33. DESERTEC Foundation, *DESERTEC Foundation Flyer*, retrieved on July 09 2012, from http://www.desertec.org/fileadmin/downloads/desertec_foundation_flyer_en.pdf
34. Ministry of Environment, Energy and Climate Change, 2012, *Licensing Status of RES projects in Greece*, retrieved on July 09 2012, from <http://www.ypeka.gr/LinkClick.aspx?fileticket=Gr3lTH00iBE%3d&tabid=701&language=el-GR>
35. REN21, 2011, *Renewables 2011- Global Status Report*, retrieved on July 15 2012, from http://www.ren21.net/Portals/97/documents/GSR/REN21_GSR2011.pdf
36. Hellenic Republic, 2006, *Law 3468 “Production of Electricity from Renewable Energy Sources and High-Efficiency Cogeneration of Electricity and Heat and Miscellaneous Provisions”*, retrieved on July 15 2012, from <http://www.ypeka.gr/LinkClick.aspx?fileticket=5B5fuUXA4Ag%3d&tabid=555&language=el-GR>

37. Greek Operator of Electricity Market, 2012, *Code for electricity transactions*, retrieved on July 15 2012, from http://www.lagie.gr/fileadmin/groups/EDSHE/PithmistikaThemata/20120201_kodikas_sinalagon_HE.pdf
38. WIKIPEDIA, retrieved on August 5 2012, from http://en.wikipedia.org/wiki/Mathematical_model
39. A. Gelman, I. Leenen, I. Van Mechelen, P. De Boeck, J. Poblome, 2009, *Bridges between deterministic and probabilistic models for binary data*, *Statistical Methodology*, Volume 7, Pages 187–209
40. C. K. Ho, G. J. Kolb, 2010, *Incorporating Uncertainty into Probabilistic Performance Models of Concentrating Solar Power Plants*, *Journal of Solar Energy Engineering*, Volume 132
41. C. K. Ho, S. S. Khalsa, G. J. Kolb, 2011, *Methods for probabilistic modeling of concentrating solar power plants*, *Solar Energy*, Volume 85, Pages 669-675
42. M. D. McKay, R. J. Beckman, W. J. Conover, 1979, *A Comparison of Three Methods for Selecting Values of Input Variables in the Analysis of Output from a Computer Code*, *Technometrics*, Volume 21
43. G. D. Wyss, K. H. Jorgensen, 1998, *A User's Guide to LHS: Sandia's Latin Hypercube Sampling Software*, Sandia National Laboratories, Albuquerque, NM, SAND98-0210
44. R. V. Lenth, 2001, *Some Practical Guidelines for Effective Sample Size Determination*, *The American Statistician*, Volume 55, Pages 187-193
45. WIKIPEDIA, retrieved on October 7 2012, from [http://en.wikipedia.org/wiki/ Fortran](http://en.wikipedia.org/wiki/Fortran)
46. H. Fangohr, 2004, *A Comparison of C, MATLAB and Python as Teaching Languages in Engineering*, *Lecture Notes in Computer Science*, Volume 3039 Berlin/Heidelberg, Springer, Pages 1210–1217
47. L. De Rose, D. Padua, 1999, *Techniques for the Translation of MATLAB Programs into Fortran 90*, *ACM Transactions on Programming Languages and Systems (TOPLAS)*, Volume 21, Pages 286 – 323
48. T. A. Dellin, M. J. Fish, 1979, *User's Manual for DELSOL: A Computer Code for Calculating the Optical Performance, Field Layout and Optimal System Design for Solar Central Receiver Plants*, Sandia National Laboratories

49. A. C. Ratzel, B. D. Boughton, 1987, *CIRCE.001: A Computer Code for Analysis of Point-Focus Concentrators with Flat Targets*, Sandia National Laboratories
50. M. C. Stoddard, S. E. Faas, C. J. Chiang, J. A. Dirks, 1987, *SOLERGY—A Computer Code for Calculating the Annual Energy from Central Receiver Power Plants*, Sandia National Laboratories
51. D. T. Gillespie, 1976, A General Method for Numerically Simulating the Stochastic Time Evolution of Coupled Chemical Reactions, *Journal of Computational Physics*, Volume 22, Pages 403-434
52. I. A. Beresnev, G. M. Atkinson, 1998, *FINSIM – a FORTRAN Program for Simulating Stochastic Acceleration Time Histories from Finite Faults*, *Seismological Research Letters* Volume 69
53. Wolfram Research, retrieved on October 13 2012, from <http://reference.wolfram.com/mathematica/guide/Mathematica.html>
54. H. R. Varian, 1993, *Economic and Financial Modeling with Mathematica*, TELOS/Spring-Verlag
55. G. L. Blankenship, R. Ghanadan, H. G. Kwatny, C. LaVigna, V. Polyakov, 1995, *Tools for integrated modeling, design, and nonlinear control*, *Control Systems*, IEEE, Volume 15, Pages 65 – 79
56. R. Adinberg, 2009, *Facilitation of Heat Transfer in Solar Thermal Energy Storage System*, Solar Energy Research Facilities, Weizmann Institute of Science
57. P. D. Schwartzman, D. V. Schwartzman, 2011, *A Solar Transition is Possible*, Institute for Policy Research & Development
58. R. Adinberg, 2011, *Simulation analysis of thermal storage for concentrating solar power*, *Applied Thermal Engineering*, Volume 31, Pages 3588-3594
59. I. L. Garcia, J. L. Alvarez, D. Blanco, 2011, *Performance model for parabolic trough solar thermal power plants with thermal storage: Comparison to operating plant data*, *Solar*, Volume 85, Pages 2443-2460
60. R. Adinberg, 2012, *Evaluation of solar thermal storage for base load electricity generation*, *EPJ Web of Conferences*, Volume 33
61. W. W. Sampson, 2009, *Modeling Stochastic Fibrous Materials with Mathematica®*, Springer

62. K. J. Hastings, 2010, *Introduction to Probability with Mathematica[®]*, CRC Press
63. MathWorks, retrieved on October 16 2012, from <http://www.mathworks.com/products/matlab>
64. WIKIPEDIA, retrieved on October 16 2012, from <http://en.wikipedia.org/wiki/MATLAB>
65. L. Prechelt, 2000, *An empirical comparison of seven programming languages*, IEEE Computer, Volume 33, Pages 23-29
66. E. Gallopoulos, E. Houstis, J.R. Rice, 1994, *Computer as Thinker/Doer: Problem-Solving Environments for Computational Science*, IEEE Computational Science & Engineering, Volume 1, Pages 11-23
67. G. R. Walker, 2001, *Evaluating MPPT converter topologies using a MATLAB PV model*, Journal of Electrical & Electronics Engineering, Volume 21, Pages 49-55
68. H. L. Tsai, C. S. Tu, Y. J. Su, 2008, *Development of Generalized Photovoltaic Model Using MATLAB/SIMULINK*, Proceedings of the World Congress on Engineering and Computer Science 2008
69. C. S. Chin, A. Babu, W. McBride, 2011, *Design, modeling and testing of a standalone single axis active solar tracker using MATLAB/Simulink*, Renewable Energy, Volume 36, Pages 3075-3090
70. P. Palenzuela, G. Zaragoza, D. Alarcón, J. Blanco, 2011, *Simulation and evaluation of the coupling of desalination units to parabolic-trough solar power plants in the Mediterranean region*, Desalination, Volume 281, Pages 379-387
71. S. Vergura, V. Di Fronzo, 2012, *Matlab based Model of 40-MW Concentrating Solar Power Plant*, International Conference on Renewable Energies and Power Quality
72. J. Blanco, P. Palenzuela, D. Alarcón, G. Zaragoza, E. Guillén, M. Ibarra, 2011, *Assessment of suitable configurations for combined Solar Power and Desalination plants*, 2nd European Conference on Polygeneration
73. N. Corral, N. Anrique, D. Fernandes, C. Parrado, G. Caceres, 2012, *Power, placement and LEC evaluation to install CSP plants in northern Chile*, Renewable and Sustainable Energy Reviews, Volume 16, Pages 6678-6685

74. P. Garcia, A. Ferriere, J. J. Bezia, 2008, *Codes for solar flux calculation dedicated to central receiver applications: A comparative review*, Solar Energy, Volume 82, Pages 189-197
75. S. Alexopoulos, B. Hoffschmidt, C. Rau, J. Sattler, 2011, *Choice of solar share of a hybrid power plant of a central receiver system and a biogas plant in dependency of the geographical latitude*, World Renewable Energy Congress, Volume 14
76. J. H. Taylor, D. Kebede, 1996, *Modeling and Simulation of Hybrid Systems in MATLAB*, Proc. IFAC World Congress
77. F. Wickelmaier, C. Schmid, 2004, *A Matlab function to estimate choice model parameters from paired-comparison data*, Behavior Research Models, Instruments & Computers, Volume 36, Pages 29-40
78. S. M. Kay, A. H. Nuttall, P. M. Baggenstoss, 2001, *Multidimensional Probability Density Function Approximations for Detection, Classification, and Model Order Selection*, IEEE Transactions on Signal Processing, Volume 49
79. WIKIPEDIA, retrieved on October 5 2012, from <http://en.wikipedia.org/wiki/Spreadsheet>
80. S. A. Oke, 2004, *Spreadsheet Applications in Engineering Education: A Review*, Int. J. Engng Ed. Volume 20, Pages 893-901
81. H. Price, 2003, *A Parabolic Trough Solar Power Plant Simulation Model*, National Renewable Energy Laboratory
82. J. Igo, C. E. Andraka, 2007, *Solar Dish Field System Model for Spacing Optimization*, in Proceedings of the Energy Sustainability Conference, Long Beach, CA, Pages 981-987
83. S. Akyol, S. Ahrens, F. Jahr, C. Rehberger, E. Luepfert, 2010, *Cost impact model for using polymer film based lightweight mirror construction in CSP plant*, SolarPaces 2010, Perpignan, Frankreich
84. A. Chatterjee, E. Bernal, S. Seshadri, O. Mayer, M. Greaves, 2011, *Linear Fresnel Reflector based Solar Radiation Concentrator for Combined Heating and Power*, AIP Conference Proceedings, Volume 1407, Pages 257-261
85. D. F. Togo, 2004, *Risk analysis for accounting models: A spreadsheet simulation approach*, Journal of Accounting Education, Volume 22, Pages 153-163

86. I. M. Premachandra, J. G. Powell, J. Shi, 1998, *Measuring the relative efficiency of fund management strategies in New Zealand using a spreadsheet-based stochastic data envelopment analysis model*, Omega, Volume 26, Pages 319-331
87. D. M. Levine, D. F. Stephan, T. C. Krehbiel, M. L. Berenson, 2008, *Statistics for managers using Microsoft® Excel*, Pearson Prentice Hall
88. H. F. Assuncao, J. F. Escobedo, A. P. Oliveira, 2003, *Modeling frequency distributions of 5 minute-averaged solar radiation indexes using Beta probability functions*, Theoretical and Applied Climatology, Volume 75, Pages 231-224
89. WIKIPEDIA, retrieved on October 22 2012, from http://en.wikipedia.org/wiki/Comparison_of_risk_analysis_Microsoft_Excel_add-ins
90. WIKIPEDIA, retrieved on October 5 2012, from <http://en.wikipedia.org/wiki/JavaScript>
91. C. J. Dixon, 2006, *A means of estimating the completeness of haplotype sampling using the Stirling probability distribution*, Molecular Ecology Notes, Volume 6, Pages 650–652
92. H. Schildt, 1988, *C++ The Complete Reference (Third Edition)*, Osborne McGraw-Hill
93. TIOBE Programming Community Index, retrieved on November 3 2012, from <http://www.tiobe.com/index.php/content/paperinfo/tpci/index.html>
94. Bjarne Stroustrup's homepage, retrieved on November 3 2012, from <http://www.stroustrup.com/>
95. J. Barton, L. Nackman, 1994, *Scientific and Engineering C++: An Introduction with Advanced Techniques and Examples*, Addison-Wesley Longman Publishing
96. S. Thrun, 2000, *Towards Programming Tools for Robots That Integrate Probabilistic Computation and Learning*, Proceedings of the IEEE International Conference on Robotics and Automation
97. WIKIPEDIA, retrieved on November 3 2012, from [http://en.wikipedia.org/wiki/Eclipse_\(software\)](http://en.wikipedia.org/wiki/Eclipse_(software))
98. M. Zhou, S. Zhou, Internet, 2007, *Open-source and Power System Simulation*, Power Engineering Society General Meeting, IEEE

99. Tonatiuh, retrieved on November 3 2012, from <http://code.google.com/p/tonatiuh>
100. R. Walker, R. Holmes, I. Hedgeland, P. Kapur, A. Smith, 2006, *A light-weight approach to technical risk estimation via probabilistic impact analysis*, Proceedings of the 2006 international workshop on Mining software repositories
101. The RETScreen User Manual, retrieved on October 23 2012, from http://www.etscreen.net/ang/d_t_guide.php
102. TRNSYS, retrieved on October 28 2012, from <http://sel.me.wisc.edu/trnsys/features/features.html>
103. TRNSYS, retrieved on October 28 2012, from <http://www.trnsys.com>
104. C.K. Ho, 2008, *Software and Codes for Analysis of Concentrating Solar Power Technologies*, Sandia National Laboratories
105. TRNSYS 17 – A TRaNsient SYstem Simulation program, *Updates in Version 17.1*
106. R. Pitz-Paal, J. Dersch, B. Milow, F. Tellez, A. Ferriere, U. Langnickel, A. Steinfeld, J. Karni, E. Zarza, O. Popel, 2007, *Development Steps for Parabolic Trough Solar Power Technologies With Maximum Impact on Cost Reduction*, Journal of Solar Energy Engineering, Volume 129, Pages 371-377
107. S. Jones, R. Pitz-Paal, P. Schwarzboezl, N. Blair, R. Cable, 2001, *TRNSYS Modeling of the SEGS VI Parabolic Trough Solar Electric Generating System*, Proceedings of Solar Forum 2001
108. P. Harper, 2009, *Trnsys Modeling of a 100 MW Combined Cycle Concentrated Solar Power Plant*, Research report, Stellenbosch University
109. S. Janjai, J. Laksanaboonsong, T. Seesaard, 2011, *Potential application of concentrating solar power systems for the generation of electricity in Thailand*, Applied Energy, Volume 88, Pages 4960-4967
110. B. Yang, J. Zhao, W. Yao, Q. Zhu, H. Qu, 2010, *Feasibility and Potential of Parabolic Trough Solar Thermal Power Plants in Tibet of China*, Power and Energy Engineering Conference 2010
111. SAM Introduction and Getting Started, retrieved on November 5 2012, from <https://sam.nrel.gov/content/resources-learning-sam>

112. K. Lovegrove, J. Wyder, A. Agrawal, D. Boruah, J. McDonald, K. Urkalan, 2011, Concentrating Solar Power in India, PDF Prepared by IT Power Group for the Australian Government Department of Climate Change and Energy Efficiency with the cooperation of the Government of India Ministry for New and Renewable Energy for AusAID Public Sector Linkages Program project. Press Release
113. K. Ummel, 2010, *Concentrating Solar Power in China and India: A Spatial Analysis and the Cost of Deployment – Working Paper 219*, Center for Global Development, Washington D.C.
114. N. Blair, M. Mehos, C. Christensen, 2008, *Sensitivity of Concentrating Solar Power Trough Performance, Cost and Financing with Solar Advisor Model*, 14th Biennial CSP SolarPACES (Solar Power and Chemical Energy Systems) Symposium, Las Vegas, Nevada
115. N. Blair, M. Mehos, C. Christensen, C. Cameron, 2008, *Modeling Photovoltaic and Concentrating Solar Power Trough Performance, Cost, and Financing with the Solar Advisor Model: Preprint*, NREL Report No. CP-670-42922
116. C. Turchi, 2010, Parabolic Trough Reference Plant for Cost Modeling with the Solar Advisor Model (SAM), NREL Report No. TP-550-47605
117. A. Dobos, C. Ho, 2010, Stochastic modeling of concentrating solar power plants using the Solar Advisor Model (SAM), SolarPaces Conference Paper
118. W.B. Stine, M. Geyer, 2001, *Power From The Sun*, retrieved on October 5 2012, from <http://www.powerfromthesun.net/book.html>
119. J. Garcia-Barbarena, P. Garcia, M. Sanchez, M. Blanco, C. Lasheras, A. Padros, J. Arraiza, 2012, *Analysis of the influence of operational strategies in plant performance using SimulCET, simulation software for parabolic trough power plants*, Solar Energy, Volume 86, Pages 53-63
120. Acciona, *Technology and Experience in Concentrating Solar Power*, retrieved on November 4 2012, from <http://www.acciona-energia.com/media/315798/Technology%20and%20experience%20in%20concentrating%20solar%20power.pdf>

121. F. Zaversky, J. Garcia-Barbarena, M. Sanchez, D. Astrain, 2012, *Probabilistic modeling of a parabolic trough collector power plant – An uncertainty and sensitivity analysis*, Solar Energy, Volume 86, Pages 2128-2139
122. National Renewable Energy Center of Spain, 2012, *CSTP plant design: Goals, processes, and computer tools*, Training workshop on concentrated solar thermal power plants, Abu Dhabi, UAE – ADNEC
123. M. Blanco, M. Sanchez, L. Ramirez, 2009, *Computer tools to assist in the design, analysis and optimization of concentrating solar power plants*, Energetica India, Volume 3, Pages 42-43
124. P. Garcia, A. Mutuberria, J. Garcia-Barbarena, M. Sanchez, M. Blanco, C. Lasheras, A. Padros, J. Arraiza, 2009, *Validation of DINACET computational scheme using Nevada solar one power plant data*, Proceeding of SolarPACES 2009 International Conference, Berlin, Germany
125. J. Feldhoff, K. Schmitz, M. Eck, D. Laing, F. Ortiz-Vives, L. Schnatbaum-Lauman, J. Schulte-Fischedick, 2011, *Comparative System Analysis of Direct Steam Generation and Synthetic Oil Parabolic Trough Power Plants with Integrated Thermal Storage*. 5th International Conference on Energy Sustainability, Washington, USA
126. J. Usaola, 2012, *Participation of CSP plants in the reserve markets: A new challenge for regulators*, Energy Policy, Volume 49, Pages 562, 571
127. S. Kalogirou, 2009, *Solar energy engineering: processes and systems*, Elsevier
128. J. Duffie, 1991, *Beckman, Solar Engineering of Thermal Processes*, John Wiley and Sons
129. WIKIPEDIA, retrieved on November 10 2012, from http://en.wikipedia.org/wiki/Coordinated_Universal_Time
130. E. Akim, D. Tuchin, 2002, *GPS Errors Statistical Analysis for Ground Receiver Measurements*, Keldysh Institute of Applied Mathematics, Russia Academy of Sciences
131. R. George, S. Wilcox, M. Anderberg, 2008, *National Solar Radiation Database (NSRDB) - 10 km Gridded Hourly Solar Database*, Solar Resource Assessment Workshop, Denver, USA

132. I. Hall, R. Prairie, H. Anderson, E. Boes, 1978, *Generation of a typical meteorological year*, Proceedings of the 1978 Annual Meeting of the American Section of the International Solar Energy Society, Denver, USA, Pages 669-671
133. International Bureau of Weights and Measurements, 2008, *Guide to the Expression of Uncertainty in Measurements*, JCGM
134. C. Choi, 2003, *Improving the accuracy of a variable step-size method for solving stiff Lyapunov differential equations*, Proceeding of the American Control Conference, Volume 3, Pages 2755-2760
135. M. Wagner, P. Gilman, 2011, *Technical Manual for the SAM Physical Trough Model*, NREL Technical Report, TP-5500-51825
136. T. Stoffel, D. Renne, D. Myers, S. Wilcox, M. Sengupta, R. George, C. Turchi, 2010, *Best Practices Handbook for the Collection and Use of Solar Resource Data*, NREL Technical Report, TP-550-47465
137. D. Gately, 2004, *Psychrometric chart celebrates 100th anniversary*, ASHRAE Journal, Volume 46, Pages 16 – 20
138. M. Wagner, M. Mehos, D. Kearney, A. McMahan, 2011, *Modeling of a parabolic trough solar field for acceptance testing: A case study*, Proceedings of the ASME 2011 5th International Conference on Energy Sustainability, Washington, USA
139. G. Kaplan, 1985, *Understanding Solar Concentrators*, Vita
140. C. Turchi, M. Mehos, C. Ho, G. Kolb, 2010, *Current and Future Costs for Parabolic Trough and Power Tower Systems in the US Market*, NREL Conference Paper, CP-5500-49303
141. M. Montes, A. Abanades, J. Martinez-Val, M. Valdes, *Solar multiple optimization for a solar-only thermal power plant, using oil as heat transfer fluid in the parabolic trough collectors*, Solar Energy, Volume 83, Pages 2165-2176
142. H. Gaul, A. Rabl, 1980, *Incidence-Angle Modifier and Average Optical Efficiency of Parabolic Trough Collectors*, Solar Energy Engineering, Volume 102, Pages 16-31
143. M. Carvalho, P. Horta, J. Mendes, M. Pereira, W. Carbajal, 2007, *Incidence Angle Modifiers: A General Approach for Energy Calculations*, Proceeding of ISES World Congress, Pages 608-612

144. M. Brandner, 2006, *Uncertainty in optical measurement applications: A case study*, Instrumentation and Measurement, Volume 55, Pages 713-720
145. D. Ginley, D. Cahen, 2012, *Fundamentals of Materials for Energy and Environmental Sustainability*, Cambridge University Press
146. H. Baehr, K. Stephan, 2006, *Heat and Mass Transfer*, Springer
147. T. Adams, 2008, *A Guide for Estimation of Uncertainty of Dimensional Calibration and Testing Results*, The American Association for Laboratory Accreditation
148. C. Kennedy, 2002, *Review of Mid- to High-Temperature Solar Selective Absorber Material*, NREL, Technical Report, TP-520-31267
149. R. Forristall, 2003, *Heat Transfer Analysis and Modeling of a Parabolic Trough Solar Receiver Implemented Engineering Equation Solver*, NREL, Technical Report, TP-550-34169
150. E. Brown, 2008, *Understanding and Expressing Measurement Uncertainties associated with Thermodynamic Metrology*, Perry Johnson Laboratory Accreditation
151. M. Eck, K. Hennecke, 2009, *Heat Transfer Fluids for Future Parabolic Trough Solar Thermal Power Plants*, Proceeding of ISES World Congress 2007, Pages 1806-1812
152. F. Zabel, D. Law, S. Taylor, J. Zuo, 2010, *Impact of Uncertainties of Heavy Oil Fluid Property Measurement*, Journal of Canadian Petroleum Technology, Volume 49, Pages 28-35
153. National Renewable Energy Laboratory, retrieved on November 15 2012, from http://www.nrel.gov/csp/troughnet/power_plant_systems.html
154. E. Prabhu, 2006, *Solar Trough Organic Rankine Electricity System (STORES) – Stage 1: Power Plant Optimization and Economics*, NREL, Sub-contract Report, SR-550-39433
155. H. Price, V. Hassani, 2002, *Modular Trough Power Plants Cycle Analysis*, Technical Report, TP-550-31240
156. J. Dersch, M. Geyer, U. Hermann, S. Jones, B. Kelly, R. Kistner, W. Ortmanns, R. Pitz-Paal, H. Price, 2002, *Solar Trough Integration into Combined*

- Cycle Systems*, Proceeding of ASME International Solar Energy Conference, 2002, Nevada, USA
157. B. Kelly, U. Hermann, M. Hale, 2001, *Optimization Studies for Integrated Solar Combined Cycle Systems*, Proceeding of ASME International Solar Energy Conference: The Power to Choose, 2001, Washington, USA
 158. I. Niknia, M. Yaghoubi, 2010, *Transient Analysis of Integrated Shiraz Hybrid Solar Thermal Power Plant*, Proceeding of World Renewable Energy Congress XI, 2010, Abu Dhabi, UAE
 159. J. Servet, G. San Miguel, D. Lopez, 2011, *Hybrid Solar – Biomass Plants for Power Generation; Technical and Economic Assessment*, Global NEST Journal, Volume 13, Pages 266-276
 160. M. Wagner, 2008, *Simulation and predictive performance modeling of utility-scale central receiver system power plants*, Master's thesis, University of Wisconsin, Madison, Wisconsin, USA
 161. K. Jaeger, 2012, *Guidance on Uncertainty Budgets for Electrical Parameters*, The American Association for Laboratory Accreditation
 162. A. Wood, 2012, *Solar Hybrid Solution*, Siemens AG at 4th Saudi Solar Forum
 163. M. Wagner, C. Kutscher, 2010, *The impact of hybrid wet/dry cooling on concentrating solar power plant performance*, Proceedings of the 4th International Conference on Energy Sustainability, ASME, Phoenix, Arizona, USA.
 164. J. Pacheco, S. Showalter, W. Kolb, 2001, *Development of a molten-salt thermo-cline thermal storage system for parabolic trough plants*, Proceeding of Solar Forum 2001, Washington DC, USA
 165. D. Mills, 2004, *Advances in solar thermal electricity technology*, Solar Energy, Volume 76, Pages 19-31
 166. B. Kelly, D. Kearney, 2006, *Parabolic Trough Solar System Piping Model*, NREL, Subcontract Report, SR-550-40165
 167. Regulatory Authority of Energy, 2010, *Evaluation guide of electricity generation projects by the use of concentrated solar radiation*, retrieved on November 30 2012 from <http://www.rae.gr>

168. M. Eck, W. Steinmann, 2002, *Direct Steam Generation in Parabolic Troughs: First Results of the DISS (Direct Solar Steam) Project*, Solar Energy Engineering, Volume 124, Pages 134-139
169. P. Svoboda, E. Dagan, G. Kenan, 1997, *Comparison of DSG vs. HTF Technology for Parabolic Trough Solar Power Plants Performance and Cost*, Conference Proceedings, ASME International Solar Energy Conference, Washington DC, USA
170. U.S. Department of Energy, retrieved on November 30 from http://apps1.eere.energy.gov/buildings/energyplus/cfm/weather_data3.cfm/region=6_europe_wmo_region_6/country=GRC/cname=Greece
171. F. Shutter, P. Heller, S. Meyen, R. Pitz-Paal, C. Kennedy, A. Fernandez-Garcia, M. Schmuecker, 2010, *A New Method to Characterize Degradation of First Surface Aluminum Reflectors*, NREL, Conference Report, CP-5500-49164
172. S. Vergura, V. Lameira, 2011, *Technical-Financial Comparison Between a PV Plant and a CSP Plant*, *Revista Electronica Sistemas & Gestao*, Volume 6, Pages 210-220
173. Menasol, 2011, *North Africa and Middle East Solar Country Profile*, retrieved on December 3 2012 from <http://www.revolve-magazine.com/home/wp-content/uploads/2011/05/MENASOL-COUNTRY-PROFILES.pdf>
174. E. Luepfert, M. Geyer, W. Schiel, A. Esteban, R. Osuna, E. Zarza, P. Nava, 2001, *EuroTrough – Design Issues and Prototype Testing at PSA*, ASME Solar Energy: The Power to Choose, Washington DC, USA
175. M. Geyer, E. Luepfert, R. Osuna, A. Esteban, W. Schiel, A. Schweitzer, E. Zarza, P. Nava, J. Langenkamp, E. Mandelberg, 2002, *EUROTROUGH – Parabolic Trough Collector Developed for Cost Efficient Solar Power Generation*, Symposium on Concentrating Solar Power and Chemical Energy Technologies, Zurich, Switzerland
176. Schott Business Unit Solar, Solar Thermal Power Plants, Schott Solar CSP GmbH, retrieved on December 5 2012 from <http://www.hvg-dgg.de/uploads/media/Fa708b-Nattermann.pdf>
177. C. Fark, 2009, *Setting the benchmark in receiver technology*, Schott Solar CSP GmbH

178. F. Burkholder, C. Kutscher, 2009, *Heat Loss Testing of Schott's 2008 PTR70 Parabolic Trough Receiver*, NREL Technical Report, TP-550-45633
179. Sonne Solar Energy Industries Corp, retrieved on December 5 2012 from <http://www.sonnecorp.diytrade.com/sdp/1212106/4/pd-5495696/9422656.html>
180. R. Mahoney, 2000, *Trough Technology – Heat Collector Element (HCE) – Solar Selective Absorbers*, Trough Workshop ASES 2000
181. U.S. Environmental Protection Agency, 2008, *Climate Leaders Greenhouse Gas Inventory Protocol Offset Project Methodology for Industrial Boiler Efficiency*, retrieved on December 6 2012 from http://www.epa.gov/climateleadership/documents/resources/industrial_boiler_protocol.pdf
182. J. Hinkley, B. Curtin, J. Hayward, Al. Wonhas, R. Boyd, Ch. Grima, A. Tadros, R. Hall, K. Naicker, A. Mikhail, 2011, *Concentrating solar power - drivers and opportunities for cost-competitive electricity*, Garnaut Climate Change Review Update 2011
183. EPA Thessaloniki SA, retrieved on January 24 from <http://www.epathessaloniki.gr/index.php?cid=80&mn=29>
184. Europe's Energy Portal, retrieved on January 24 from <http://www.energy.eu/>
185. Hellenic Republic, 2003, *Presidential Decree 299/2003: Determination of lower and upper depreciation rates*, retrieved on January 25 from <http://www.taxheaven.gr/laws/law/index/law/126>